Functional and Biochemical Characterization of KCNQ1/KCNE1 Subunit Interactions in the Cardiac I_{Ks} Potassium Channel

Priscilla Jay Chan

Submitted in partial fulfillment of the
requirements for the degree of
Doctor of Philosophy
in the Graduate School of Arts and Sciences

COLUMBIA UNIVERSITY

2011

ABSTRACT

Functional and Biochemical Characterization of KCNQ1/KCNE1 Subunit Interactions in the Cardiac I_{Ks} Potassium Channel

Priscilla Jay Chan

The I_{Ks} potassium channel, critical to control of heart electrical activity, requires assembly of pore-forming alpha subunits (KCNQ1) and accessory beta (KCNE1) subunits. I_{Ks} is the slowly activating component of delayed rectifier K^+ current in the heart and is a major contributor to the timing of repolarization of the cardiomyocyte membrane potential. Inherited mutations in either I_{Ks} channel subunit are associated with cardiac arrhythmia syndromes, including long QT syndrome (LQTS), short QT syndrome (SQTS) and familial atrial fibrillation (FAF).

The biophysical properties of I_{Ks} channel current are dramatically altered when KCNE1 associates with the KCNQ1 channel. Functional tetrameric channels can be formed by KCNQ1 alone, but co-assembly with KCNE1 is required for the unique kinetics necessary to regulate human cardiac electrical activity as well as for the channel's functional response to the sympathetic nervous system. Specifically, KCNE1 co-assembly results in a depolarizing shift in the voltage dependence of activation, an increase in the single channel conductance, and an increase in current density. I_{Ks} channel current is also characterized by slow activation and deactivation kinetics, with little or no inactivation, in contrast to the KCNQ1 homomeric channel, which is characterized by fast activation and deactivation kinetics and clear inactivation.

We wanted to understand how KCNE1 modulates the KCNQ1 channel functionally and investigate the structural determinants of this modulation. In Chapter II, we explore the role(s) of KCNE1 in the context of two KCNQ1 atrial fibrillation associated mutations, S140G and V141M. In contrast to published results, we find distinct dependence on the KCNE1 subunit for V141M, but not for S140G. Having determined the importance of KCNE1 for V141M functionally, we continued to explore the role of KCNE1 structurally for this mutation. Using cysteine substitution in both KCNQ1 and KCNE1 subunits, we monitored spontaneous disulfide bond formation and find that V141C crosslinks to KCNE1, while S140C does not. Having established the functional and structural importance of KCNE1 for V141M, we proposed that there could be mutations in KCNE1 that could reverse the consequences of slow deactivation in the V141M mutation. In Chapter III, we engineer amino terminal KCNE1 mutations and demonstrate that this domain is important for controlling deactivation, but not activation, kinetics of the KCNQ1 channel. We find two KCNE1 mutations, L45F and Y46W, which when co-expressed with either V141M or S140G mutations in KCNQ1, help restore the mutant channel back towards a wild-type I_{Ks} channel. From these results, we propose that the amino-terminal domain could play an important role in mediating the rate of deactivation in KCNQ1/KCNE1 channels. After testing mutations on KCNE1 that could affect normal channel function, we continued with a project to study mutations on KCNQ1 that would have similar dramatic effects on the channel. In Chapter IV, we mutated KCNQ1 residue S140 to Threonine and found that S140T co-assembled with KCNE1 produced a channel having functional characteristics opposite to that of S140G/KCNE1 channels. In contrast to S140G/KCNE1 channels, where channels tend

to stay open due to very slow deactivation kinetics, S140T/KCNE1 channels tend to be stabilized in the closed state and require more depolarized pulses to open channels. In addition, we find that a mutation at position Y46 in KCNE1, when co-expressed with the S140T mutation in KCNQ1, helps restore the mutant channel back towards a wild-type channel. Again, here we provide evidence that the amino terminal end of KCNE1 could play a role in controlling deactivation. In Chapter V, we investigated the importance of where KCNE1 is located in the channel and also how KCNQ1/KCNE1 subunits assemble using a tandem construct, with 1 KCNE1 subunit tethered to 2 KCNQ1 subunits (EQQ). To investigate the significance of KCNE1 location, we explored the functional consequences of having the S140G or V141M mutations in the proximal (closest to KCNE1) or distal (farthest from KCNE1) KCNQ1 subunit. We find that having a mutation in the proximal subunit is subject to modulation by KCNE1, but not the distal subunit. Using crosslinking, we want to confirm proper assembly of the heterotetrameric channel to verify that KCNE1 assembles between S1 from one KCNQ1 subunit and the S6 domain of an opposing KCNQ1 subunit.

Taken together, we demonstrate that the proximity between the N-terminus of KCNE1 and the S1 domain of KCNQ1 could play a role in modulating deactivation kinetics of KCNQ1. These findings will be of great importance in understanding normal I_{Ks} channel function, which will be essential for maintaining proper heart function.

TABLE OF CONTENTS

LIST OF FIGURES AND TABLES

ABBREVIATIONS

AF = Atrial Fibrillation

AKAP = A kinase-anchoring protein

CTX = charybdotoxin

CTX-Mal = charybdotoxin with maleimide group

Cys = cysteine

DTT = 1,4-dithio-DL-threitol

E1 = KCNE1

EQ = tandem construct linking one KCNE1 to one KCNQ1 subunit

EQQ = tandem construct linking one KCNE1 to two KCNQ1 subunits

ER = endoplasmic reticulum

FAF = familial atrial fibrillation

FRET = fluorescence resonance energy transfer

gof = gain-of-function

JLNS = Jervell-Lange Nieslsen Syndrome

LQTS = Long QT Syndrome

MTSES = methanethiosulfonate-ethylsulfonate

NEM = N-ethylmaleimide

NMR = nuclear magnetic resonance

PKA = protein kinase A

PP1 = protein phosphatase 1

p-helix = pore-loop helix

Q1 = KCNQ1

SNS = sympathetic nervous system

SQT = Short QT Syndrome

TCEP = tris(2-carboxyethyl)phosphine)

TEA = tetraethylammonium

TIRF = total internal reflection fluorescence

TM or TMD = transmembrane or transmembrane domain

VSD = voltage-sensing domain

WT = wild-type

ACKNOWLEDGEMENTS

This thesis would not have been possible without the scientific guidance, mentorship, and support from many people along the way. First of all, I would like to thank my thesis advisor, Rocky Kass, for his guidance and support throughout the entire process. From him, I've learned invaluable lessons about scientific communication and perseverance, which I will take with me throughout my career. Without Rocky, I would not have had this opportunity, so I am greatly appreciative that he took me on as a student. I hope that I have been able to contribute to his lab in some way, although I know it will never amount to how much I have learned from him and this lab. Secondly, I would like to thank the entire Kass Lab, past and present, without whom, through scientific discussions, lunch conversations, and various shenanigans, I could not have completed this thesis.

I would also like to thank my thesis committee members, Arthur Karlin and Steven Marx, both of whom I have also learned a lot from and appreciate that I could converse with them frequently about my project. To Arthur, I am very grateful for the extra time and effort that he took to help me think about my project and to troubleshoot problems. When talking to him, he always made science especially fun to talk and think about. To Steven, I appreciate his support and the time he took to help me with any questions I had, and he has also been very supportive by being on every committee with me throughout this entire process, from my qualifying exam to the thesis defense.

I would especially like to thank David Chung and Cecile Terrenoire for teaching me everything about patch clamp electrophysiology and data analysis. I am very grateful to David Chung for being in the lab when I started, in addition to being a good friend, I was able to have someone to discuss my project freely with and toss around ideas about our overlapping projects.

Cecile Terrenoire is someone in the lab who I literally, would not have survived without, in addition to always being available to answer any questions I had and taking the time to explain something, she is also a true friend who I can always talk to about anything. I would like to thank Lei Chen and Ian Glaaser, both of which I was able to ask any questions relating to molecular biology or biochemistry to, even though sometimes they had conflicting answers. Ian has also been very helpful being the senior student in the lab and I am grateful to him for being able to repeatedly ask him any questions about the pharmacology courses and program. I would also like to thank John Bankston, Jeremiah Osteen, Kevin Sampson, and George Wang for their help during my thesis. John for always taking an interest in the experiments I was doing and helping me think about them, Jeremiah for his helpful advice and for being another person I could talk to freely about my project with, and Kevin, whom I am very grateful to for his guidance and advice on how to present and analyze results in an effective way. I would like to especially thank Jenny Rao, whom I've probably asked to prepare numerous maxi-preps and flasks of cells for me over the years, but also for being a friend who I can share my interests with, including running and biking with and making wontons. I am also grateful to the new people in the lab, Michael Bohnen and Seth Robey, for being in the lab with positive attitudes and enthusiasm for science near the end of my journey and also Dazhi Xiong for being extremely helpful in completing additional experiments for my thesis and manuscript.

I am particularly thankful to my fellow classmate in the Pharmacology Program, Tahilia Rebello, without whom, I again literally would not have survived this process. If she had not been there every step of the way, I don't think I would be finishing this thesis now. I would also like to thank my mom and dad and sister for their unconditional love and never-ending support for anything I aspire to do. Although they may be far away in California, they would offer the

best and most helpful advice. A special thank you to my grandmother, Fung Oi Yue, who always had the time to ask how I was doing, even though she had 9 other grandchildren and 7 children of her own to worry about. She taught me to work hard and finish whatever I start. If she were here today, I hope that I have made her proud by finishing this thesis. And lastly, to my husband, Hyman Chung, who somehow always knows how to make everything infinitely better with fun and laughter and makes me feel like I am capable of accomplishing anything. Without his support and love, I would not have had the strength and motivation to finish this thesis.

To my grandmother, Fung Oi Yue, and parents, Simon and Betty Chan

CHAPTER I

INTRODUCTION

Physiology

In order for the mammalian heart to function properly, a coordinated sequence of electrical impulses, that initiates in the atria and propagates to the ventricles, is required. This electrical activity comes from the generation of action potentials, which are a net result of the sequential activation and inactivation of ion channels that conduct depolarizing inward (Na^+ and Ca^{2+}) and repolarizing outward (K^+) currents. Potassium currents are particularly important in the repolarization phase of the action potential and help to stabilize the resting potential in cell membranes. Repolarization is attributed to the efflux of K^+ ions due to activation of several voltage-gated potassium channels.

The Cardiac I_{Ks} channel is comprised of KCNQ1 and KCNE1

Potassium (K^+) channels in the heart are important for the regulation of action potential duration and control of the cellular resting membrane potential. Noble and Tsien first identified in sheep Purkinje fibers that there are two potassium-sensitive components, that contribute to the delayed rectifier K^+ current in order to control action potential duration (Noble and Tsien, 1969). These two components were later defined pharmacologically as I_{Kr} and I_{Ks}. I_{Kr} was described as the rapidly activating component, which could be blocked by class III anti–arrhythmic drugs, while I_{Ks} was classified as the slowly activating outward component of the delayed rectifier K^+ current and was drug insensitive (Sanguinetti and Jurkiewicz, 1990). The molecular identity of

$I_{Ks,}$ consisting of a tetramer of pore-forming alpha subunits, KCNQ1, and the accessory beta subunit, KCNE1, remained unknown for several more years.

KCNE1 was discovered before KCNQ1 and was thought to form the basis of the I_{Ks} current because it produced a slowly activating outward potassium current when expressed in *Xenopus* oocytes (Takumi et al., 1988). However, the idea that KCNE1 formed functional channels on its own caused a fair amount of debate because it is a single membrane spanning protein containing only 129 amino acids and it did not share the same characteristics as other voltage gated K^+ channels (Murai et al., 1989; Folander et al., 1990; Takumi et al., 1991). In later studies, it was shown that KCNE1 did not conduct currents when expressed in mammalian cell lines: ClC-2, CHO, and Jurkat cell lines (Lesage et al., 1993). The controversy was eventually settled when KCNQ1 was discovered in a positional cloning study that was investigating the gene responsible for Long QT Syndrome (LQTS) (Wang et al., 1996b). In this study, the authors establish KCNQ1 as the chromosome 11-linked LQT1 gene responsible for the most common inherited cardiac arrhythmia.

Further studies clarified that KCNE1 is not a K^+ channel itself, but is an essential subunit that assembles with KCNQ1 to form the I_{Ks} channel complex (Barhanin et al., 1996; Sanguinetti et al., 1996). Both groups observed that when KCNE1 was expressed in mammalian cells, COS-7 and CHO, they saw no detectable current, but when co-expressed with KCNQ1, they saw a slowly activating outward current, almost identical to cardiac I_{Ks}. They performed further experiments that involved co-expression of KCNQ1 and KCNE1 in *Xenopus* oocytes, which resulted in currents with much greater current amplitude than currents from KCNE1 expression alone. From these results, both groups concluded that KCNE1 is not a K^+ channel itself, but is an accessory subunit that assembles with KCNQ1 in order to produce the slow outward

potassium current. The experiments initially characterizing KCNE1 were performed in oocytes, and to explain the current that was exhibited by from these cells, it was concluded that KCNE1 was assembling with an endogenous K^+ channel to produce current. Thus, the link between the LQT associated gene, KCNQ1, and I_{Ks} was established and gave physiological significance to this current in the heart.

Long QT Syndrome

Long QT Syndrome (LQTS) is a disorder of the cardiac repolarization process, in which there is prolongation of the QT interval (QTc ≥ 0.46 seconds) affecting every 1 in 7,000 people of the general population. LQTS is associated with recurrent syncope due to a transient, rapid, polymorphic ventricular tachycardia, also known as torsade de pointes, and sudden death. This disorder can be acquired or inherited. Acquired LQT can result from treatment with many types of drugs, including certain anti-arrhythmic medications or treatment for metabolic abnormalities. The inherited form of LQTS is predominantly an autosomal dominant disorder, known as Romano-Ward Syndrome, and can be caused by specific mutations in ion channel genes. LQTS was found to be mapped to different loci in the human genome and these loci have been named chronologically in order of their discovery. Subsequently, using linkage analyses, the genes for LQT2 was discovered to be linked to the hERG potassium channel (Curran et al., 1993) and LQT3 was found to be linked to the cardiac SCN5A sodium channel (Wang et al., 1995). However, the gene for LQT1 was determined later and was found to be linked to the cardiac KCNQ1 potassium channel gene (Wang et al., 1996b). The most common mutations occur in the first 3 identified LQT genes (LQT1-LQT3), with more than 50% occurring in KCNQ1, which is associated with LQT1. Currently, there are 13 inherited forms of LQT identified.

There is also an autosomal recessive variant of LQTS known as Jervell and Lange-Nielson syndrome, which is characterized by QT prolongation and hearing loss.

Atrial Fibrillation

Atrial fibrillation (AF) is characterized by rapid and irregular activation of the atrium. It is caused mainly by multiple circuit-reentry, due to shortening of the action potential and reduction of the effective refractory period (Nattel, 2002). AF affects nearly 1% of the general population and prevalence increases with age. Many disease associated gain-of-function mutations have been found in KCNQ1. These disease phenotypes include short QT syndrome (Bellocq et al., 2004), sudden infant death syndrome (Rhodes et al., 2008), and atrial fibrillation (Chen et al., 2003c; Hong et al., 2005; Lundby et al., 2007; Das et al., 2009). Two mutations that cause atrial fibrillation, S140G and V141M, are of interest to us because they are both located in the S1 transmembrane region of KCNQ1 and have little or no effect on I_{Ks} channel function unless KCNQ1 is co-assembled with the beta subunit, KCNE1. This will be the subject of Chapter II of the current investigation.

In the study by Chen et al, a missense mutation in KCNQ1, S140G, was identified in 16 members of a single family (Chen et al., 2003c). This group characterized this mutation in a heterologous system and showed that co-expression of KCNQ1 S140G assembled with KCNE1 resulted in constituitively open channels, which exhibited instantaneous activation in response to membrane depolarization. They conclude that the S140G mutation causes a shortened action potential because of the increased outward K^+ current due to the slow closing of channels, which in turn, was driving the membrane potential back to the resting membrane potential more quickly, thus shortening the repolarization phase of the atrial action potential. Another report of a point

mutation associated with AF, V141M, was studied a few years later (Hong et al., 2005). Here, a case of AF and short QT syndrome was diagnosed *in utero*. The functional phenotype of the V141M mutation, co-assembled with KCNE1, produced channels similar to that which was described for channels containing the S140G mutation, exhibiting voltage-independent currents. However, recently, it was shown that both of these mutations are in fact, not voltage-independent, but actually exhibit extremely slow deactivation kinetics, so that it requires a longer time course for the channels to close (Restier et al., 2008). Further examination of these mutant channels show that the instantaneous current seen previously (Chen et al., 2003c; Hong et al., 2005), was due to the accumulation of open channels caused by incomplete deactivation between depolarizing pulses due to mutation-altered channel deactivation kinetics. In the study by Lundby et al, the functional consequences of point mutation, Q147R, in KCNQ1 was characterized, in which a patient exhibited AF and QT prolongation (Lundby et al., 2007). Q147R was found to cause loss-of-function when co-expressed with KCNE1 and gain-of-function when co-expressed with KCNE2. This group hypothesized that depending on the distribution of KCNE1 and KCNE2 subunits in the heart, the Q147R mutation in KCNQ1 could offer an explanation for AF and prolonged QT interval in the same patient. In Das et al, the S209P mutation located in the S3 domain of KCNQ1 mutation was characterized (Das et al., 2009). Compared to the wild-type KCNQ1/KCNE1 channel, the S209P mutant activates more rapidly, deactivates more slowly, and exhibits a hyperpolarizing shift in the voltage dependence of activation. What is interesting about all these AF-associated mutations is that all report that co-assembly with KCNE1 is needed to see mutation-altered changes in channel function.

Other physiological roles of KCNQ1

KCNQ1 is expressed mainly in the heart, but also in the kidney, intestine, pancreas, and the inner ear (Yang et al., 1997b). A KCNQ1 knockout mouse study reported that in KCNQ1 -/- mice, no cardiac abnormalities were observed, but they exhibited deafness, cochlear disruption and gastric hyperplasia (Lee et al., 2000). This study illustrates that KCNQ1 is important in the inner ear, and that loss-of-function in this gene can lead to Jervell-Lange Nielson syndrome (JLNS), which is associated with deafness and QT prolongation.

KCNQ1 in the inner ear

In the ear, endolymphatic fluid produced by the stria vascularis surrounds the sensory hair cells of the cochlea and has a high concentration of potassium and a low concentration of sodium. I_{Ks} channels are necessary to maintain the high resting potential of +100 mV of the inner ear (Tyson et al., 1997). Mutations in either subunit of the I_{Ks} channel can lead to JLNS-associated deafness due to the absence of K^+ secretion into the endolymph of the scala media of the inner ear (Neyroud et al., 1997; Schulze-Bahr et al., 1997; Drici et al., 1998). Complete homozygous functional loss of the pore-forming KCNQ1 subunit can lead to enough K^+ depletion to cause deafness.

KCNQ1 in the colon

In the intestine, KCNQ1 assembles with KCNE3 and is co-localized in crypt cells to form constituitively conducting channels (Schroeder et al., 2000). They report that KCNQ1/KCNE3 channels may form the potassium channel that is important for cyclic AMP-stimulated intestinal chloride secretion, which could be important in treating secretory diarrhea and cystic fibrosis. More recently, it was reported that KCNQ1 also assembles with KCNE2 in the stomach to

control gastric acid secretion (Dedek and Waldegger, 2001). One group shows that targeted deletion of the KCNE2 subunit gene ablates gastric acid secretion and predisposes mice to gastric neoplasia (Roepke et al., 2010). They report that there is a balance between KCNE2 and KCNE3 and that if KCNE2 is depleted in gastric cells, KCNE3 is upregulated and vice versa. They indicate that KCNQ1 cannot function in the absence of both KCNE2 and KCNE3 in gastric parietal cells.

Voltage-gated K^+ Channels

Voltage-gated ion channels are membrane embedded pore-forming proteins that help establish and control the voltage gradient across the plasma membrane of cells by allowing the flow of ions down their electrochemical gradient. They are activated by changes in electrical potential difference near the channel. They are present in the membranes of many different cell types and are especially important in neurons and cardiomyocytes.

Voltage gated K^+ channels represent the most diverse family of ion channels in the heart and are the targets of several anti-arrhythmic drugs that help prolong the action potential duration (Tamargo et al., 2004). The first voltage gated K^+ channel was successfully cloned from *Drosophila* and is currently known as the *Shaker* channel (Jan and Jan, 1997). Flies displayed abnormal leg shaking in response to ether exposure and they seemed to be missing a K^+ current in their leg and flight muscles, so it was postulated that the defect was due to a K^+ channel gene. This was the starting point of the investigations that led to the discovery of the diverse family of K^+ channels we know of today. The K^+ channel family is diverse due to the wide range of hetero-tetramers that can be formed utilizing different subunits from within the same K^+ channel family. This diversification is even more increased due to their ability to co-assemble with non-pore forming accessory beta subunits, also known as the KCNE proteins.

KCNQ1 belongs to the classical voltage-gated potassium channel family, consisting of 676 amino acids, which forms six membrane-spanning domains, including the pore region (Figure 1-1). This main K^+ channel pore-forming protein is translated from a single gene, but the channel is made up of four separate subunits, which come together in the membrane to form functional channels (MacKinnon, 1991; Papazian, 1999). To date, there are five known members of the KCNQ1 family (KCNQ1 – 5). KCNQ proteins contain six TM domains, in which S1-S4 make up the voltage-sensing domain (VSD) and S5-S6 constitute a single pore-domain. All KCNQ proteins have six positively charged amino acids in the S4 domain located at every 3rd residue, except for KCNQ1, which only has four charges. Membrane depolarization causes a physical outward movement of S4, which induces further conformational changes that open the channel to allow K^+ permeation. The p-loop contains the pore signature sequence, (TxTTx)GYG, that dictates K^+ selectivity, and is now considered the K^+ selectivity signature motif (MacKinnon, 1995).

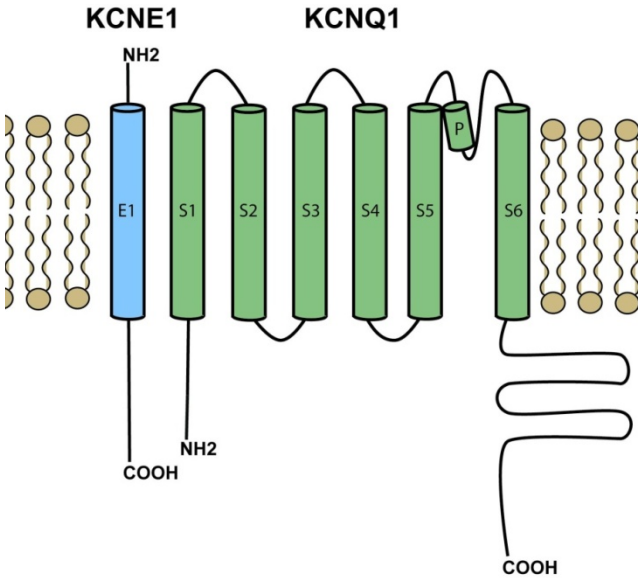

Figure 1-1. **KCNQ1 and KCNE1 comprise the I_{Ks} channel.** (A) Schematic of KCNE1 (blue) and KCNQ1 (green).

KCNE1, on the other hand, is a single membrane-spanning protein of only 129 amino acids (Figure 1-1). There are five members of the KCNE family (KCNE1-5), in which KCNE1 is the founding member of this family and subsequently, KCNE2-KCNE5 were discovered by homology searching using databases (Takumi et al., 1988; Abbott et al., 1999; Piccini et al., 1999). The KCNQ1 channel is unique in that it can be modulated by all 5 KCNE1 proteins. KCNE2, aside from associating with the hERG channel to form I_{Kr}, the rapidly activating inward rectifier current, also assembles with KCNQ1 to form a voltage-independent channel (Tinel et al., 2000). KCNE2 co-assembly with KCNQ1 leads to currents with an apparently instantaneous activation, a rapid deactivation process; and a linear current±voltage relationship. In addition to the gating effects, there was a decrease in the amplitude of the outward current (Tinel et al., 2000). Aside from the heart, there is evidence demonstrating that KCNE2/KCNQ1 channels are expressed in the stomach and may play a role in gastric acide secretion and gastric cancer cell proliferation (Roepke et al., 2010). Similarly, KCNE3 associates with KCNQ1 to form a constituitively open channel, important for gastric K^+ secretion (Schroeder et al., 2000). KCNE4 is an inhibitor of KCNQ1 channel activity (Grunnet et al., 2002). To date, the function of the KCNE5 protein has not been established, but functional studies show that KCNE5 induces both a time- and voltage-dependent modulation of the KCNQ1 current. Interaction of the KCNQ1 channel with KCNE5 shifts the voltage activation curve of KCNQ1 by more than 140 mV in the positive direction (Angelo et al., 2002).

Functional Characteristics of KCNQ1/KCNE1

The I_{Ks} channel is formed by co-assembly of KCNQ1 and KCNE1 (Barhanin et al., 1996; Sanguinetti et al., 1996). The biophysical properties of the KCNQ1 current are dramatically

altered when this subunit associates with KCNE1 (Figure 1-2). In the presence of KCNE1, there is an increase in current amplitude, a slow onset of activation, a depolarizing shift in the voltage dependence of activation, an increase in the single channel conductance, and removal of inactivation. I_{Ks}has a linear current voltage relationship, in contrast to the KCNQ1 current alone.

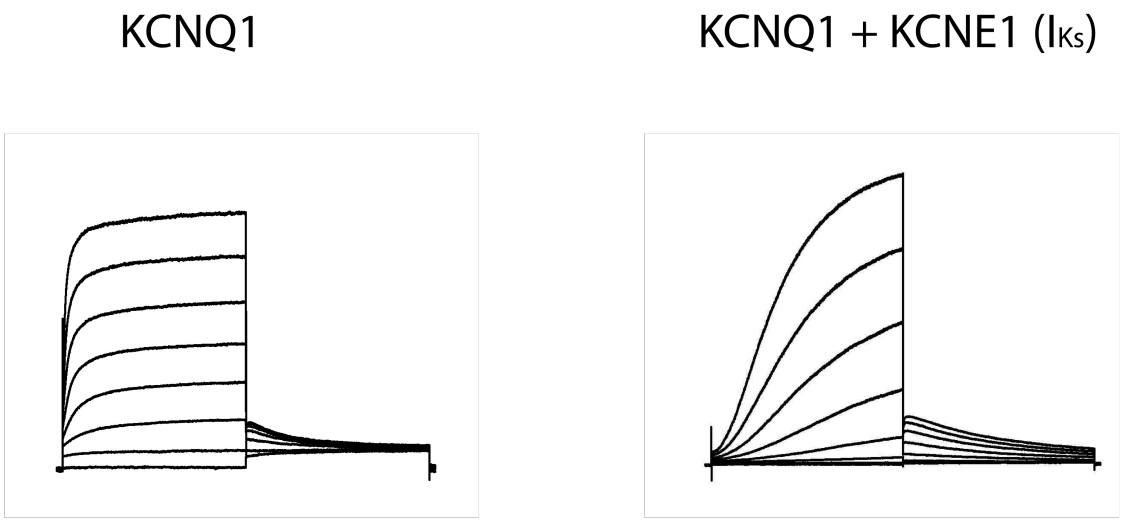

Figure 1-2. **KCNE1 co-assembly with KCNQ1 dramatically alters channel biophysical properties.** Family of current traces for KCNQ1 (A) and KCNQ1 + KCNE1 (B). Cells were depolarized from -40 mV to +80 mV in 20 mV increments for 2 s and then repolarized to -40 mV for 2 s. Interpulse holding potential was -80 mV.

KCNQ1 subunits can form functional channels on their own. These homomultimeric channels are characterized by their rapidly activating currents, reaching full activation within 1 second (Sanguinetti et al., 1996; Yang et al., 1997b; Wang et al., 1998) and undergoing inactivation during depolarization. An inactivation hook can be seen in recordings as a hook in the tail currents, which is produced because the rate of recovery from inactivation is faster than deactivation, thus what we see are channels opening upon repolarization followed by a very slow rate of deactivation (Pusch et al., 1998; Tristani-Firouzi and Sanguinetti, 1998). The extent of inactivation can be quantified by measuring these inactivation hooks.

The mechanism of how KCNE1 modulates KCNQ1 is unclear. Many studies have been done to determine points of contact between KCNE1 and KCNQ1 (Haitin et al., 2008; Shamgar et al., 2008; Xu et al., 2008; Chung et al., 2009; Lvov et al., 2010; Zheng et al., 2010). There is evidence showing that the transmembrane region of KCNE1 interacts with the KCNQ1 pore to regulate channel activity (Tapper and George, 2000; Melman et al., 2004) and that the C-terminus controls deactivation kinetics (Takumi et al., 1991; Tapper and George, 2000; Chen et al., 2009). These findings will be reviewed in more detail as they are important in the current investigation in trying to understand and determine a unifying mechanism for KCNE1 modulation of KCNQ1 channels.

Regulation of I_{Ks}

The sympathetic nervous system is responsible for up- and down-regulating many homeostatic mechanisms in living organisms, including increasing the rate and force of contraction in the heart. Cardiovascular diseases, such as hypertension and heart failure, are often associated with sympathetic nervous system (SNS) overactivity. Conversely, exercise has been shown to reduce hypertension and decrease elevated SNS activity.

SNS stimulation leads to activation of beta-adrenergic receptors, which results in protein kinase A (PKA) - mediated phosphorylation of I_{Ks} channels. The functional regulation of the I_{Ks} channel by PKA requires the A kinase-anchoring protein (AKAP) Yotiao (Marx et al., 2002). Yotiao forms a macromolecular complex with the channel and recruits key enzymes such as PKA and protein phosphatase 1 (PP1) to control the phosphorylation state of I_{Ks}. Voltage-gated K^+ channels do not exist only as independent proteins responding to changes in the transmembrane potential, but as macromolecular complexes that are able to integrate a wide range of cellular signals which can fine tune channel activities (Marx et al., 2002).

Structural Characteristics of I_{Ks}

The question of how KCNE1 modulates KCNQ1 has been a question concerning investigators since it was first discovered that this accessory subunit assembles with KCNQ1 to recapitulate the cardiac I_{Ks} current (Barhanin et al., 1996; Sanguinetti et al., 1996). Although there are many hypotheses on this subject, there is no unifying answer as to how this accessory subunit is able to cause such dramatic changes on channel function. However, the following review will summarize many of the studies attempting to address the mechanism of KCNE1 modulation, including studies involving stoichiometry, structural models, and structure-function studies of KCNE1/KCNQ1 interactions.

Stoichiometry

It was determined 20 years ago that voltage-gated K^+ channels are comprised of a tetramer of alpha subunits that come together to form a single ion conduction pore (MacKinnon, 1991). During this time, it was still being debated whether KCNE1 was the only subunit in the I_{Ks} channel complex, so the initial studies were not the best, but they helped us understand how to address the question of stoichiometry. Wang and Goldstein first attempted to determine the stoichiometry of KCNE1 in the channel complex (Wang and Goldstein, 1995). This group used various ratios of KCNE1 mutants (D77N) co-expressed with wild-type KCNE1, which produced non-conducting channels. They concluded that there are two functional KCNE1 subunits in each channel based on binomial distribution analysis. Another study determined that there were at least 14 KCNE1 subunits in each channel (Tzounopoulos et al., 1995). However, their investigation was flawed due to their use of a KCNE1 mutant (S69A) expressed with wild-type

KCNE1, which caused variable expression. Their error is possibly a result of not controlling for the changes in current amplitude with this particular mutant.

After it was discovered that KCNQ1 assembles with KCNE1 to constitute the I_{Ks} channel complex (Barhanin et al., 1996; Sanguinetti et al., 1996), many groups started to investigate the number of KCNE1 subunits that could associate with the tetrameric KCNQ1 channel. I_{Ks} gating kinetics are affected by the amount of KCNE1 cRNA that is injected into *Xenopus* oocytes (Blumenthal and Kaczmarek, 1994), so it is likely that the assembly and stoichiometry of KCNE1 and KCNQ1 subunits is important in determining how these subunits come together to exhibit the slow activating I_{Ks} current. The Kass lab addressed this question by using tandem constructs, forcing a fixed stoichiometry of either 1:1 or 2:1 ratios of KCNQ1 to KCNE1 subunits (Wang et al., 1998). Using the 1:1 fusion protein, where one KCNE1 subunit is linked to one KCNQ1 subunit, (named mK24 for minK K^+ channel 2,400 base pairs), they find that it exhibits current identical to I_{Ks}. In addition, they find that channels formed by the mK24 constructs can be further modulated by co-expression of additional KCNE1 protein. For the 2:1 fusion protein, two KCNQ1s linked to one KCNE1, they again observe currents similar to I_{Ks}. These results suggest that since KCNE1 is able to modulate the mK24 fusion protein, there is the possibility of multiple stoichiometries when this channel is expressed at the cell surface membrane.

The Goldstein group revisited the stoichiometry question in 2003, where they came to the conclusion that the ratio of KCNQ1:KCNE1 in the channel complex was 4:2, consistent with their original finding. Using a charybdotoxin (CTX) sensitive KCNQ1 construct, they assess KCNE1 stoichiometry in I_{Ks} channels using biophysical and biochemical techniques. CTX is a useful probe of K^+ channels because it binds with one-to-one stoichiometry to occlude the ion

conduction pore (Miller et al., 1985; MacKinnon and Miller, 1988; Goldstein and Miller, 1993). They observe that CTX block of KCNQ1/KCNE1 channels formed from a fixed 2:1 stoichiometric construct (two KCNQ1s and one KCNE1) matched the inhibition from channels formed from KCNQ1 and KCNE1 co-expression, whereas constructs formed from a 1:1 construct (one KCNE1 and one KCNQ1) did not exhibit similar block. Using biochemical methods, they used a monoclonal antibody to quantify radiolabled CTX channels formed from either 2:1 or 1:1 tandem constructs on the cell surface. They confirmed with these experiments that they believe the stoichiometry to be 4:2. However, the idea of multiple stoichiometries was not ruled out in this investigation because they were using fixed constructs.

A study done by the Kobertz group reports a 4:2 KCNQ1:KCNE1 stoichiometry in *Xenopus* oocytes (Morin and Kobertz, 2007, 2008). They use a modified CTX sensitive KCNQ1 construct and were able to count individual KCNE1 subunits in the channel complexes. They modify CTX to specifically react with cysteine residues in the N-termini of KCNE1 subunits. In addition, they modify CTX to become a cysteine reactive inhibitor by engineering a maleimide group to the CTX mutant (CTX-Mal). Maleimide groups protect cysteines because they form an irreversible thioether bond with the cysteine and make it stable to reducing agents. In these experiments, they use an iterative subunit counting approach, where they apply CTX-Mal to the channels, in which the maleimide group should react with an N-terminal cysteine residue on KCNE1. From this reaction, the KCNE1 cysteine residue is permanently modified and is prevented from reacting with subsequent CTX-Mal treatments. At this point, the CTX block is irreversible until the CTX-Mal is washed out and the maleimide group is cleaved off of CTX with a reducing agent (TCEP). The whole cycle is repeated until the CTX block becomes completely reversible with washout. With this method, they were able to determine the

stoichiometry to be 4:2. However, they performed their functional experiments at a voltage (+20 mV), which did not allow all channels to be open. The $V_{1/2}$ of activation for I_{Ks} channels is 7.5 ± 0.9 mV (Sanguinetti et al., 1996), so at +20 mV, all available channels are not open yet, so without fully activating all channels, it is hard to say whether all the channels are fixed in this 4:2 ratio. In addition, they injected only a single KCNQ1/KCNE1 injection ratio so it is possible that at this one particular ratio, only a 4:2 stoichiometry is feasible, but with other ratios, there could be variable stoichiometries.

The most recent investigation concerning the stoichiometry of KCNQ1/KCNE1 was published by the Isacoff group (Nakajo et al., 2010). In this study, the authors present the finding that the stoichiometry of the KCNQ1 and KCNE1 complex is variable, ranging from 4:1 to 4:4, in which up to 4 KCNE1 subunits can associate with the KCNQ1 tetramer. They say that the stoichiometry is dependent on the expression densities of KCNQ1 and KCNE1. Total Internal Reflection Fluoresence (TIRF) is used to observe the fluorescence of a single molecule to count individual KCNE1 subunits in the KCNQ1 complexes. In this study, they counted bleaching steps of fluorescently tagged KCNE1 proteins and were thus able to count the number of subunits in each complex. When the tagged KCNE1 was co-expressed with KCNQ1, they observed a large number of complexes with three or four bleaching steps, indicating that more than two KCNE1 subunits could assemble with the channel complex. They also tested a fusion protein with two KCNQ1s linked to one KCNE1, thus a forced 4:2 stoichiometry and found this complex could be further modulated with additional KCNE1 protein, but the fusion protein with one KCNQ1 and one KCNE1 could not be further modulated, indicating that 4 is the maximal number of KCNE1 subunits that can associate with the KCNQ1 tetramer.

Structural models

Structural information about a protein provides a foundation for interpreting current functional and biochemical studies and provides a road map for future studies. To date, there is no crystal structure of the I_{Ks} channel due to technical limitations (Van Horn et al., 2011). However, many K_v channels have been successfully expressed and purified for crystallization and we have been able to generate testable hypotheses using these models and apply them to the I_{Ks} channel.

The first crystal structure of a potassium channel was KcsA and although this channel is a two membrane-spanning K^+ channel, its amino acid sequence is actually very similar to those of eukaryotic six membrane-spanning K^+ channels. In particular, its sequence in the pore region, located between the membrane-spanning segments and containing the K^+ channel signature selectivity sequence, is almost identical to that found in the Drosophila *Shaker* and vertebrate voltage-gated K^+ channels, (Doyle et al., 1998). Mackinnon's group went on to reach a number of important conclusions about the architecture of the potassium channel using site-directed mutagenesis, electrical measurements, and crystallization techniques. They crystallize the bacterial K^+ channel, K_vAP (Jiang et al., 2003a) and the first mammalian K_v channel, K_v1.2, which is a member of the *Shaker* K^+ channel family (Long et al., 2005a). From the latter study, this group was able to determine the structural basis of voltage sensing and gating, which involves an electromechanical coupling of the S4 voltage sensor to the pore through the S4-S5 linker. This linker constricts or dilates the pore in order to open and close the channel. However, at this point, these K^+ channel structures only reflect the channel in the open states because of the absence of a hyperpolarized electrical potential during crystallization, so a closed state model of a K^+ channel is yet to be determined. Yet, there have been several structural models based on

biophysical and structure-function studies that have allowed us to speculate on the closed states of the K^+ channel (Smith et al., 2007).

To study the KCNQ1 channel, the $K_v1.2$ open state crystal structure was used as a template for homology modeling (Figure 1-3) (Smith et al., 2007). In the initial study of $K_v1.2$, the electron density for specific regions of the channel, including the loops connecting S1-S2, S2-S3, and S3-S4 and the voltage sensor, were weak. In order to fill in the gaps of the $K_v1.2$ template, Rosetta software was used and an ensemble of possible structures was generated to help predict a model for the entire channel. A closed state model of KCNQ1 was also generated based on previous closed state models of $K_v1.2$ (Yarov-Yarovoy et al., 2006). From this KCNQ1 structural model, Smith and colleagues predicted a location for KCNE1, hypothesizing that KCNE1 could sit in an intersubunit cleft, involving the S1-S3 segments in the KCNQ1 channel. Interestingly, this cleft is associated with many known gain-of-function (gof) disease mutations, which have been reported to depend on KCNE1 (Chen et al., 2003c; Hong et al., 2005; Lundby et al., 2007). They offer an explanation for how these gof mutations could stabilize the open state in the presence of KCNE1.

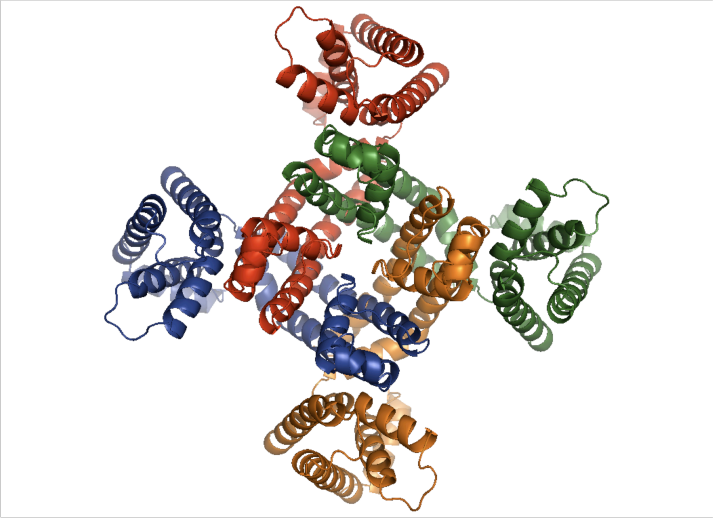

Model from Smith, *et al*. *Biochemistry,* **46**, 14141 -14152 (2007).

Figure 1-3. **Extracellular view of KCNQ1 Tetramer.**

Following the KCNQ1 model, the Sanders group published another study where they incorporate KCNE1 into the channel complex, based on the known functional and biochemical studies at the time (Kang et al., 2008). They dock KCNE1 to KCNQ1, showing that the extracellular end of KCNE1 forms an interface with the upper regions of S1, S5, and S6 of three different KCNQ1 subunits in the open state. They also generate a closed state model, where they suggest that KCNE1 sits on and restricts movement of the S4-S5 linker, the element that connects the voltage sensor to the gate. They conclude that, the point of contact between KCNE1 and the S4-S5 linker, is an adhesive interaction that must be overcome in order to transition from the closed to open states, offering an explanation for the slow activation of I_{Ks} (Kang et al., 2008).

The structure of KCNE1 was studied by a number of groups using solution nuclear magnetic resonance (NMR) methods. NMR spectroscopy and scanning mutagenesis studies indicate that the TMD of KCNE1 (residues 44-67) adopt an alpha helical structure (Aggeli et al.,

1998; Chen and Goldstein, 2007; Tian et al., 2007b). Aggeli and Yang performed NMR studies of a 27-residue stretch (42-68) of the TM domain of this protein. The NMR studies established that the TMD residues have an R-helical conformation, the helix being looser near the N-termini and more stable in the central region of the molecule (Aggeli et al., 1998). In another study, KCNE1 was overexpressed in *E. coli* and purified. KCNE1 was then reconstituted in detergent micelle solutions and injected into *Xenopus* oocytes. Several concerns with this technique are whether KCNE1 is correctly folded in these micelles and whether they could associate with and modulate KCNQ1 channels. However, this group successfully performed NMR experiments with these KCNE1 micelles and concluded that the KCNE1 TMD (residues 45-71) includes several alpha helices, at which there is a break in helicity at residues 59-61 and that the distal C-terminus (107-129) is disordered (Tian et al., 2007a). Chen and Goldstein perform serial perturbation analysis on the first 23 residues of the TMD of KCNE1 (44-66), by substituting residues with tryptophan (hydrophobic), asparagine (polar uncharged) and arginines (polar charged) and characterizing the resultant functional changes. Their results suggest the presence of different secondary structures within the transmembrane domain of KCNE1. In agreement with previous studies, they also conclude that there is a break in helicity in the mid TMD around residue 56. Their results suggest that the proximal region of the KCNE1 TMD (residues 44-55) is alpha helical and sits at the lipid-protein boundary and that the distal portion (residues 56-66) interacts within the channel center, coming close to the ion conduction pathway, in agreement with this groups previous investigations into the location of KCNE1 (Goldstein and Miller, 1991; Wang et al., 1996a; Sesti et al., 2000; Chen et al., 2003b).

The Kobertz group investigated the secondary structure of the C-terminus of KCNE1 (Rocheleau et al., 2006). Using alanine and leucine scanning mutagenesis, they observed two

classes of KCNE1 mutants, which were segregated into those that had high or low impact changes on gating properties. They conclude that the cytoplasmic C-terminus of KCNE1 is a kinked alpha helix and is broken into two segments by a proline residue (P77).

KCNE1 proteins have two well conserved *N* –linked glycosylation sites, N5 and N26, indicating that KCNE1 can be differentially glycosylated and can exist in immature or mature forms. In one study, Chandrasekhar et al. demonstrates that the majority of KCNE1 proteins localize to the endoplasmic reticulum (ER) when expressed alone in mammalian cells and thus exist in the immature form (Chandrasekhar et al., 2006). However, coassembly of KCNE1 proteins with KCNQ1 channel subunits promotes KCNE1 protein trafficking to the cell surface. Subsequently, glycosylation of KCNE1 will occur at the cell surface and the mature form of KCNE1 will be expressed, producing functional KCNQ1/ KCNE1 channels.

Structure Function Studies

The structural mechanisms by which KCNE1 modulates K^+ channels are important in determining their roles in human physiology and cardiac related diseases. There have been a number of investigations addressing the question of KCNE1 modulation, which will be reviewed here, including the location of KCNE1 in the channel complex, the sites of interaction between KCNQ1 and KCNE1, and the role of these possible sites of interaction.

Studies on KCNE1

Location in the I_{Ks} channel complex

For many years, there was considerable controversy concerning whether KCNE1 lined the inside of the ion conduction pathway or was located outside of the pore. Investigators used

cysteine scanning mutagenesis studies or pore-blocking drugs to determine the location of the TMD of KCNE1 within the KCNQ1 channel complex. Drugs, such as tetraethylammonium (TEA), was used in functional studies because it blocked K^+ channel pores (MacKinnon and Yellen, 1990; Yellen et al., 1991). One group observed that prior treatment of TEA to channels slowed methanethiosulfate-ethylsulfonate (MTSES) blockade with cysteine mutations in KCNE1 (Wang et al., 1996a). MTSES reagents normally react with exposed cysteines (Akabas et al., 1992; Kurz et al., 1995; Pascual et al., 1995) and the Wang group argued that these reagents could not react with the KCNE1 cysteine mutations because TEA was already blocking the channel pore. Therefore, they concluded that KCNE1 must be located in the pore. Another group came to the same conclusion that KCNE1 lines the pore by studying cysteine mutations in KCNE1 and using the thiol reactive transition metal, cadmium (Cd^{2+}), to monitor accessibility. Mutated KCNE1 residues in the TMD (F54C, G55C) exhibited Cd^{2+} blockade, so they hypothesized that this could only happen if Cd^{2+} was binding in and occluding the pore. The mutation at G55C also altered ion selectivity in the channel, so they concluded that KCNE1 must lie in the pathway of ion conduction (Tai and Goldstein, 1998). However, this group neglected the presence of a native cysteine, 331, in the KCNQ1 pore. So what they saw in their results was due to Cd^{2+} block in the pore, but it was likely due to the native cysteine residue that was actually located in the pore, and not in KCNE1.

Other studies show that KCNE proteins lie outside of the conduction pathway. Studies by Tapper and George recognized that the cysteine residue in the pore, C331, was responsible for Cd^{2+} sensitivity and that KCNE1 does not lie in the permeation pathway of the channel (Tapper and George, 2001). Kurokawa and Kass Lab colleagues studied TEA-sensitive KCNQ1 mutants (K318I, V319Y) and argued that blockade of the channel by TEA does not affect the

accessibility of KCNE1 residue 54 and 55 to external cadmium (Kurokawa et al., 2001). The Kass Lab showed that engineering a TEA sensitive site into pore region did not affect TEA sensitivity, in the absence or presence of KCNE1. When these TEA-sensitive constructs were co-expressed with cysteine substituted KCNE1 constructs, G55C and F54C, the channel showed increased sensitivity to Cd^{2+}, indicating there was a pore-independent mechanism of block by Cd^{2+}. Currently, the location of KCNE1 is generally accepted to be peripheral to the KCNQ1 channel as evidenced by KCNE1/KCNQ1 structural models (Kang et al., 2008).

Recently, there have been many investigations trying to determine the specific interactions between KCNE1 and KCNQ1. Two groups show that KCNE1 makes contacts with KCNQ1 in their extracellular loops by monitoring spontaneous disulfide formation between various cysteine substitutions in both subunits (Xu et al., 2008; Chung et al., 2009). Chung and colleagues establish the location of KCNE1 to be situated between S1 and S6 of opposing KCNQ1 subunits.

These studies demonstrate that we have a general idea of where KCNE1 is located within the channel complex, in the periphery of the channel complex, with proximity to the S1 domain of one subunit and the S6 domain of another subunit. However, KCNE1 must associate with KCNQ1 in a specific manner in order to modulate gating and current amplitude, thus it is important to identify where KCNE1 is interacting with KCNQ1. These KCNQ1/KCNE1 interactions may involve one or many subregions of KCNE1 in order for modulation to occur, which will be reviewed shortly.

N-terminus

Although, the role of the N-terminus of KCNE1 has been implicated in affecting pH sensitivity of KCNQ1 assembled channels (Peretz et al., 2002; Heitzmann et al., 2007) and

involved in determining stoichiometry of the assembled channel (Chen et al., 2003b; Morin and Kobertz, 2008), the KCNE1 N-terminus has not been studied in terms of modulation of the KCNQ1 channel. Stilbenes and fenamates, small molecule activators of the I_{Ks} channel complex, were found to be dependent on the KCNE1 amino terminus for their pharmacological effect (Abitbol et al., 1999). Mutation or deletion of residues 39-42 in the N-terminus abolish these activators effects and suggest that this region of KCNE1 may be involved in interactions with KCNQ1.

Transmembrane domain (TMD)

The importance of the KCNE1 transmembrane domain (TMD) in terms of KCNQ1 modulation remains unresolved. One group engineered synthetic peptides that included just the TM domain of KCNE1 and expressed them with KCNQ1 channels (Aggeli et al., 1998). However, these channels exhibited fast activating currents reminiscient of KCNQ1 channels expressed alone, indicating that the TMD alone cannot control modulatory activity of the channel. On the other hand, Melman and colleagues published a series of studies, emphasizing the importance of the TMD of KCNE1 and its role in controlling activation properties of the KCNQ1 channel. They studied modulation of KCNQ1 by KCNE1 and KCNE3, where they generated chimeras of KCNE1 and KCNE3, and swapped the TMD residues 57-59 in KCNE1 (FTL) with the equivalent residues 71-73 in KCNE3 (TVG) (Melman et al., 2001). They demonstrated that these three TMD residues in both KCNE1 and KCNE3 were responsible for conferring activation properties when co-assembled with the KCNQ1 channel. In this study, when KCNQ1 was co-assembled with KCNE1 chimera containing residues TVG, they observed a constituitively open channel, reminiscient of KCNQ1/KCNE3 channels (Schroeder et al., 2000). Conversely when KCNQ1 was expressed with KCNE3 containing FTL residues, they saw a

slowly activating channel, typical of a KCNQ1/KCNE1 channel (Barhanin et al., 1996; Sanguinetti et al., 1996). In further studies, the same group named this stretch of amino acids the "activation triplet" and identified that a single residue was sufficient to confer the changes in activation kinetics, Thr 58 for KCNE1 and Val 72 for KCNE3 (Melman et al., 2002).

C-terminus

There are many studies investigating the importance of the C-terminus of KCNE1 and its modulatory role with KCNQ1 channels. One group engineered synthetic peptides from the carboxy terminal region (aa 67-93) of KCNE1 and injected these peptides into *Xenopus* oocytes. The resultant channels exhibited I_{Ks}-like currents, indicating that this region was sufficient for potassium channel activity (Ben-Efraim et al., 1996). However, these studies relied upon the modulation of an endogenous oocyte K^+ channel (Sanguinetti et al., 1996). It is possible that more than one region of KCNE1 is necessary for modulation of KCNQ1 channels.

In 1991, Takumi was the first to demonstrate that both the TMD and C-terminus of KCNE1 was important for potassium channel activity. Using deletion and truncation mutants, they measured channel activity of the resultant mutant combinations and found both were important for channel activity (Takumi et al., 1991). Tapper and George demonstrate that the TMD of KCNE1 is important for KCNQ1 association, but it is the C-terminus that is necessary for channel activity (Tapper and George, 2000). Co-expression of KCNQ1 with a KCNE1 C-terminal deletion mutant resulted in rapidly activating potassium current resembling currents from channels assembled with only KCNQ1, indicating an important modulatory role for the C-terminus region of KCNE1. As a control, they needed to verify that KCNE1 was associating with the channel, so they engineer a G55C mutation, located in the TMD, which confers

susceptibility to cadmium block. Currents recorded from KCNQ1 and the KCNE1 G55C /C-terminal deletion mutant exhibited cadmium block, indicating that KCNE1 is associated with the channel, but perhaps the C-terminus is needed to control channel activity. To determine which regions of KCNE1 were necessary for both association and modulation, this group created chimeras between KCNE1 and a Na^+ channel beta1 subunit. They concluded that both the TMD and the C-terminus of KCNE1 are necessary for modulation and that the C-terminus alone is not sufficient for modulating channel activity, contrary to previous reports (Ben-Efraim et al., 1996). However, the Melman group would argue the opposite, that the TMD is important for modulatory activity and that the C-terminus anchors and positions the KCNE1 subunit into the channel (Melman et al., 2001). In 2004, the Kobertz group set out to determine whether the TMD or C-terminus was responsible for modulation with the KCNQ1 channel, using chimeras of KCNE3 and KCNE1 (Gage and Kobertz, 2004). For KCNE3, they find that the TMD was sufficient for assembly and modulation because the activation triplet, actively modulated KCNQ1 activation, in agreement with the results from Melman's group. However, for KCNE1, they find that the equivalent activation triplet in TMD of KCNE1 is passive, and that the KCNE1 C-terminal domain is the region that controls gating.

More recent work on the I_{Ks} channel has focused primarily on the importance of the C-terminus in altering deactivation properties of the channel. The MacDonald group suggests that the KCNE1 C-terminus may be involved in modulating KCNQ1 channel deactivation and be important for assembly (Chen et al., 2009). This group analyzed the effects of the C-terminal mutant, D76N, and truncation of the entire C-terminus on channel function and assembly. They observed that truncation of the C-terminus reduced the association of KCNE1 to KCNQ1 channels, resulting in less channels expressed at the surface, as evidenced by a western blot

showing that the KCNE1 with the C-terminus deleted does not produce fully mature KCNE1 protein. Functional studies of channels assembled with KCNQ1 and KCNE1 with the C-terminus deleted, reduced current density and shifted the voltage dependence in the depolarizing direction. They conclude that there are several roles of the C-terminus of KCNE1 with KCNQ1 channel function, including channel assembly and control of deactivation kinetics. Thus far, it is likely that both the TMD and C-terminus of KCNE1 are necessary for its modulatory properties with the KCNQ1 channel.

There are several groups who have characterized specific interactions of the C-terminus of KCNE1 and different regions of the KCNQ1 channel. The Romey group first reported that the C-terminus, but not any other region of KCNE1, physically interacts with the pore-loop of KCNQ1 using a yeast two-hybrid screen (Romey et al., 1997). Haitin et al uses fluorescence resonance energy transfer (FRET) to show that the KCNQ1 C-terminal helix C tetramerization domain interacts with the C-terminus of KCNE1 (Haitin et al., 2008). Lvov et al finds that the C-terminus of KCNE1 interacts with S6 and the S4-S5 linker using cysteine crosslinking (Lvov et al., 2010). Zheng et al characterizes a physical interaction between the intracellular C-termini of both KCNE1 and KCNQ1 (Zheng et al., 2010). Using deletion mutants of both the KCNQ1 and KCNE1 C-termini and co-immunoprecipitation methods, they indicate that the KCNE1 C-terminus binds to a region of KCNQ1 just after the S6 TM segment but before the tetramerization domain. The tetramerization domain of KCNQ channels is located in the distal portion of the C-terminus (Howard et al., 2007; Wiener et al., 2008).

There have been studies investigating other roles of the C-terminus of KCNE1 besides modulation of KCNQ1. Rochealeau and Kobertz published a study that supports a protein-protein interaction with the C-termini of KCNE1/KCNQ1 (Rocheleau et al., 2006). Using

alanine and leucine scanning mutagenesis, they functionally observe two classes of KCNE1 mutants, which are segregated into those that had high or low impact changes on gating properties. Based on the functional data, they conclude that the cytoplasmic C-terminus of KCNE1 is a kinked alpha helix and is broken into two segments by a proline residue (P77). In accordance with previous crystal structures of voltage gated K^+ channels, the high impact face of KCNE1 is involved in protein-protein interactions with the voltage-sensing domain (Jiang et al., 2003a; Jiang et al., 2003b; Long et al., 2005b). These results provide a structural region in which studies involving KCNQ1 gating and intracellular regulation can be investigated. Studies investigating regulation of I_{Ks} channel function support an important role for the C-terminus of KCNE1. Mutations in the cytoplasmic domain of KCNE1 have also been shown to disrupt PKA mediated modulation of the KCNQ1 channel (Kurokawa et al., 2003; Kurokawa et al., 2009). The C-terminus also has effects in channel trafficking and recycling (Seebohm et al., 2007; Xu et al., 2009).

Current working model of KCNE1 modulation of KCNQ1

In the closed state, the S4-S5 linker interacts with the C-terminal end of S6 from another subunit to lock it in closed conformation, while the N-terminal end makes contacts between the voltage sensor and pore domains. The Sanders group speculates that KCNE1 slows channel activation by interacting with and restricting the movement of the S4-S5 linker, when the channel opens (Kang et al., 2008).

Studies on KCNQ1

S6 (Pore)

The process by which voltage-gated ion channels open in response to changes in membrane potential is activation. The activation gate is the key element that physically opens and closes the ion conduction pathway. In KCNQ1 channels, the S5-S6 helices make up the pore domain in one subunit, and it is essential that four subunits come together to form a single ion permeation pathway. Interactions between KCNE1 and the S6 domain of KCNQ1, which constitutes part of the pore region, are not surprising. Due to the unique properties that are exhibited when KCNE1 associates with KCNQ1, including slowing activation kinetics, it is likely that KCNE1 would have a physical interaction with the activation gate in order to slow opening. The discovery of the crystal structure of KcsA provided much of the initial information about the position and nature of the gate, since this channel consists of only two domains, which constitute the pore region (Doyle et al., 1998).

Several interactions between KCNE1 and the S6 domain of KCNQ1 have been identified. Studies from our group and others demonstrate that the extracellular residues flanking the TM region of the S6 domain (V324C) form spontaneous crosslinks with KCNE1 residue (L42C) (Xu et al., 2008; Chung et al., 2009). Melman et al. showed that KCNE1 TMD residues 57-59 interact with S6 KCNQ1 residues 338-340, using electrophysiological and biochemical methods (Melman et al., 2001; Melman et al., 2002). In another study, an interaction between TMD of KCNE1 and S6 segment KCNQ1 was identified (Tapper and George, 2001). They found that Cd^{2+} coordinated two cysteines, L51C in KCNE1 and I328C in S6 KCNQ1. In addition, a prediction of the KCNE1 helix showed that other residues exhibit proximity: TMD residues on KCNE1 (F54 and G55) are close to the pore domain of KCNQ1 (Cys331) (Tapper and George, 2001). The yeast two-hybrid studies by Romey et al also support a KCNE1/ S6 KCNQ1 interaction (Romey et al., 1997). The Melman group continued their studies on KCNE1

regulation of KCNQ1 channel gating by determining sites of interaction between the two subunits (Melman et al., 2004). They generated chimeras of KCNQ1 and K^+ channels that do not associate with KCNE1. Using co-immunoprecipitation studies, they concluded that KCNE1 binds to the S6 segment of the pore to mediate control of gating. Using tryptophan scanning mutagenesis and functional studies, Panaghie and Abbot confirm Melman's results and conclude that a point of interaction exists between the TMD of KCNE1 (T58) and the S6 pore domain of KCNQ1 (F340) (Panaghie et al., 2006). Although many putative interaction points have been identified between KCNE1 and the S6 domain of KCNQ1, a crystal structure of this complex channel would be helpful in defining an interface between the KCNE1 and the KCNQ1 subunits.

S4 (Voltage Sensor)

The mechanism by which voltage-gated channels detect changes in membrane potential and translate this to the activation gate to open the channel is the subject of many investigations. The $K_V1.2$ structure provides detailed information about the organization of the voltage-sensing domain (VSD), consisting of S1-S4 helices, and how it surrounds the pore (Long et al., 2005a). The gate is controlled by the S4 voltage sensor, which contains charges, known as gating charges, that move when the membrane electric field changes. There are roughly four to eight positively charged residues, mostly arginines, located at every third position in the S4 helix. When the gating charges move across the electric field, due to changes in membrane voltage, they generate an electric current called gating current. This gating current is a useful readout for voltage sensor movement.

Some investigators believe that these voltage-sensing arginines face the hydrophobic core of the lipid bilayer (Jiang et al., 2003b), while others believe they face a polar protein crevice (Ahern and Horn, 2004; Durell et al., 2004; Bezanilla, 2005). Others showed that the S4

arginines could interact with negatively charged residues in other VSD helices (Papazian et al., 1995; Tiwari-Woodruff et al., 2000). There are three models of voltage sensing that have been proposed in the past decade, in which the transporter model and the helical screw model argue that the arginines are protein exposed, while the paddle model argues that the argnines are lipid exposed. In the transporter model, the S4 helix rotates and tilts as it moves from one crevice to another, totaling a movement of 2-3 Å across the membrane. In the helical screw model, the S4 helix rotates and translocates along its axis, while moving its gating charges across the electric field upon depolarization, with a net movement of 5-13 Å. In the paddle model, S4 and the extracellular part of S3 (S3b) form a helical hairpin, or paddle. In the resting state, the paddle is located deep in the membrane almost in contact with the intracellular solution, and upon depolarization, the paddle makes a net movement of 15-20 Å across the membrane to the extracellular side. In a more recent study, a group solved the crystal structure of a 'paddle chimaera model', which includes the voltage sensor paddle from $K_V2.1$ transferred into $K_V1.2$ (Long et al., 2007). They conclude from the crystal structure that one entire face of the paddle is exposed to lipid membrane. Although there are many theories supporting that the lipid environment surrounds the voltage sensor, the matter remains is still to be determined.

There have been studies investigating how KCNE1 affect the kinetics of S4 voltage sensor movement and equilibration rate. State dependent accessibility studies using MTS reagents have previously been used to assess movement S4 segment in several voltage gated channels (Larsson et al., 1996; Yang et al., 1997a; Bell et al., 2004; Vemana et al., 2004). There is biochemical evidence showing a physical interaction with one of the arginines in S4 (A226C) KCNQ1 and an extracellular residue on KCNE1, E44C (Nakajo and Kubo, 2007). However, the investigators neglected to mutate out a native cysteine, located at position 136, in the S1 domain.

Their results may not reflect a true physical interaction between the S4 segment and KCNE1 because the results could be mixed with crosslinking between S1 (C136) and KCNE1 (E44C), which is a possibility (Xu et al., 2008; Chung et al., 2009). However, the Nakajo and Kubo group also demonstrate that in the presence of KCNE1, MTSET modification rates for S4 cysteine mutants were 10 fold slower in the presence of KCNE1 vs. in the absence of KCNE1, indicating that S4 movement is slow and that S4 is responsible for the slow gating kinetics of the I_{Ks} channel. However, Rochealeau and Kobertz perform a study to address voltage sensor equilibrium and rates in K^+ channels in response to Nakajo and Kubo's study (Rocheleau and Kobertz, 2008). They find that MTSET modification rates for the S4 cysteine mutants were independent of depolarization pulse duration. They find that upon depolarization, the voltage sensors reach equilibrium quickly in the presence of KCNE1 and conclude that the slow gating of the channel complex is not due to slow moving voltage sensors, but could be due to the cytoplasmic domain of KCNE1 slowing gate opening. It is undetermined whether the modulatory effects of KCNE1 on the voltage sensor or the activation gate is through a direct or allosteric mechanism, but these studies suggest KCNE1 involvement may be through an allosteric mechanism.

Panaghie and Abbott performed an alanine scan of S4 and came across two findings: they find that there is charge paucity in the carboxy end of the S4 segment and that the KCNQ1 activation gate is coupled to S4 in KCNQ1/KCNE3 channels (Panaghie and Abbott, 2007). They compared the effective charge on KCNQ1 and homologous K^+ channels and found that KCNQ1 had the least amount of positive S4 charge. They added arginine to two sites on KCNQ1 and found that they could convert originally constitutive KCNQ1/KCNE3 channels to non-constitutive channels. They did the converse to KCNQ4/KCNE3 channels. KCNQ4 has two

extra arginines than KCNQ1 and when they removed these two C-terminal arginines, they found that non-constitutive KCNQ4/KCNE3 channels converted to constituitive channels. Thus, charge paucity in C-terminal region of S4 is responsible for unique gating properties of KCNQ1 and KCNE1.

More recently, there have been studies monitoring voltage sensor movement of the KCNQ1 channel. In a recent study from our group, voltage clamp fluorometry studies showed that the presence of KCNE1 alters voltage sensor movement that is necessary to open the channel gate (Osteen et al., 2010). When KCNE1 is present, multiple voltage sensors must move before the channel can open. In the absence of KCNE1, there are two possibilities, either all four KCNQ1 voltage sensors move at the same time to allow the transition to the fully open state or the four KCNQ1 voltage sensors move independently but the KCNQ1 channel transitions to the fully open state through a series of sub-conductance states.

S1

There has been interest in the S1 domain of KCNQ1 because of it is the location of several gain-of-function mutations (Chen et al., 2003c; Hong et al., 2005; Lundby et al., 2007). Following the publication of the initial KCNQ1 structural models, several groups published results investigating interactions between KCNE1 and the S1 domain of KCNQ1 (Xu et al., 2008; Chung et al., 2009). In Xu et al, they show that KCNE1 makes different contacts with KCNQ1 in the open and closed states using cysteine crosslinking and functional measurements. The authors conclude that these state dependent contacts are caused by a rotation of KCNE1 as the KCNQ1 channel opens and that KCNE1 is located between S1, S4 and S6 of three different KCNQ1 subunits. However, their functional experiments may be flawed because the pseudo wild-type KCNQ1 construct that they use clearly has slowed deactivation kinetics compared with

wild-type KCNQ1. So it is likely that their state dependent experiments are unclear due to the fact that the construct they use exhibits slow deactivation kinetics, thus allowing the channel to be stabilized in the open state. In the study by Chung and colleagues, we monitored spontaneous disulfide formation between cysteine-substituted residues in the extracellular flanking regions of KCNE1 and KCNQ1. Our group positions KCNE1 between the S1 and S6 domains of opposing KCNQ1 subunits (Chung et al., 2009).

Haitin and colleagues investigate a role for the S1 domain in steering S4 voltage sensor movement during channel gating (Haitin et al., 2008). They substitute cysteines in S4 residues (S225, I227, R228) and monitor channel currents in *Xenopus* oocytes. They find that there are several intra and inter subunit interactions, namely between voltage sensors of two different subunits (I227C-I227C) and also between cysteines substituted at S4 (R228C) residues and S1 (C136) residues within one subunit.

Restier and colleagues demonstrate that two KCNQ1 gof mutant (S140G and V141M) channels close when held at hyperpolarized voltages for extended periods of time, indicating a defect in deactivation of the channel (Restier et al., 2008). A salt bridge mechanism was used to explain how these mutant channels become trapped in the open state either due to stabilization of an open state salt bridge or slowing the formation of a closed state salt bridge between the S2 and S4 domains in the KCNQ1 channel. Although this mechanism is one possibility for how these mutant channels become trapped in the open state, the mechanism of how KCNE1 is involved in these salt bridge interactions and how it is involved in slowing the deactivation process in the presence of these KCNQ1 mutations, remains unresolved.

There are several studies suggesting that the S1 domain is involved in channel gating. In one study, Lee and colleagues propose that there are two interfaces involved in the gating of K_V

channels, one which involves the S4-S5 linker that guides voltage sensor movement directly to channel opening and closing, and the other involves S1 of the voltage sensor and the pore-loop helix near the extracellular surface. They postulate that this 2nd interface acts as an anchor point to allow effective communication between the voltage sensor and gate (Lee et al., 2009). They use disulfide cross-linking to find proximity between S1 and the pore-loop, and specifically a cross-link between T47C and V183C in K_vAP was found (Lee et al., 2009). Although these residues are in a bacterial K^+ channel, they correspond to residues Thr144 in S1 and Tyr299 in the Pore-loop of K_v7.1. If Thr144 (S1 Q1) and Tyr 299 (Pore-loop) residues crosslink in the Q1 channel, it would support a role for S1 in constraining the pore region in order to control gating. These interactions between S1 and the pore region are also implicated in the KCNQ1 structural models (Smith et al., 2007). The KCNQ1 structural model predicts an interface between S1 and S5/p-loop regions of two adjacent subunits in the open state. This interface includes four of five known gain of function mutations in KCNQ1: S140G and V141M in S1, I274V in S5, A300T in the p-loop helix (the fifth mutation is V307I, not included in interface). This group hypothesizes that the interface helps to stabilize the open state and could help explain the mutation-induced changes in channel function.

Although there is evidence indicating that existence of many interactions between KCNE1 and KCNQ1, the mechanism of KCNE1 modulation is still unclear. By determining the positioning of KCNE1 in the channel complex, we can use this information to determine the stoichiometry of the KCNQ1 and KCNQ1 subunits, the binding sites of KCNE1, and eventually the mechanism of how KCNE1 modulates gating of the I_{Ks} channel.

METHODS

Molecular biology and cell culture

Human KCNE1 (Murai et al., 1989) was subcloned into the p3XFLAG-CMV-14 Expression Vector (Sigma-Aldrich E4901, St. Louis, MO) to generate a C-Terminal FLAG-tagged KCNE1. Human KCNQ1 (Sanguinetti et al., 1996) was subcloned into the pCDNA3.1 Expression Vector (Sigma). Pseudo wild-type KCNQ1 C136V / C214A / C331A (pWT) was generated for both functional and biochemical experiments. All mutations were engineered into pWT KCNQ1 and KCNE1 cDNA with the QuikChange Site-Directed mutagenesis kit (Agilent Technologies, Santa Clara, CA). Biochemical experiments were conducted with these constructs. Human KCNE1 with an N-terminal HA tag was used for functional studies. Chinese hamster ovary (CHO) cells (American Type Culture Collection, Manassas, VA) were cultured in Ham's F-12 culture media with 10% FBS in a 37°C incubator with 5% CO_2.

EQ and EQQ Tandem Constructs

EQ construct was engineered by linking the C-terminus of KCNE1 to the N-terminus of KCNQ1. EQQ construct was engineered by inserting an additional KCNQ1 subunit into the EQ construct. Cys substitutions were made in a pseudo-wild-type background (pWT: C214A, C331A) for the following EQ constructs: $E_{K41C}Q_{I145C}$; $E_{L42C}Q_{V324C}$ and EQQ constructs: $E_{K41C}Q_{I145C}Q$; $E_{K41C}QQ_{I145C}$; $E_{L42C}Q_{V324C}Q$. The human rhinovirus (HRV-3C) protease (Novagen) consensus cleavage site, LEVLFQGP, which is cleaved between the Q and G, was inserted into the C-terminus of KCNE1 to create a cleavage site between KCNE1 and KCNQ1.

Electrophysiology

CHO cells were transfected with wild-type (WT) or mutant KCNQ1 alone or co-transfected with WT or mutant KCNE1, and with eGFP (0.4 μg of each cDNA) and plated on 35 x 10 mm tissue culture dishes as previously described (Marx et al., 2002). Electrophysiological measurements were carried out 48h after transfection. Currents were recorded at 25°C using the whole-cell patch clamp configuration with an Axopatch 200A amplifier (Molecular Devices, Union City, CA) as previously described (Kurokawa et al., 2003). Series resistance was 2-3 MΩ. The physiological K^+ external solution contained (in mM): 132 NaCl, 4.8 KCl, 1.2 $MgCl_2$, 1 $CaCl_2$, 5 glucose, 10 HEPES, pH was adjusted to 7.4 with NaOH. Internal solution contained (in mM): 110 K^+ aspartate, 1 $MgCl_2$, 1 $CaCl_2$, 11 EGTA, 5 K_2ATP, 10 HEPES. Cells were chosen based on eGFP fluorescence.

As indicated in the text, in some experiments recordings were carried out in solutions containing elevated K^+ concentration (120 mM) to increase the driving force and allow resolution of deactivating tail currents over a broad range of negative voltages. The elevated K^+ external solution contained (in mM): 17.8 NaCl, 120 KCl, 1.2 $MgCl_2$, 1 $CaCl_2$, 5 glucose, 10 HEPES, pH was adjusted to 7.4 with NaOH. In all other experiments, recordings were carried out in a solution containing physiological K^+ concentration (5 mM).

Data Analysis

Data were collected using Clampex 8.0 (Molecular Devices, Union City, CA) and analyzed as described previously (Kurokawa et al., 2003) with Clampfit 8.0 (Molecular Devices) and Origin

7.0 (OriginLab Corp, Northampton, MA).Statistical data analysis was assessed with Student's *t* test; differences at $p < 0.05$ were considered to be significant.

Voltage Clamp Protocols

To record the conductance–voltage (G–*V*) relationship for I_{Ks}, cells were voltage clamped at a negative holding potential (−80, -100 mV, or −120 mV). Test potentials were applied to a series of isochronal activation voltages with a fixed incremental increase between successive pulses (e.g. −100 to +40 mV in 20 mV steps) for 2 s, and activation was determined from deactivating tail currents measured at voltages indicated in the text for specific experiments. The interval between test pulses was 15 or 20 s, as described in figure legends.

To compare activation kinetics for channels with differing voltage dependences, voltages were chosen where open probabilities were similar. Time to half activation ($t_{1/2}$) was measured during 2 s pulses, taken at the voltage closest to the $V_{1/2}$ acquired from the G-*V* relationship for each subunit combination. To calculate the $t_{1/2}$, the current at the beginning of the test pulse (I_o) was subtracted from the maximal outward current at the end of the pulse (I_{max}) and this value was divided by 2. The time (in seconds) corresponding to this calculated value is used as the $t_{1/2}$ value.

Kinetics of deactivating tail currents were analyzed using 2 s depolarizing steps to +20 mV triggered every 15 seconds from a holding potential of –100 mV and followed by 2 s repolarizing steps ranging from –80 to –120 mV (20-mV increments). I_{Ks} rate of deactivation (τ_{deact}) measured at –80mV, -100 mV, and -120 mV was obtained by fitting the tail current with a single exponential.

Crosslinking

The cross-linking procedure and the calculation of the cross-linking band have been described previously (Chung et al., 2009). CHO cells were co-transfected with mutant cDNAs of KCNQ1 C136V/C214A/C331A (pWT KCNQ1) and FLAG-KCNE1 (1.0 μg each) using PLUS reagent and Lipofectamine (Invitrogen, Carlsbad, CA). Cells were incubated for 48h at 37°C in the presence of 5% CO_2. Crosslinking occurred in the presence of ambient oxygen; no external oxidizing agents were added. The adherent cells were surface-biotinylated with EZ-Link Sulfo-NHS-LC-Biotin (Thermo Fisher Scientific, Waltham, MA), the reaction was stopped with glycine methyl ester, the cells were lysed, and, after sedimentation of insoluble material, the supernatant was mixed with Ultralink Immobilized NeutrAvidin Protein Plus beads (Thermo Fisher Scientific) to bind the biotin-labeled membrane proteins, which were eluted from the beads by treatment for 3 min at 90°C in 8 M Urea, 4% SDS, 200 mMTris pH 8.0, and 2 mM EDTA, all as previously described (Liu et al., 2008b). Dithiothreitol (DTT) to a final concentration of 20mM was added to half of each eluate. Samples were incubated at 50°C for 20 min, bromophenol blue was added, and the samples in SDS sample buffer were electrophoresed on 4–20% acrylamide gels. The gels were transferred to nitrocellulose, and the blot was blocked with Blocking Buffer for Near Infrared Fluorescent Western Blotting (Rockland Immunochemicals Inc, Gilbertsville, PA) and incubated with goat anti-KCNQ1 C-20 antibody (1:1000, Santa Cruz Biotechnology, Santa Cruz, CA) and mouse anti-FLAG M2 antibody (1:2000, Sigma-Aldrich, St. Louis, MO). Membranes were washed and incubated with donkey anti-goat AlexaFluor 680-labeled antibody (1:5000, Invitrogen, Carlsbad, CA) and donkey anti-mouse IRDye 800-labeled antibody (1:5000, LI-COR Biosciences, Lincoln, NE). Fluorescent signals were detected using the Odyssey Infrared Imager (LI-COR).

Crosslinking with EQ and EQQ Constructs

The cell lysate was mixed with Neutravidin-Sepharose beads (Pierce Chemical Co.) for 60 min at 4°C. In a typical sample, cell lysate from a 25 cm^2 flask in 500-µl lysis buffer was mixed with 60 µl of a 50% slurry of Neutravidin beads, previously washed and suspended in lysis buffer. The beads were washed seven times with lysis buffer (without NEM and protease inhibitors) and two additional times with HRV buffer (in mM, 150 NaCl, 50 Tris, pH 7.5, 1 EDTA, 0.5% Triton X-100). The beads were mixed with 5 U of HRV-3C protease (Novagen) in 50 µl HRV-3C buffer and nutated overnight at 4°C. To elute bound protein and fragments released by cleavage, we added 100 µl 8 M urea, 4% SDS, 200 mM Tris, pH 8, and heated the mixture to 90°C for 2 min. After a short spin, the supernatant was collected. A 30-µl portion was treated with 2 µl of 400 mM DTT to reduce disulfides. Both the unreduced and the reduced portions were electrophoresed, transferred to nitrocellulose, and immunoblotted by sequential treatment with anti-KCNQ1 antibody (Santa Cruz Biotechnologies) and mouse anti-FLAG M2 antibody (1:2000, Sigma-Aldrich, St. Louis, MO). Membranes were washed and incubated with donkey anti-goat AlexaFluor 680-labeled antibody (1:5000, Invitrogen, Carlsbad, CA) and donkey anti-mouse IRDye 800-labeled antibody (1:5000, LI-COR Biosciences, Lincoln, NE). Fluorescent signals were detected using the Odyssey Infrared Imager (LI-COR).

CHAPTER II

Characterization of KCNQ1 Atrial Fibrillation Mutations Reveals Distinct Dependence on KCNE1

Background and Significance

Several studies that report spontaneous crosslinking between substituted cysteine residues on KCNE1 and KCNQ1 have positioned KCNE1 between the first and sixth transmembrane helices (S1 and S6, respectively) of opposing KCNQ1 subunits, consistent with the current KCNQ1 structural model (Kang et al., 2008; Xu et al., 2008; Chung et al., 2009). In this segment of S1, two gain-of-function (gof) disease mutations associated with atrial fibrillation (AF), S140G and V141M, are located in adjacent residues. When KCNQ1 containing either AF-associated mutation in S1 (S140G or V141M) is co-expressed heterologously with KCNE1, the resultant channels activate immediately in response to depolarizing pulses applied from holding potentials similar to typical myocyte resting potentials (Chen et al., 2003c; Hong et al., 2005). Subsequent analysis has revealed that the instantaneous current is due to accumulation of open channels caused by incomplete deactivation between pulses at these holding potentials (Restier et al., 2008). To date, this channel property is believed to be manifested only in the presence of KCNE1 for both mutations (Restier et al., 2008).

Here, we explore the role(s) of KCNE1 in translating the effects of the KCNQ1 AF mutations S140G and V141M into pathological channel function by characterizing the mutations in the absence and presence of KCNE1. We have explored the structural proximity of KCNE1 relative to the two AF mutations located in S1 KCNQ1, using a biochemical assay to monitor disulfide bridge formation between introduced cysteines. Our results demonstrate that even

though both mutations exhibit extremely slow deactivation kinetics in the presence of KCNE1, they have distinct dependencies on this accessory subunit. The V141M mutation, but not S140G, requires co-assembly of KCNQ1 and KCNE1 to alter channel deactivation kinetics. The S140G mutation in the KCNQ1 channel itself is sufficient to dramatically slow the deactivation process. Biochemical evidence correlates function with structure, revealing orientation of the two subunit proteins such that on S1 KCNQ1, V141 but not S140 is positioned close to KCNE1, providing a structural basis for the distinct subunit dependence of channel function conferred by these two AF mutations.

Results

Part I – KCNQ1 AF Mutants (S140G and V141M) Depend Differently on KCNE1

Function of S140G and V141M in the absence of KCNE1

The functional effects of the S140G and V141M mutations were characterized in cells expressing only KCNQ1 channels. Because previous studies (Chen et al., 2003c; Bendahhou et al., 2005) have shown that tail currents for the S140G mutation are difficult to measure in physiological K^+ solution (5 mM), the following experiments were carried out in external solutions containing elevated K^+ concentration (120 mM, see Methods). This environment allowed the resolution of tail currents over a broader range of negative voltages. Control experiments (Figure 2-1) verified that elevated K^+ did not affect the voltage-dependence of KCNQ1 channel function compared with experiments in physiological K^+ solution. As had been shown for V141M channels in *Xenopus* oocytes (Hong et al., 2005), we confirm that channels encoded by V141M resemble WT KCNQ1 channels, both in voltage dependence of activation and deactivation kinetics (Figure 2-2A and 2-2C). However, the $V_{1/2}$ of activation for S140G

channels is significantly more negative than WT KCNQ1 channels, with a hyperpolarizing shift of -30 mV from WT KCNQ1 (Figure 2-2D). In addition, S140G channels exhibited significantly slower deactivation at -100 mV compared to both WT KCNQ1 and V141M channels (Figure 2-2E).

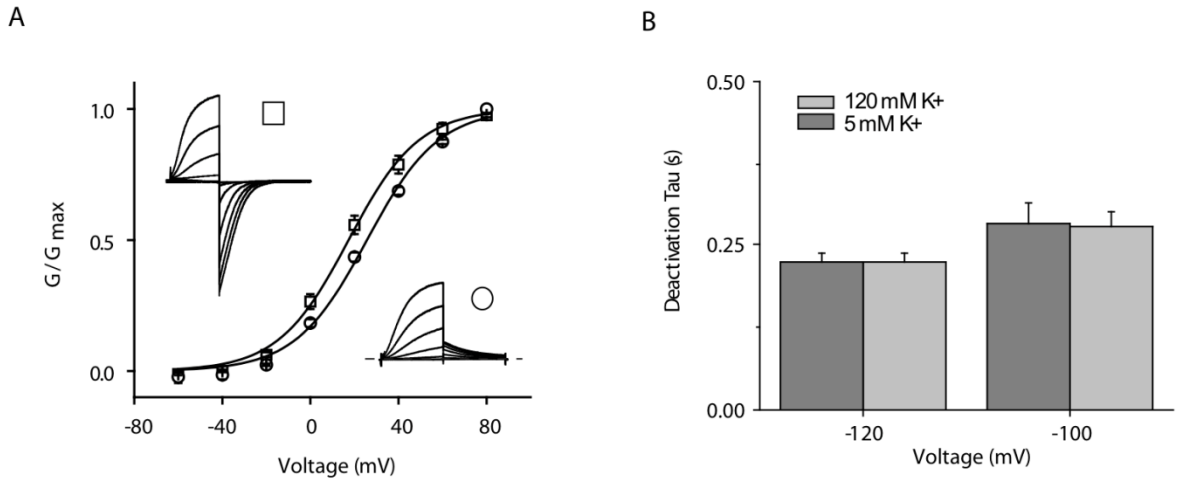

Figure 2-1. **Function of wild-type KCNQ1 and wild-type KCNE1 (120 mM K^+ vs. 5 mM K^+)** (A) G-*V* relationship and (B) Deactivation tau for KCNQ1/KCNE1 measured in 120 mM K^+ vs. 5 mM K^+ external solution. KCNQ1/KCNE1 (120 mM K^+): Holding potential = -120 mV. Cells were depolarized from -120 mV to + 80 mV in 20 mV increments. Tail currents were measured at -120 mV for 5 s (*left inset).* KCNQ1/KCNE1 (5 mM K^+): Holding potential = -80 mV. Test pulses were applied once every 11 seconds from -60 mV to +80 mV. Tail currents were measured at -40 mV for 2 s (*right inset)*.

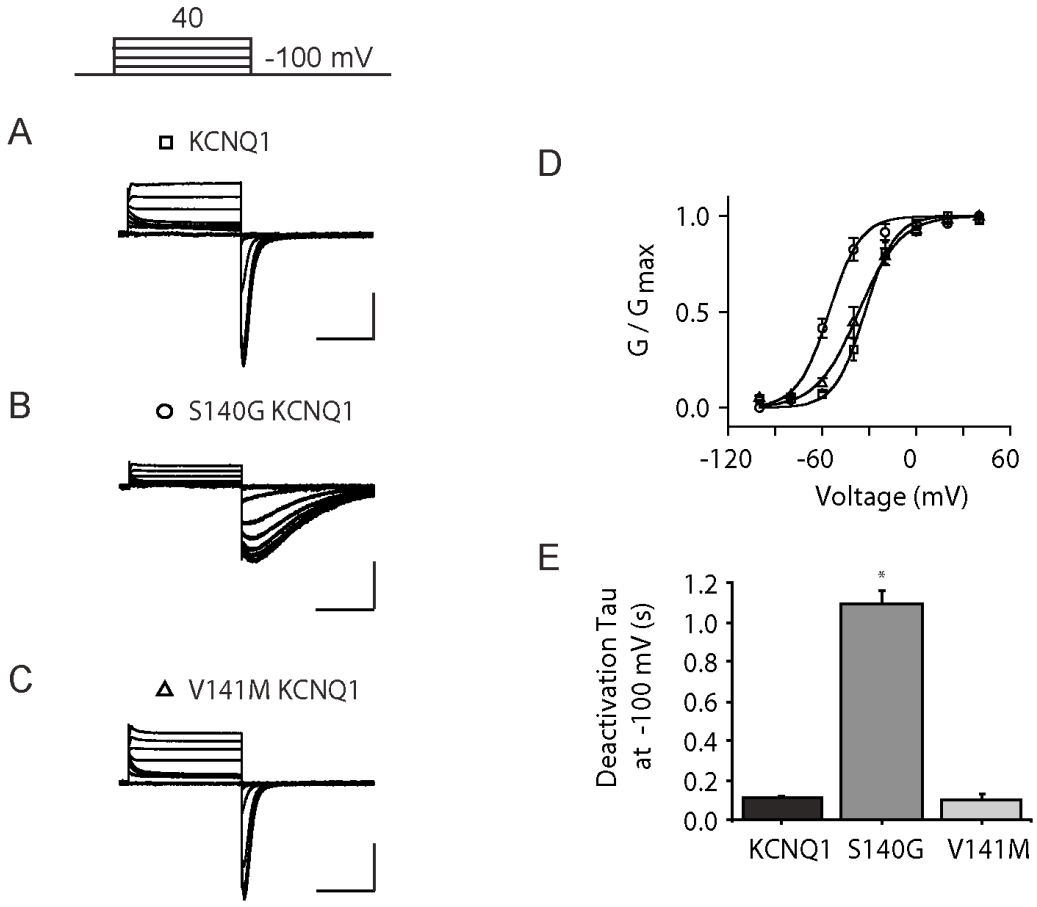

Figure 2-2. **S140G but not V141M slows deactivation of homomeric KCNQ1 channels.** Representative families of currents traces in cells expressing WT KCNQ1 (A), S140G (B), and V141M (C) in the absence of KCNE1. Currents in response to 2 s pulses from -100 mV to +40 mV in 20 mV increments from a -100 mV holding potential. (D) Normalized isochronal (2 s) activation curves for KCNQ1 (squares), S140G (circles), and V141M (triangles). (E) Deactivation time constant (tau) obtained at -100 mV from single exponential fits to tail currents following conditioning pulses (+20 mV, 2 sec). For all current traces of vertical scale is 50 pA/pF and horizontal scale is 1.0 s. Data are shown as mean ± s.e.m. * ($p < 0.05$)

Function of S140G and V141M in the presence of KCNE1

Activation Kinetics

The impact of KCNE1 co-expression on channel properties was investigated with KCNQ1 carrying either of these two AF-associated mutations. A pulse protocol consisting of 2-s isochronal activating pulses to +20 mV was applied at a very slow rate (once every 20 seconds) to ensure that the majority of channels were closed prior to the next test pulse as we measured the impact of KCNE1 co-expression on activation gating. Representative current traces for S140G and V141M, assembled with KCNE1, reveal channels that exhibit the slow onset of activation seen in WT I_{Ks} channels (Figure 2-3A to 2-3C). The voltages for half maximal (isochronal) activation for channels consisting of KCNE1 co-expressed with three KCNQ1 variants were measured to compare voltage dependence of activation gating. Both S140G / KCNE1 channels ($V_{1/2}$ = 1.5 ± 2.7 mV, *n*=4) and V141M / KCNE1 channels ($V_{1/2}$ = 2.4 ± 1.0 mV, *n*=3) exhibit hyperpolarizing shifts in voltage dependence, compared to WT KCNQ1 / KCNE1 channels ($V_{1/2}$ = 17.5 ± 2.6 mV, *n*=6) (Figure 2-3D). Next, I_{Ks} activation kinetics were compared by measuring the time ($t_{1/2}$) at which I_{Ks} current is half maximally activated at the voltage closest to the $V_{1/2}$ for each subunit combination. KCNE1 co-expression caused no significant change in activation kinetics of the S140G ($t_{1/2}$ = 1.5 ± 0.04 s, *n*=4) and V141M ($t_{1/2}$ = 1.45 ± 0.06 s, *n*=4) assembled channels ($p > 0.05$ for S140G / KCNE1 vs. V141M / KCNE1). Although activation kinetics of both S140G and V141M channels assembled with KCNE1 were statistically significant from KCNQ1/KCNE1 ($t_{1/2}$ = 1.15 ± 0.31 s, *n*=6) (Figure 2-3E), this was not important.

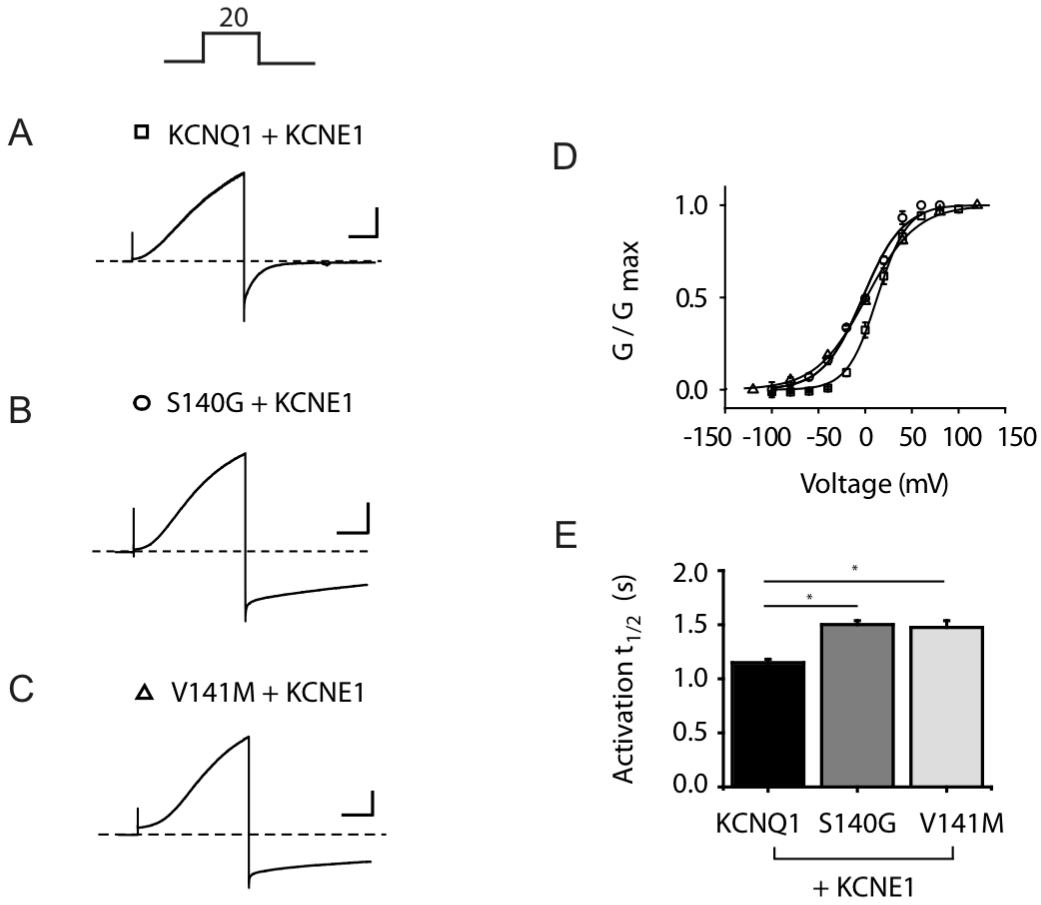

Figure 2-3. **S140G and V141M mutations minimally affect KCNQ1/KCNE1 activation kinetics.** Representative current traces are shown for KCNQ1 (A), S140G (B), and V141M (C), each co-expressed with KCNE1. Holding potential = -80 mV (KCNQ1) and -100 mV (S140G and V141M). Cells were pulsed to -120 mV (KCNQ1 and S140G) and -140 mV (V141M) to ensure that all channels were closed prior to the depolarizing pulse (+20 mV, 2 sec). (B) Normalized isochronal (2 s) activation curves for KCNQ1 (squares), S140G (circles), and V141M (triangles). (C) Activation $t_{1/2}$ for KCNQ1, S140G, and V141M. For all current traces: vertical scale is 100 pA/pF and horizontal scale is 0.5 s. Dotted lines indicate zero current. Data are shown as mean ± s.e.m. * ($p < 0.05$)

Deactivation Kinetics

Deactivation kinetics of the S140G and V141M mutant channels co-expressed with KCNE1 were subsequently investigated. To compare deactivation kinetics for the different KCNQ1/KCNE1 pairs, the deactivation time constants (tau) were measured from tail currents at -120 mV in response to a 2 s depolarizing pulse (Figure 2-4A and 2-4B). Deactivation for S140G / KCNE1 channels (τ_{deact} = 4.09 ± 0.23 s, n=5) is significantly slower than that for WT KCNQ1 / KCNE1 channels (τ_{deact}= 0.24 ± 4.2 s, n=6, $p < 0.05$ for S140G / KCNE1 vs. KCNQ1/ KCNE1). For V141M / KCNE1 channels, deactivation is significantly slower than both KCNQ1 and S140G assembled channels (τ_{deact} = 6.71 ± 0.64 s, n=4, $p < 0.05$ vs. KCNQ1 / KCNE1 and $p < 0.05$ vs. S140G / KCNE1) (Figure 2-4C).

Another way to evaluate the effect of KCNE1 on channel deactivation is to examine the fold change in deactivation of the KCNQ1 mutations in the absence and presence of KCNE1. The fold change is the ratio of deactivation tau from the KCNQ1 / KCNE1 subunit conditions: deactivation tau from the KCNQ1 subunit alone. These results are summarized in a log plot, showing deactivation at -120 mV for all KCNQ1 variants and KCNE1. KCNE1 co-expression on V141M subunits reveals a dramatic effect, slowing deactivation roughly fifty fold compared to KCNQ1/KCNE1 channels (V141M: 51.39 ± 5.57, n=8 and KCNQ1 = 2.74 ± 0.14, n=9) (Figure 2-4C). The fold change in deactivation for S140G / KCNE1 channels (S140G: 7.75 ± 0.99, n=9) is also significantly greater than that of WT KCNQ1/KCNE1 channels.

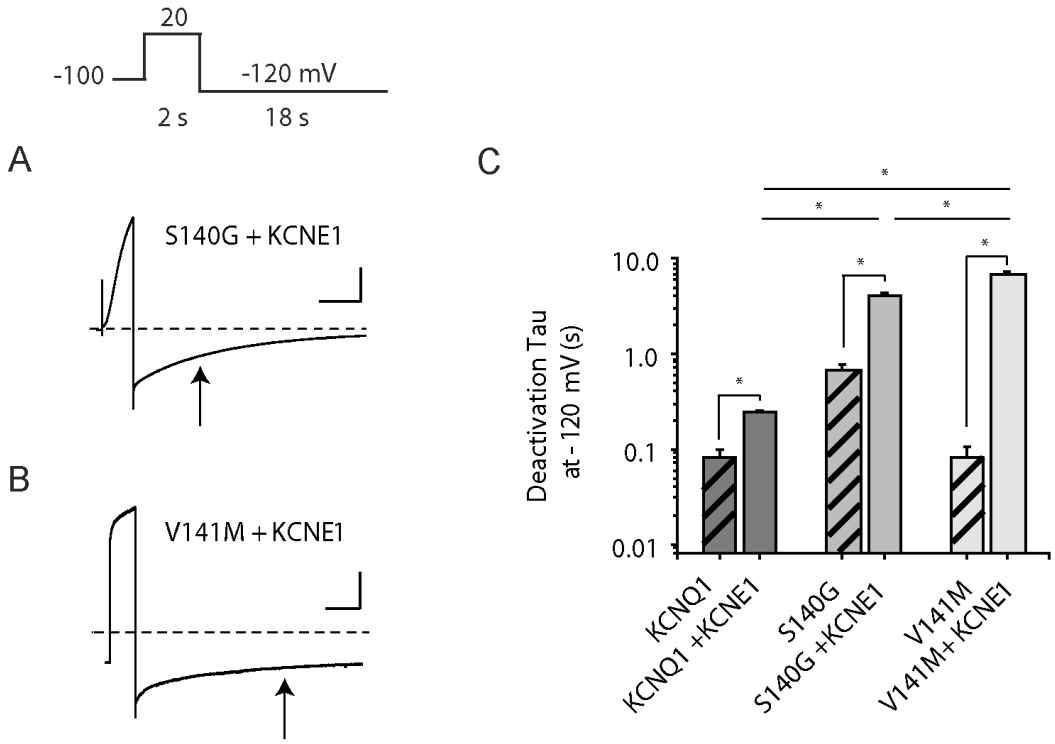

Figure 2-4. **KCNE1 slows deactivation of V141M heteromeric channels to a greater extent than S140G channels.** Representative current traces are shown for S140G (A) and V141M (B), each co-expressed with KCNE1. Arrows indicate the tau for each subunit combination. (C) Deactivation time constant (tau) at -120 mV is represented in a log plot for KCNQ1, S140G, and V141M, each co-expressed without and with KCNE1 (n = 4-9). Hatched bars represent KCNQ1, S140G, and V141M without KCNE1. For S140G/KCNE1 and V141M/KCNE1 current traces: vertical scale is 50 pA/pF and 100 pA/pF, respectively, and horizontal scale is 2.5 s. Dotted lines indicate zero current. Data are shown as mean ± s.e.m. * ($p < 0.05$)

Crosslinking of KCNQ1 (S140C or V141C) to KCNE1

The functional data suggest possible physical differences in the location of KCNQ1 residues S140 and V141 relative to KCNE1 in assembled channels. We thus sought to determine the proximity of S140 and V141 relative to KCNE1 at the level of the membrane interface by individually substituting cysteines in KCNQ1 and KCNE1 and monitoring spontaneous disulfide

bridge formation. These residues (S140 and V141) are located one turn into the helix of the S1 transmembrane domain and when mutated to cysteines, they are believed to be exposed to water, ready to deprotonate to the reactive thiolate form. Due to their proximity to the membrane, they are also subject to spontaneous oxidation in the endoplasmic reticulum or on the cell surface (Liu et al., 2008a).

Two KCNQ1 Cys-substituted mutants (S140C and V141C) and twelve KCNE1 Cys-subsituted mutants (G40C to L51C) were generated. S140C and V141C were made in a pseudo-wild-type (pWT) construct in which the three native cysteines in the transmembrane domain of KCNQ1 were mutated out: C136 was mutated to valine, while C214 and C331 were mutated to alanines. These mutations did not alter function significantly in the channel (Figure 2-5A and 2-5B). It was necessary for C136 to be mutated out in order to prevent crosslinking within the S1 domain to S140C or V141C (Figure 2-5C).

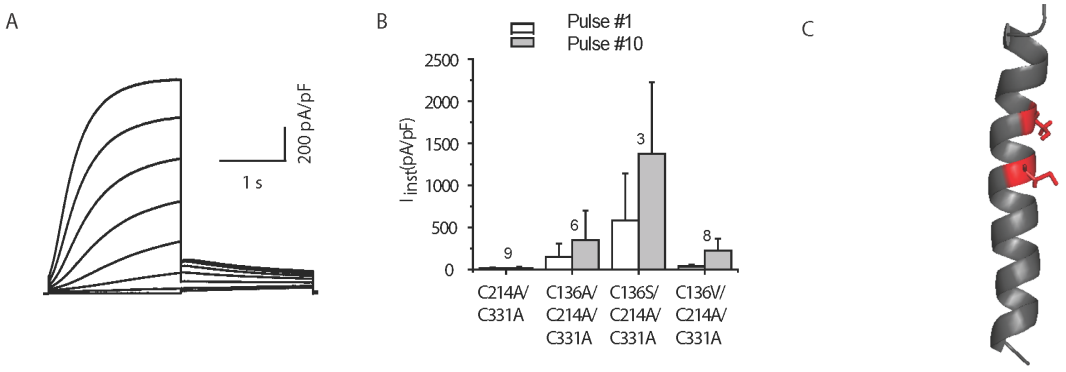

Figure 2-5. **Function of Pseudo-WT KCNQ1 (pWT).** (A) Family of current traces for pWT construct with mutations (C136V, C214A, C331A). (B) Plot of instantaneous current (pA/pF) measured from the first pulse (white bars) and the tenth pulse (gray bars) for various pWT constructs. Number of observations is noted above bars. (C) Schematic illustration of S1 KCNQ1 with residues C136 and S140 highlighted in red to demonstrate proximity within the helix.

The extent of crosslinking was calculated as follows: (KCNQ1/KCNE1 + X/2)/ (KCNQ1/KCNE1 + KCNQ1 + $KCNQ1_2$ + X). Calculations were based on the intensities of four bands: the monomeric KCNQ1 band (~74 kD), the crosslinked KCNQ1/KCNE1 band (~110 kD), the $KCNQ1_2$ band (KCNQ1 dimer ~150 kD), and a band labeled X (~250 kD) (Figure 2-6) (Chung et al., 2009). For each condition, averaged data are expressed as mean ± S.E. Statistical data analysis was assessed with Student's *t*-test: differences at $p < 0.05$ were considered to be significant.

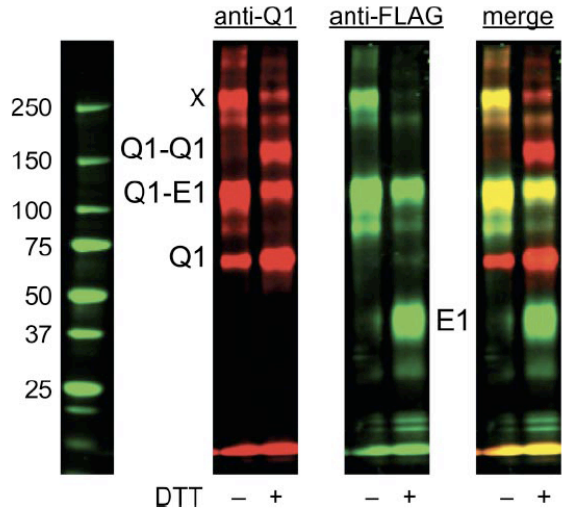

Figure 2-6. **Full Length Blot of Crosslinking Bands.**
KCNQ1 is represented as a red signal and KCNE1 as a green signal. The merged red and green in the cross-linked KCNQ1/KCNE1 band is yellow. The samples in the right lanes were reduced with DTT in sample buffer. X indicates a band of molecular weight greater than 250 kDa. The molecular weights of the markers are in kDa.

The KCNE1 residues were chosen for cysteine substitution due to their location in the region of KCNE1 predicted to be aligned with the region where S140 and V141 are located (Kang et al., 2008; Chung et al., 2009). The crosslinking percentage is plotted for the twenty-four

cysteine pairs tested (Figures 2-7B and 2-7C). Sample immunoblots are shown for crosslinking results obtained from S140C and V141C, in the absence and presence of a reducing agent, dithiothreitol (DTT). The extent of crosslinking is summarized for S140C and twelve KCNE1 Cys mutants, in which there is <10% disulfide bond formation (Figure 2-7B). This result suggests that S140 is not positioned towards KCNE1. However, this is not the case for V141. In this case, there is evidence of disulfide bond formation between V141C and two Cys mutants on KCNE1: E43C and A44C. V141C / E43C exhibited 35 ± 4.3% (n=5) crosslinking, while V141C / A44C exhibited 78 ± 2.4% (n=11) cross-linking (Figure 2-7C), which are comparable to the high degree of crosslinking that was found for the extracellular flanks between KCNE1 and the S1 and S6 domains of two KCNQ1 subunits (Chung et al., 2009). The extent of crosslinking is taken as a measure of relative proximity of the substituted cysteines (Liu et al., 2008a). These results are consistent with the predicted three-dimensional arrangement of the transmembrane helices of KCNQ1 and the placement of KCNE1 within the channel complex (Smith et al., 2007; Kang et al., 2008).

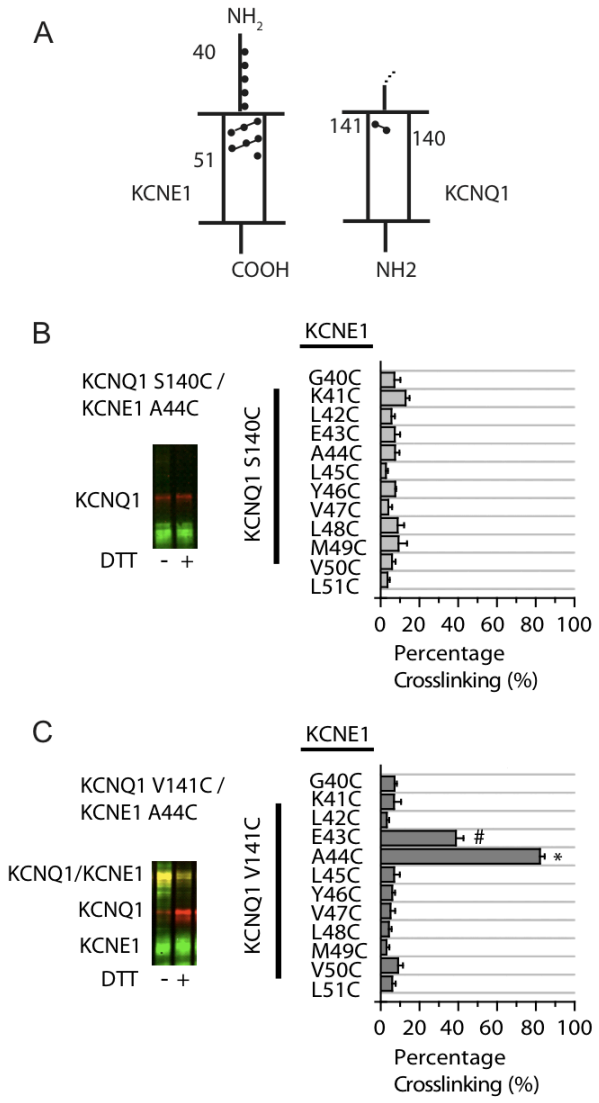

Figure 2-7. **Crosslinking of substituted cysteines in KCNQ1 and KCNE1 reveals orientation of S140 and V141 relative to KCNE1.** (A) Schematic illustration of S1 domain of KCNQ1 and KCNE1, indicating the region that was tested for cross-linking, as shown by green (KCNE1 residues) and red (KCNQ1 residues) dots. The numbers represent amino acid position. The dashed line above KCNQ1 indicates continuation of the channel. (B and C) Sample immunoblots are shown for the indicated pairs of Cys mutants of KCNQ1 and KCNE1. KCNQ1 is shown as a red signal and KCNE1 is shown as a green signal. The merged red and green signals indicate the crosslinked KCNQ1/KCNE1 band, which is shown as a yellow signal. The samples in the right lanes were reduced with 10 mM DTT in sample buffer. (B) Bar graph showing percentage of spontaneous crosslinking for S140C with KCNE1 residues G40-L51 (n = 3-6); (C) Bar graph showing percentage of spontaneous crosslinking for V141C with KCNE1 residues G40-L51 (n =

4-11). Calculations were based on the intensities of the bands, as described in Methods. Data are shown as mean ± s.e.m. Symbols (*, #) indicate a significant difference ($p < 0.05$) using Student's *t*-test.

Function of Single Cysteine Mutants

The functional characteristics of the single cysteine mutants were tested for the residues that exhibited crosslinking: V141C, A44C, and E43C. Substitution of a cysteine at position V141 did not alter activation but slowed deactivation, in agreement with previous oocyte recording (Restier et al., 2008) (Figure 2-8). The KCNE1 mutations at positions 43 and 44 did not alter channel function on their own, in the absence and presence of DTT. However, in the presence of DTT, there is a depolarizing shift in voltage dependence of activation for all single cysteine mutants, consistent with the effect of DTT alone in the pseudo WT channel (Chung et al., 2009). Further, the presence of DTT did not significantly alter deactivation time constants for all the single cysteine mutants tested.

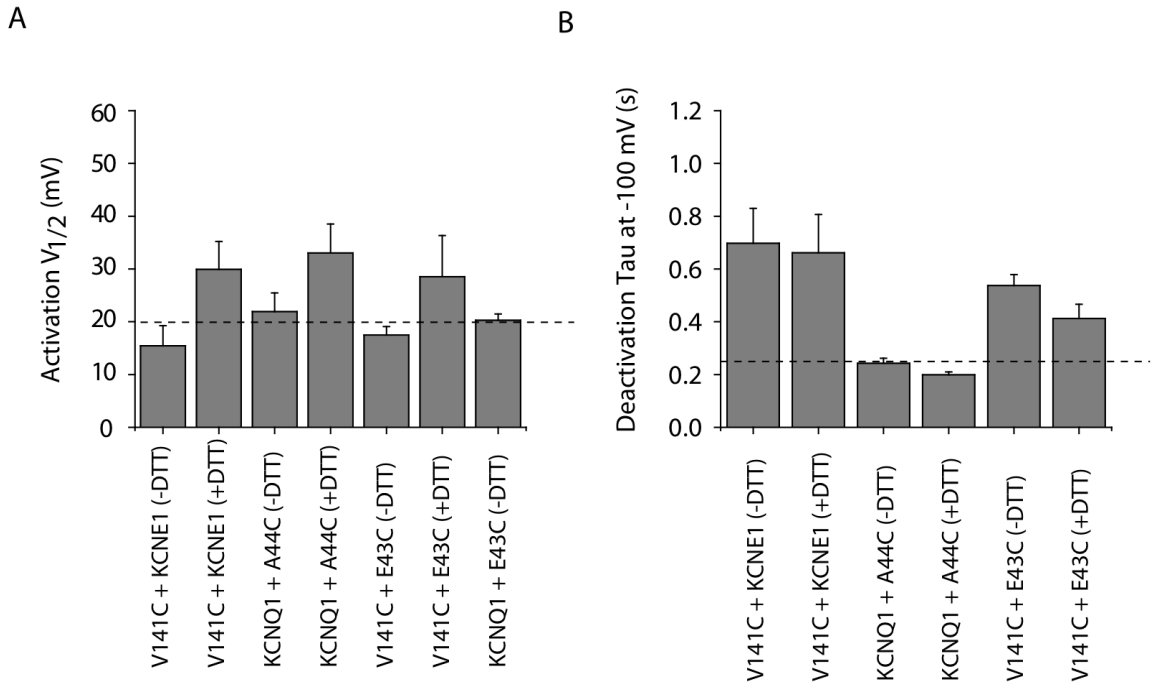

Figure 2-8. **Functional Consequences of Single Cysteines.** (A) Activation $V_{1/2}$ measured from normalized isochronal (2 s) activation curves: KCNQ1 / KCNE1 (dashed line), V141C / KCNE1 (- / +DTT), KCNQ1 / A44C (- / + DTT), V141C / E43C (- / + DTT), and KCNQ1 / E43C. (B) Deactivation time constant (tau) measured at -100 mV: KCNQ1 / KCNE1 (dashed line), V141C / KCNE1 (- / + DTT), KCNQ1 / A44C (- / + DTT), and V141C / E43C (- / + DTT) (*n* = 3-5). Data are shown as mean ± s.e.m.

Function of Crosslinking Pairs: V141C/A44C and V141C/E43C

The functional consequences of crosslinking V141C / A44C or V141C / E43C were minor. When these pairs are co-expressed, impact of crosslinking was a DTT-sensitive slowing of deactivation for V141C / A44C channels compared to KCNQ1 / KCNE1 channels (Figure 2-9A). There were DTT-sensitive shifts in the voltage dependence of activation (V141C / A44C (-DTT) $V_{1/2}$ = 34.9 ± 2.7 mV, *n*=5, $p < 0.05$ vs. V141C / A44C (+DTT): $V_{1/2}$ = 46.3 ± 2.9 mV, *n*=5) (Figure 2-9B). This shift, however, is consistent with the effect of DTT alone in the pseudo WT channel and likely is independent of the reduction of the crosslink (Chung et al., 2009). There was no significant difference in deactivation at -100 mV for V141C / A44C channels, in the absence and presence of the reducing agent, DTT (V141C / A44C (-DTT): τ_{deact} = 1.08 ± 0.06 s, *n*=5, $p > 0.05$ vs. V141C / A44C (+DTT): τ_{deact} = 0.82 ± 0.21 s, *n*=5) (Figure 2-9C). The slow deactivation kinetics that we see in the V141C / A44C (+DTT) uncrosslinked channel comes from the single cysteine engineered at V141 because there is no significant difference between these channels and channels with only a single cysteine at V141 ($p > 0.05$ for V141C / A44C (+DTT): τ_{deact} = 0.82 ± 0.21 s, *n*=5 vs. V141C / KCNE1: τ_{deact} = 0.66 ± 0.15 s, *n*=5) (Figure 2-9B and Figure 2-8B). There is also no significant difference in channel deactivation between KCNQ1 / A44C channels, with and without DTT, and KCNQ1 / KCNE1 channels indicating the cysteine engineered at A44 on KCNE1 does not have a big effect on channel function (Figure 2-

8B). Thus, crosslinking does not perturb the native conformation of the channel, giving confidence in the physiological significance of the cross-link determined orientation of V141 and S140 relative to the KCNE1 subunit.

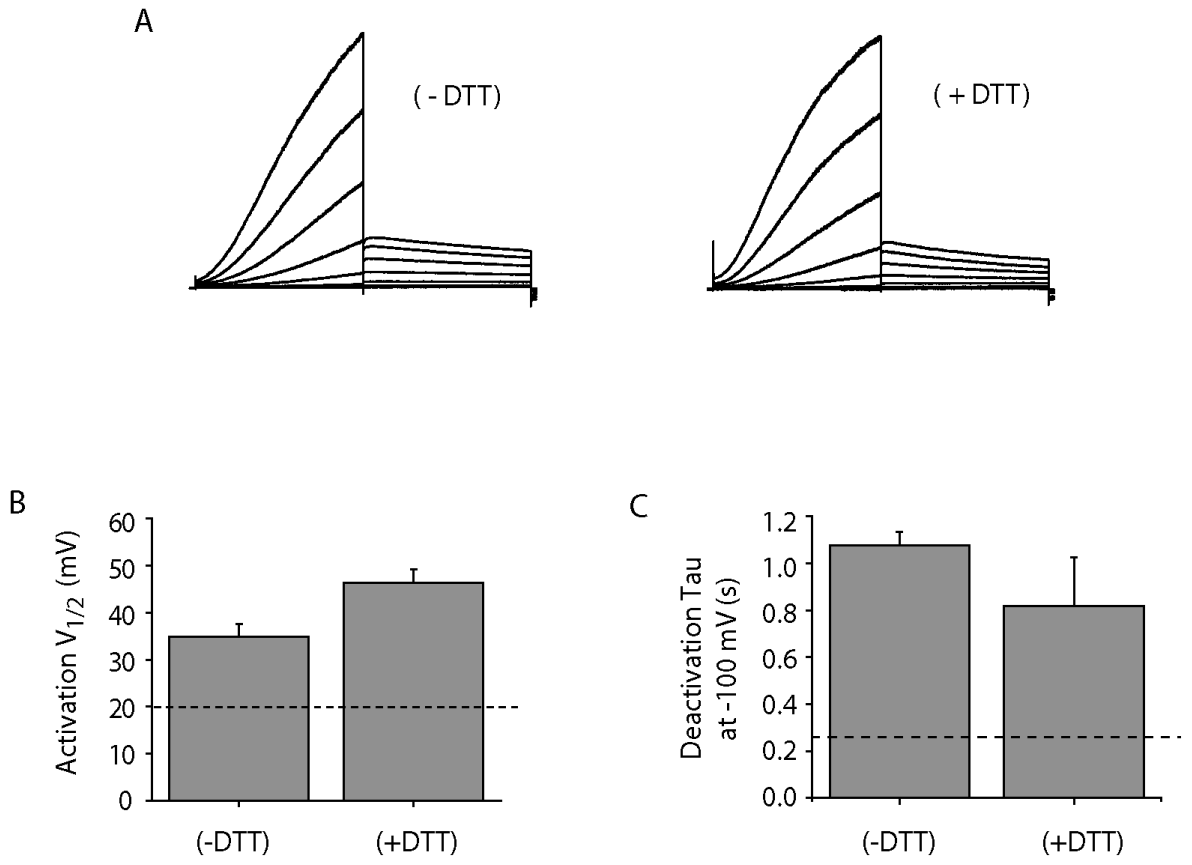

Figure 2-9. **Functional Consequences of Crosslinking Pair V141C / A44C are minor.** (A**)** Representative current traces for: V141C / A44C (- DTT) and V141C / A44C (+ DTT). Currents in response to 2 s pulses from -60 mV to +80 mV in 20 mV increments from -80 mV holding potential. Tail currents were measured at -40 mV. For DTT conditions, currents were measured after 10 minute perfusion of 10 mM DTT. (B) Activation $V_{1/2}$: KCNQ1/KCNE1 (dashed line), V141C / A44C (-DTT), and V141C / A44C (+ DTT). (C) Deactivation time constant (tau) measured at -100 mV: WT KCNQ1/KCNE1 (dashed line), V141C / A44C (- DTT), and V141C / A44C (+ DTT), (*n* = 3-5). Data are shown as mean ± s.e.m.

In summary, the results in Part I reveal KCNE1-dependence for the V141M mutation and not for S140G. These results are supported by biochemical crosslinking data demonstrating that residue V141 is positioned close to and is facing KCNE1, revealing a specific orientation of the KCNQ1 and KCNE1 subunits. The crosslink at V141C and A44C also demonstrates a suggested point of close proximity between KCNQ1 and KCNE1, functionally and structurally. The evidence for proximity in the upper TM region of the KCNQ1/KCNE1 channel is unique in that this region is structurally close and mutations at these specific residues would perturb the channel's properties. Another study demonstrated how a functional interaction in this region could affect channel function, specifically KCNE1 mutant A44W was coexpressed with the WT KCNQ1 channel (Goldstein et al 2008). The investigators demonstrated that KCNQ1/A44W channels exhibited very slow deactivation kinetics, compared to KCNQ1/KCNE1 channels. Combined with our results, these two particular residues, V141 on KCNQ1 or A44 on KCNE1, if either residue is mutated to a larger residue, the data demonstrate that channel deactivation is altered, at least in the case of V141M or A44W. Whether KCNE1 is affecting channel function in its other regions, in the TM domain by interacting with the channel pore (Melman et al 2008) or the C-terminus by interacting with the S4-S5 linker (Smith et al., 2007), these functional interactions in the upper TM region of the channel are affecting the normal mechanism of channel gating, with a preferential effect on deactivation kinetics.

Part II – KCNQ1 Intersubunit Crosslinking with S140C

Our data from Part I revealed crosslinking between KCNQ1 residue, V141C, and KCNE1 residues, 43 and 44, demonstrating proximity between S1 KCNQ1 and KCNE1 in this

extracellular region. This proximity suggests that V141 may have a direct interaction with KCNE1, and that the interaction between KCNE1 A44 / KCNQ1 V141 could be the structural basis for the mutation-induced slowing of deactivation kinetics in the V141M mutant channel. There was no evidence of crosslinking between S140C and any residues from the N-terminal region of KCNE1, suggesting that S140 is not close enough or positioned correctly to interact directly with KCNE1. This result is consistent with the fact that S140G does not depend on KCNE1 to disrupt channel function, so how is this mutation able to cause such dramatic changes in channel deactivation within the KCNQ1 homo-multimeric channel? We set out to investigate what regions in the channel complex residue S140 could be facing and interacting with, by substituting cysteines into candidate regions that could be in close proximity with S140 and then monitored disulfide bond formation.

Previous reports have suggested that S140 and V141 make contacts across the subunit-subunit interface with residues located near the tops of S5 from one KCNQ1 subunit and the pore-loop helix (p-helix) from a second KCNQ1 subunit (Smith et al., 2007). Specifically, they hypothesize that L137 in S1 KCNQ1 makes contact with I274 in S5 of another KCNQ1 subunit (Figure 2-10A). In the S1 domain of KCNQ1, S140 is located one turn up the helix from L137, and hypothetically could make contacts with Y278 in S5 of another KCNQ1 subunit. If this is a point of interaction, then it could offer one explanation for how the S140G mutation is able to stabilize the open state by interacting with the pore domain of KCNQ1 in the absence of KCNE1. In another study, disulfide crosslinking was used to find proximity between the S1 segment and the pore-loop, and a crosslink between T47C (S1) and V183C (pore-loop) in K_vAP was found (Lee et al., 2009). Although these residues are in a bacterial K^+ channel, they correspond to residues T144 in the S1 segment and Y299 in the pore-loop of K_v7.1. Since S140 is pointing

into the channel, towards the VSD, it is possible that this residue is positioned near the pore. If T144 (S1 KCNQ1) and Y299 (pore-loop) residues crosslink in the KCNQ1 channel, it supports the hypothesis that the S1 helix is close to the p-helix and could explain how the S140G mutation is slowing deactivation kinetics in the channel in the absence of KCNE1. However, when KCNE1 is assembled with the S140G mutant channel, how is the behavior of KCNE1 affected by the S140G mutation in KCNQ1? Preliminary results have been obtained for crosslinking between KCNE1 and the p-helix (Figure 2-10B), so KCNE1 could be further slowing deactivation kinetics of the S140G mutation by making contact with the p-helix (Figure 2-10C). Here, we investigated the possibility that S140C KCNQ1 would be in close proximity to the p-helix residues or the S5 segment of the adjacent KCNQ1 subunit.

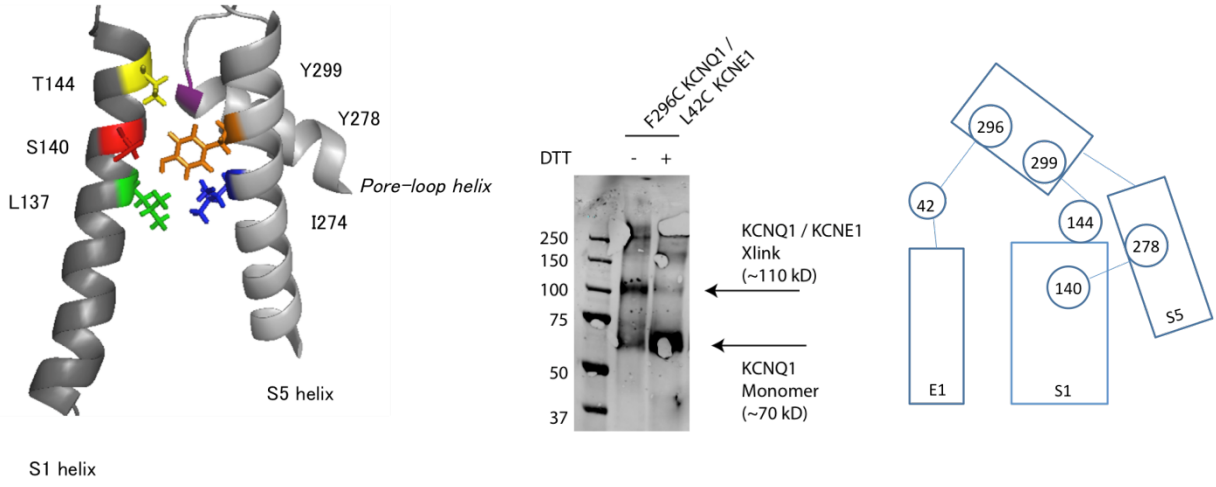

Figure 2-10. **Potential sites of interaction between the S1, S5, and pore-loop helices of two KCNQ1 subunits.** (A) Schematic illustration of S1 helix (left, dark gray) and S5 and pore-loop helices (right, light gray) from two adjacent KCNQ1 subunits. Potential sites of interaction: L137 (green) and I274 (blue), S140 (red) and Y278 (orange), T144 (yellow) and Y299 (purple), amino acids are represented in stick representations. (B) KCNE1 crosslinks to P-loop Helix of KCNQ1: western blot of crosslinking pair F296C KCNQ1 and L42C KCNE1**,** in the absence and presence of 10 mM DTT. (C) Schematic illustration of possible interactions between the S1, S5, pore-loop, and KCNE1 helices.

Crosslinking to Pore-loop helix residues (E295-A300)

KCNQ1 Cys-substituted mutants (E295C – A300C) were engineered into the S140 KCNQ1 pWT construct in which three native cysteines in the transmembrane domain of KCNQ1 were mutated out, as described previously. For these experiments, it was necessary to generate double cysteine mutant KCNQ1 constructs in order to properly assay intersubunit crosslinking. The limitation of only one cysteine in each KCNQ1 subunit is that we would only be able to observe half the amount of crosslinking because these proteins normally form a tetramer. If there are two cysteines in each subunit, one in S1 and one in the pore-loop, we should be able to see a tetramer if there is crosslinking (Figure 2-11).

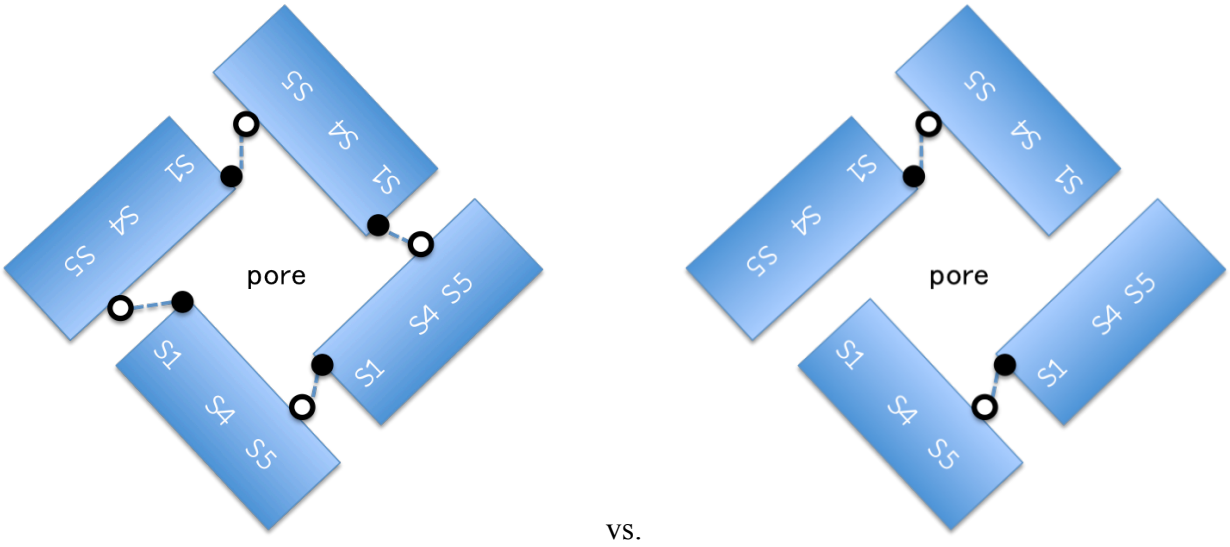

Figure 2-11. **Proposed crosslinking between the S1 and S5 helices of two KCNQ1 subunits.** Schematic illustration of hypothetical crosslinking in KCNQ1 tetramer with double cysteine mutations (A) and single cysteine mutations (B) in S1 (filled circles) and S5 (open circles). Each KCNQ1 subunit is represented as a rectangle (blue) with S1, S4, and S5 regions labeled.

The pore-loop helix residues were chosen for cysteine substitution due to their location in the channel predicted to be aligned with the region where S140 is located (Figure 2-10A) (Kang

et al., 2008). The immunoblots are shown for crosslinking results obtained between S140C and p-helix residues E295C to A300C, in the absence and presence of a reducing agent, dithiothreitol (DTT) (Figure 2-12). We see a DTT-sensitive crosslinking band (~150 kD) for pairs S140C/G297C and S140C/S298C (Figure 2-12A). Additionally, we monitored p-helix crosslinking with V141C and observed DTT-sensitive crosslinking to the same p-helix residues, V141C/G297C and V141C/S298C (Figure 2-12B). Although we expected to see this KCNQ1 crosslinked dimer band (~150 kDa) between S140C and a p-helix residue, an important negative control did not turn out. When KCNQ1 constructs containing only G297C or S298C were tested, we observed a band that was DTT-sensitive at the same molecular weight (~150 kDa) (Figure 2-12C). We could not separate out the p-helix cysteine substituted residues that were crosslinking to each other and those that were crosslinking to S140C or V141C. Thus, we could not proceed with these p-helix cysteine residues to assay intersubunit crosslinking to the S1 segment of KCNQ1.

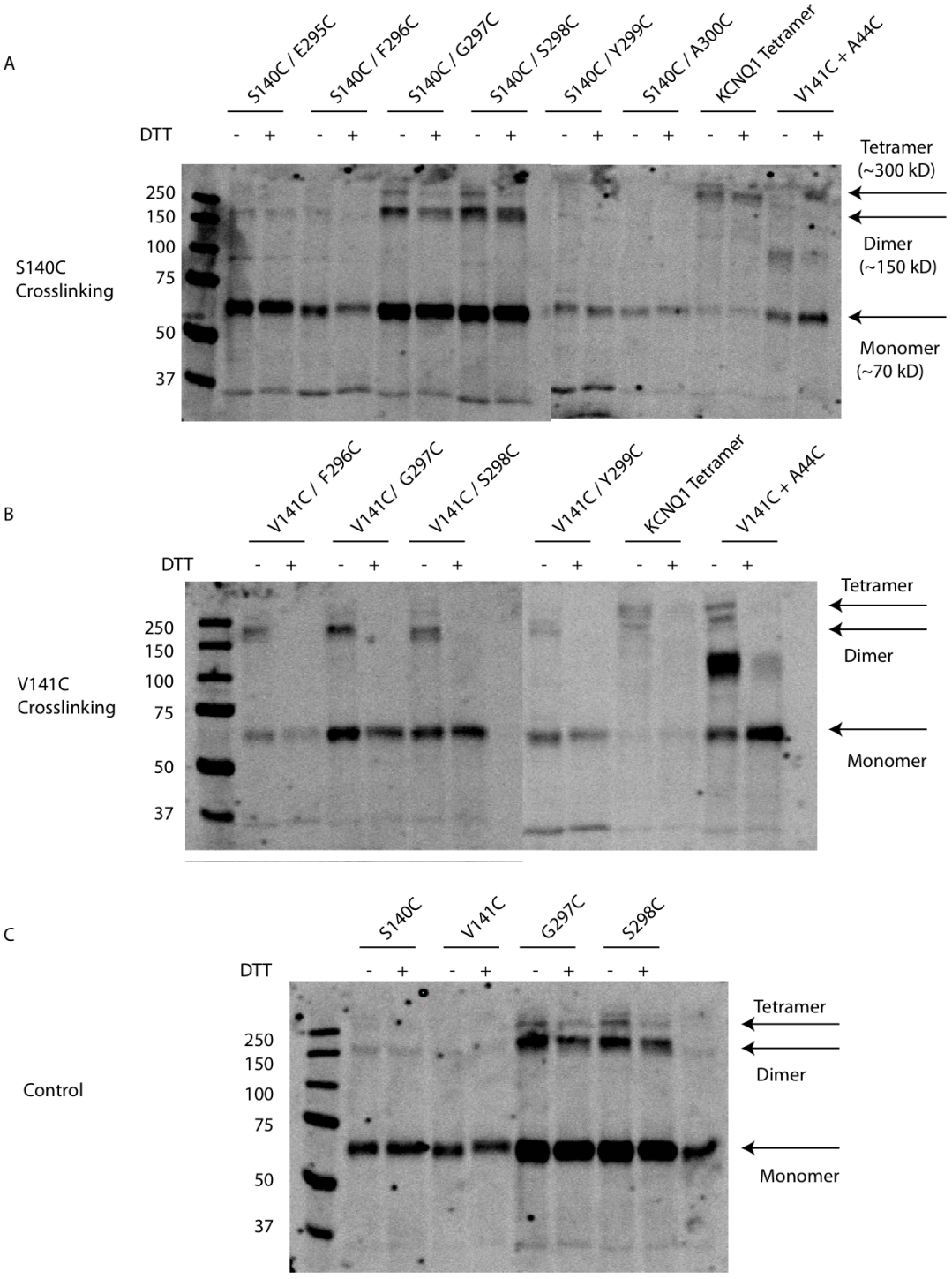

Figure 2-12. **S140C does not crosslink to the pore-loop helix.** Western blots of S140C (A) and V141C (B) double cysteine KCNQ1 mutants tested for crosslinking, in the absence and presence of 10 mM DTT. Controls included: KCNQ1 tetramer and V141C + A44C co-expression. Molecular weights: KCNQ1 monomer (~70 kD), KCNQ1 dimer (~150 kD),

KCNQ1 tetramer (~300 kD). (C) Control western blot of single cysteine mutants: S140C, V141C, G297C, and S298C.

Crosslinking to S5 residues (S276-L282)

The S5 residues (S276 – L282) were chosen for cysteine substitution due to their location in the channel predicted to be aligned with the region where S140 is located (Figure 2-10A) (Kang et al., 2008). Again, here we engineered double cysteine mutants to assay intersubunit crosslinking. Crosslinking results were obtained for pairs S140C/ S276C to S140C/ L282C, in the absence and presence of a reducing agent, dithiothreitol (DTT) (Data not shown). All cysteine pairs exhibited little to no crosslinking, however the KCNQ1 monomer expressed well, indicating that the protein was being expressed. There was faint crosslinking for a specific pair, S140C / Y278C, so we hypothesized whether there was crosslinking but we couldn't see it because expression was low. One explanation for the low expression could be because the KCNQ1 proteins are crosslinked in the ER and could not traffic to the membrane surface. Because these proteins are crosslinked, the channels could be in a conformation that renders it not functional, thus the proteins stay trapped in the ER. So far, all crosslinking experiments have been selecting for surface membrane proteins, so we do not know if there are proteins trapped in the ER. To test the above hypothesis, we repeated the same crosslinking experiments, this time without selecting for surface proteins and instead collected the whole cell lysates. The immunoblots now show increased expression for the KCNQ1 monomer and for specific KCNQ1 pairs: S140C / Y278C and S140C / F279C (Figure 2-13A and 2-13B). However, the results were not repeatable and inconsistent so it was difficult to interpret the results. In conclusion, we decided not to pursue with these experiments.

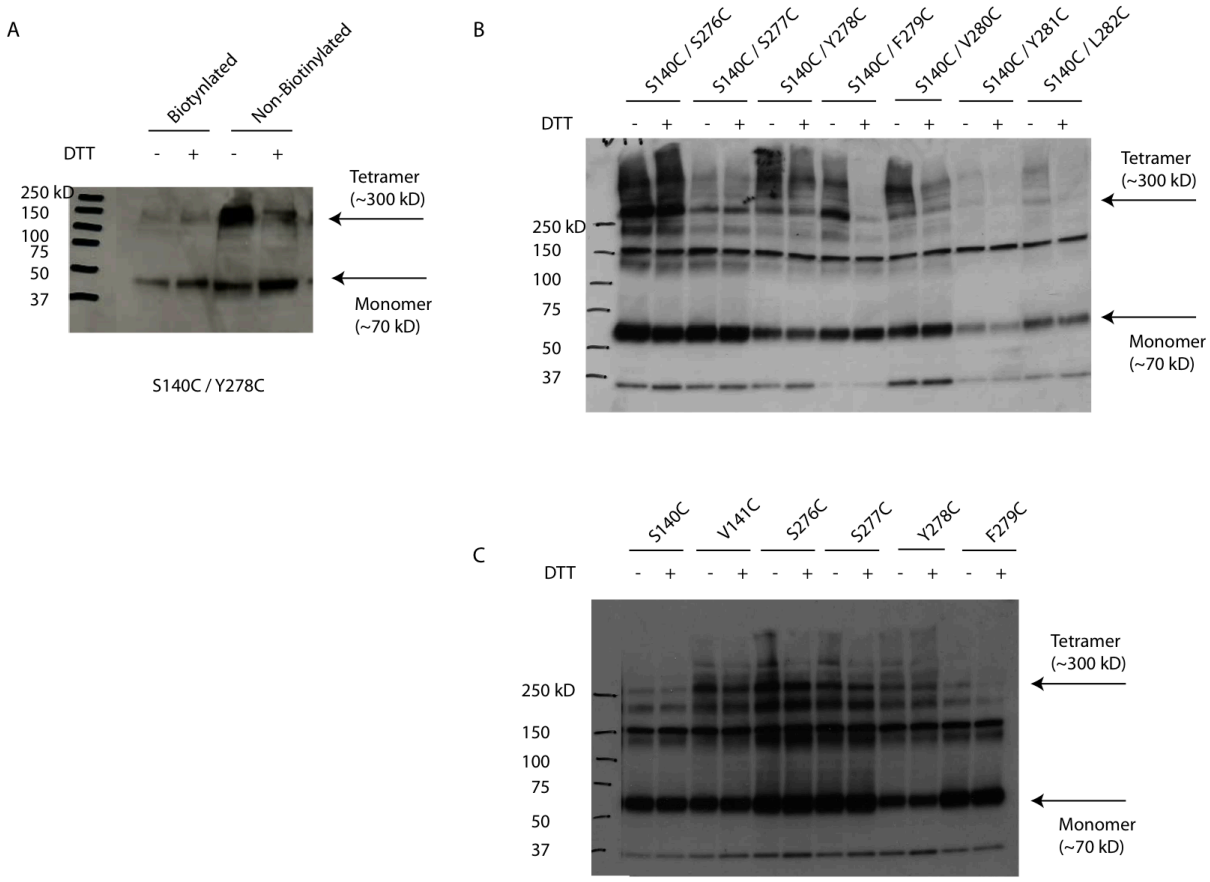

Figure 2-13. **S140C does not crosslink to the S5 helix.** Western blots of (A) biotinylated and non-biotinylated mutant S140C/ Y278C. (B) Double cysteine KCNQ1 mutants tested for crosslinking, in the absence and presence of 10 mM DTT. Molecular weights: KCNQ1 monomer (~70 kD), KCNQ1 dimer (~150 kD), KCNQ1 tetramer (~300 kD). (C) Control western blot of single cysteine mutants: S140C, V141C, S276C-F279C.

Part III - State Dependence of Crosslinking

Thus far, we have not determined what regions in the KCNQ1 channel complex that residue S140 may be interacting with to induce slow deactivation kinetics. In the experiments performed so far, crosslinking is presumably happening in the closed state of the channel, so we set out to investigate whether we could monitor crosslinking in the open states of the channel. It

is believed that disulfide bonds are formed and rearranged in the endoplasmic reticulum of the cell (Woycechowsky and Raines, 2000), where the membrane potential is relatively negative (Hwang et al., 1992). Thus, at this hyperpolarized -130 mV potential, voltage gated K^+ channels are closed. All crosslinking results so far are happening in the closed state of the channel. However in previous reports, experiments were done to test state dependence of crosslinking and one study suggested that certain crosslinks could be formed in either the open or closed states of the channel (Xu et al., 2008; Chung et al., 2009). We set out to test the state dependence of crosslinking with our cysteine-substituted residues to determine whether we observe crosslinking of S140C or V141C to any KCNE1 residues in the open state of the channel. We used an elevated K^+ environment and engineered open state mutations into the KCNQ1 channel to monitor crosslinking in the open state.

Crosslinking Residues

The KCNQ1 Cys-substituted mutants (S140C and V141C) and the five KCNE1 Cys-subsituted mutants (G40C to A44C) were used for the following experiments. The crosslinking pair, V141C + A44C, was used as a positive control because it exhibited ~80% crosslinking.

High K^+ External Solution

Previously, elevated K^+ concentration (120 mM) was used for functional experiments to increase driving force and allow resolution of deactivating tail currents over a broad range of negative voltages. In this high K^+ environment, the reversal potential is 2.32 mV and given that voltage gated KCNQ1 channels have a $V_{1/2}$ of 17.5 mV, there should be open channels in this depolarized environment. Thus, we set out to test crosslinking in the open state using these conditions for crosslinking pairs: V141C + A44C and S140C + A44C. We find that there is no

significant difference in crosslinking for V141C + A44C in 5 mM K^+ versus 120 mM K^+ (Figure 2-14). S140C + A44C did not exhibit any crosslinking in either K^+ environment (Data not shown).

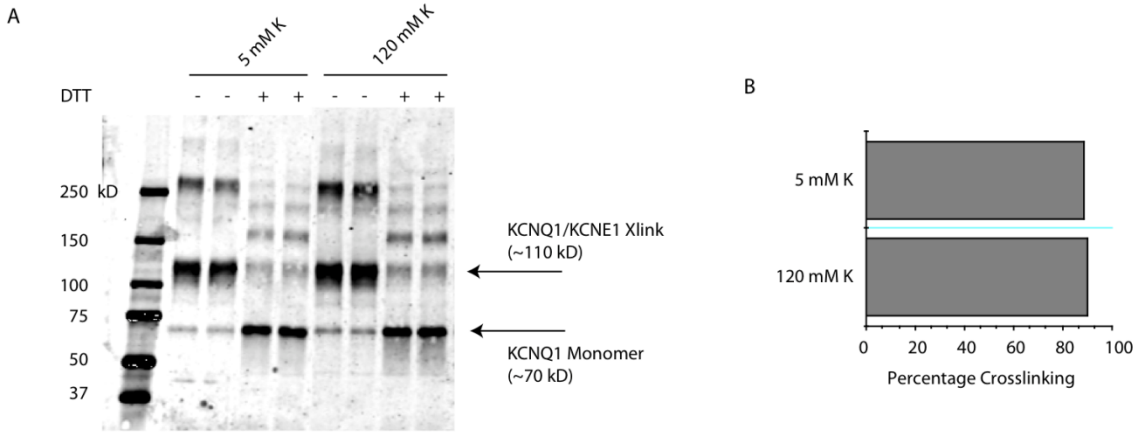

Figure 2-14. **Different K^+ concentrations do not reveal open state crosslinking.** (A) Western blot of V141C + A44C in 5 mM K^+ vs 120 mM K^+ **,** in the absence and presence of 10 mM DTT. (B) Bar graph showing percentage of spontaneous cross-linking for V141C and A44C. Calculations were based on the intensities of the bands, as described in Methods.

S1 Open State Mutant

Another method to assay state dependent crosslinking was to engineer open state mutations into the background of the KCNQ1 channel. For these experiments, the S140G and V141M mutations were chosen as the open state mutants because we had previously characterized them functionally. These channels have a $V_{1/2}$ of 1.5 mV (S140G/KCNE1) and 2.4 mV (V141M/KCNE1) and thus would preferentially have channels in the open state in physiological (5mM) K^+ concentrations, where the reversal potential is ~-80 mV. In these experiments, we find that there is no crosslinking observed for S140C and Cys-KCNE1 residues

in the background of the open state mutation (V141M) (Figure 2-15A). For V141C and Cys-KCNE1 channels with open state mutation (S140G), we observe the same amount of crosslinking as channels without the open state mutation (Figure 2-15B). This method also was not successful as a proper way to assay state dependent crosslinking.

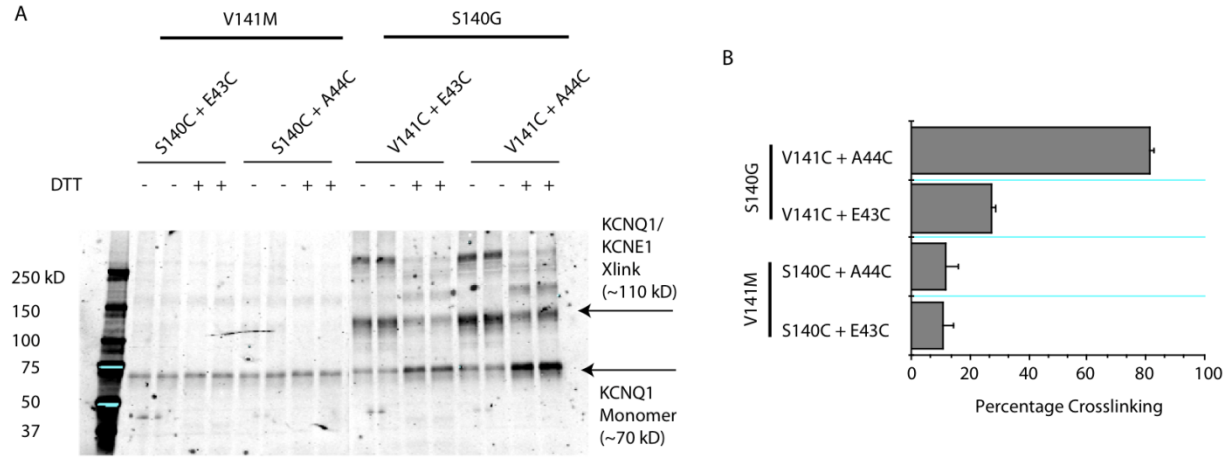

Figure 2-15. **Open state mutation in S1 does not reveal open state crosslinking.** (A) Western blot of crosslinking pairs with open state mutations listed above immunoblot**,** in the absence and presence of 10 mM DTT. (B) Bar graph showing percentage of spontaneous crosslinking for crosslinking pairs. Calculations were based on the intensities of the bands, as described in Methods. Data are presented as mean ± s.e.m.

S4 Open State Mutant

Although S140G and V141M were favored as open state mutations, they weren't the most appropriate choice for our experiments. The residues that were chosen for cysteine substitution were adjacent to the open state mutation, S140G V141C and S140C V141M. Thus, the S140G and V141M mutations might inhibit or affect the crosslinkng because they are right next to the cysteine substituted residue, so we had to find an open state mutation that was further

away from the cysteine residue. Previously, Panaghie and Abbott reported that the loss of single S4 charges at positions R231 or R237 produced constitutively active KCNE1/KCNQ1 channels (Panaghie and Abbott, 2007). We chose R231A to use for our experiments. We find that S140C channels with the S4 open state mutation did not produce any crosslinking results with the KCNE1 cysteine substitutions tested (Figure 2-16). While crosslinking with V141C and KCNE1 residues produced similar results with or without the S4 R231A mutation in the background. This method did not prove to help us monitor crosslinking in the open state either.

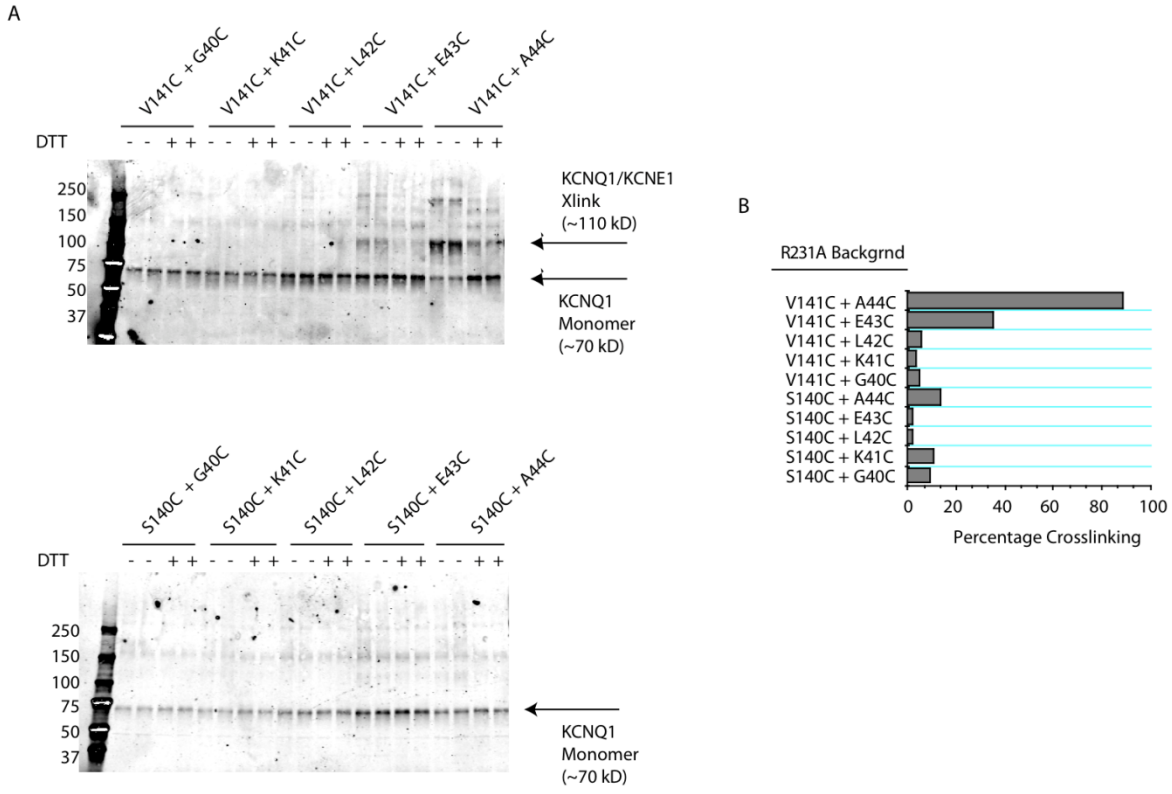

Figure 2-16. **Open state mutation in S4 does not reveal open state crosslinking.** (A) Western blot of S140C and V141C crosslinking pairs with R231A open state mutation**,** in the absence and presence of 10 mM DTT. (B) Bar graph showing percentage of spontaneous crosslinking for crosslinking pairs. Calculations were based on the intensities of the bands, as described in Methods.

Discussion

We find that KCNE1 plays a critical role in distinguishing two independent effects underlying the atrial fibrilliation-associated KCNQ1 mutations S140G and V141M. While both mutations disrupt deactivation in the presence of KCNE1, our experiments establish that S140G is able to slow channel deactivation in the absence of this subunit, in contrast to previous reports (Chen et al., 2003c). We find that the V141M mutation in the KCNQ1 subunit alone is indistinguishable from the WT KCNQ1 subunit, confirming previous reports that this mutant phenotype requires the presence of KCNE1 (Hong et al., 2005). The marked impact of KCNE1 on deactivation of the V141M channel occurs despite that fact that there is no effect of the mutation on WT KCNQ1 homomeric channel function. This indicates an important role for KCNE1 in determining the disease phenotype of the V141M assembled channels.

Based on our functional experiments, biochemical crosslinking was performed in order to establish a structural basis for the differential KCNE1 dependence of these two mutant phenotypes. KCNE1 has previously been shown by spontaneous disulfide crosslinking to be positioned in the I_{Ks} channel in a manner that allows KCNE1 communication with S1 and S6 of different KCNQ1 subunits (Xu et al., 2008; Chung et al., 2009). Our crosslinking results build onto this placement of KCNE1 within the assembled channel. We demonstrate that V141C, but not S140C, spontaneously crosslinks with cysteines introduced in KCNE1 at positions 43 and 44. These results reveal a specific orientation of S1 whereby V141 is in close proximity to KCNE1, consistent with the KCNQ1 structural model (Figure 2-17) (Kang et al., 2008). With this positioning, it is clear why there is such a dramatic effect on channel function when KCNQ1 with the V141M mutation is assembled in the tetrameric channel in the presence of KCNE1. In the absence of KCNE1, it is likely that the V141 residue is not close to any region of the channel

where it could affect channel function, which is in agreement with this mutation having no functional impact on KCNE1-free homomeric KCNQ1 channels. On the other hand, S140 is the neighboring residue on the S1 alpha helix and its position can be inferred to be rotated back towards the S2-S4 helices within its own subunit. Thus, it is not in a favorable position to form crosslinks with KCNE1 residues, but points in a direction that would allow it to impact the environment where S2 and S4 are located (Figure 2-17B). This prediction is consistent with our functional results showing that mutation of the S140 residue alone is sufficient to slow deactivation of homomeric KCNQ1 channels in the absence of KCNE1.

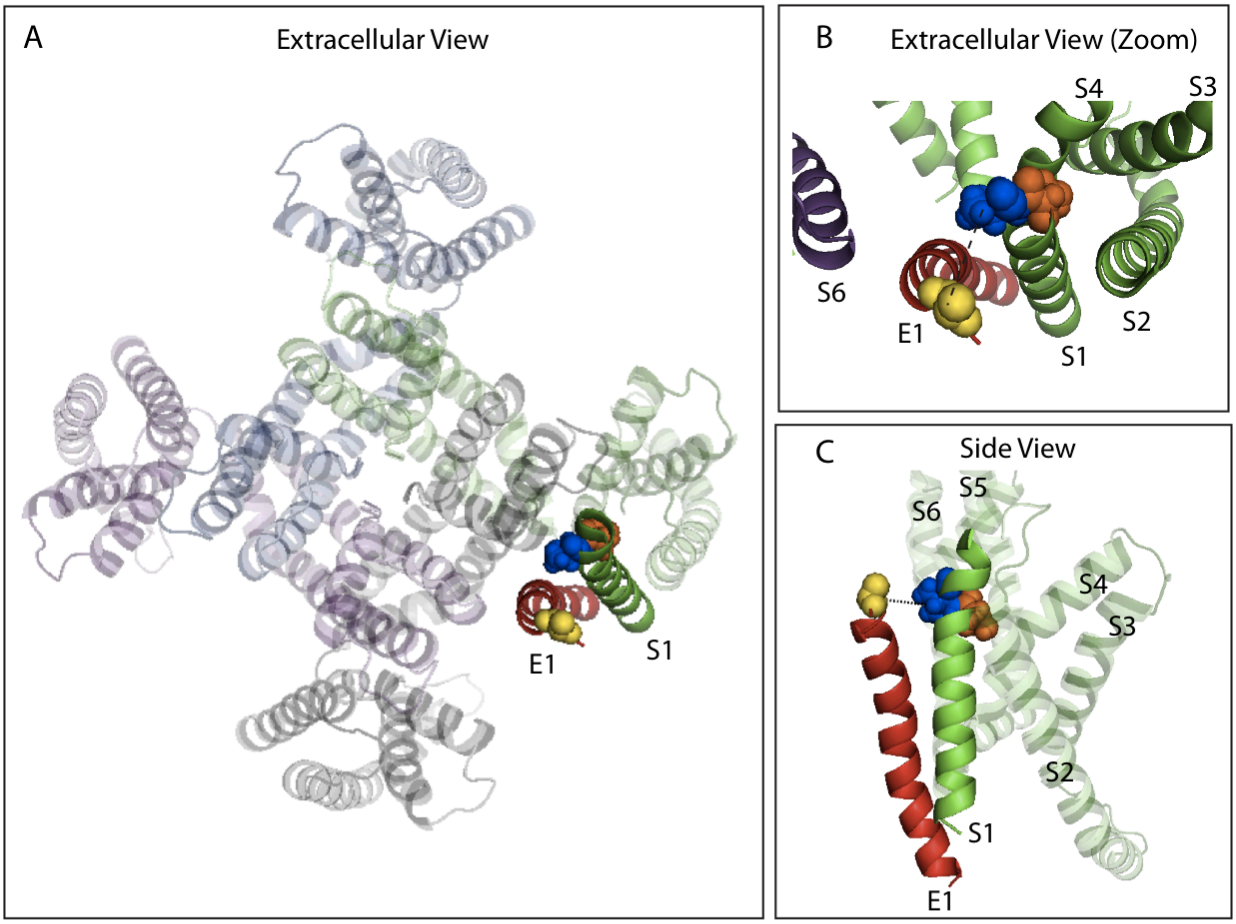

Figure 2-17. **Predicted Orientation of S1 KCNQ1 relative to KCNE1.**
(A) Extracellular view of KCNQ1 tetramer and KCNE1 transmembrane domain in the open state from *Kang et al.* (B) Extracellular view of KCNE1 (red) and S1 KCNQ1 (green) from *Kang et al.* V141 (blue) and S140 (orange) in S1 KCNQ1 and A44 (yellow) in KCNE1 are in space-fill representations. V141 points towards A44, while S140 points towards S2-S4 domains of the same KCNQ1 subunit (gray). (C) Side view of KCNE1 and single subunit of KCNQ1 taken from *Kang et al.* open state model.

The functional consequences of the crosslink at V141C / A44C and V141C / E43C were observed to be minor, indicating that crosslinking does not perturb the native conformation of the channel; consequently these residues are likely in a relatively fixed position in the native state of the channel. Taken together, our results suggest an important region of proximity between the amino terminal end of KCNE1, near the transmembrane region and the extracellular end of KCNQ1 S1, that is particularly important in controlling deactivation kinetics of the KCNQ1/KCNE1 assembled channel. Based on these results, we propose that this KCNE1 / KCNQ1 S1 interaction may mediate the KCNE1-induced changes in WT KCNQ1 deactivation.

The requirement of KCNE1 for the most severe phenotype observed with these inherited mutations raises the interesting and important question of whether the pathological phenotype of these mutations may depend on the relative expression of KCNE1 in the heart and the resulting stoichiometry of KCNE1 in these channels. Mutation carriers in the S140G family have varied clinical phenotypes from no effect to AF to mild Long QT (Chen et al., 2003c). The molecular mechanism of AF involves multiple-circuit-reentry, which is due to shortening of the action potential duration (APD) and reduction of the effective refractory period (ERP) (Nattel 2002). In the Chen et al. study, the S140G mutation caused an increase in outward potassium current at depolarized potentials, which would stabilize the resting membrane potential, leading to a shortening of the atrial ERP, thus leading to a shorter QT interval. However, it is harder to

explain why some patients exhibited prolonged QT intervals. Several hypotheses include the effect of another mutation in the atria, which could contribute to long QT phenotype, inadequate correction of the QT interval, or the alteration of other ionic currents, such as Ca^{2+} or Na^{+}, which may prolong the APD, thus leading to a net prolongation of the QT interval.

Whether the stoichiometric ratio of KCNE1 to KCNQ1 is fixed at 2/4 as suggested by the work of the Kobertz group (Morin and Kobertz, 2008) or variable as suggested by recent single molecule imaging experiments (Nakajo et al., 2010); our work would strongly suggest a mandatory proximity of KCNQ1 to a nearby KCNE1, especially in the case of V141M, subunit if the assembled channel is to be characterized by the key pathological phenotype: markedly slowed deactivation. In heterozygote patients, the number of KCNQ1 subunits carrying the disease causing mutation will vary from 1 to 4 in assembled channels, and thus alter the potential contributions of KCNE1/KCNQ1 interactions underlying arrhythmia risk. Similarly, if, in fact KCNE1/KCNQ1 stoichiometry is variable and may even vary during disease (Mustapha et al., 2007), then the severity of the disease phenotype, particularly for V141M mutation carriers, will be highly variable. Further, by this mechanism, chamber specific variation in KCNE1 (Soma et al. 2010) may well play a role in these mutations predominant effect occurring in the atria. Testing the impact of subunit assembly, availability and stoichiometry on the severity of the underlying disease mechanism therefore represents a major goal of future studies.

In summary, our work reveals KCNE1-dependence for the V141M mutation and not for S140G. These results are supported by biochemical crosslinking data demonstrating that residue V141 is positioned close to and is facing KCNE1, revealing a specific orientation of the KCNQ1 and KCNE1 subunits. The crosslink at V141C and A44C also demonstrates a suggested point of close proximity between KCNQ1 and KCNE1, functionally and structurally. Additionally, the

dependence on a neighboring KCNE1 for the full functional phenotype presents a mechanism by which diverse chamber specific or patient specific functional effects can occur.

The attempts to monitor intersubunit and state dependent crosslinking were not successful. However, the hypotheses surrounding the idea that residue S140 is interacting with a part of the channel to induce slow deactivation kinetics could provide insight into the mechanism of how this mutation functions. These hypotheses will likely require experimentation with different methods.

CHAPTER III

Amino-terminus of KCNE1 Controls Deactivation Kinetics

Background and Significance

Kang et al. describes that the N-terminus of KCNE1 is situated in the gain-of-function (gof) cleft (including four of five known mutations, S140G, V141M, I274V, and A300T) and that this placement stabilizes the open state of the channel (Kang et al., 2008). Our biochemical crosslinking studies revealed proximity between KCNQ1 V141C / KCNE1 A44C and KCNQ1 V141C / KCNE1 E43C, which may be important in acting as part of the anchor point involved in closed to open transitions in K_v channel gating (Lee et al., 2009). These findings and our data draw attention to the N-terminal region of KCNE1 and its impact on channel function.

Results

N-terminal KCNE1 Mutations

The amino terminus of KCNE1 was screened for residues that might counter the functional consequences of the two KCNQ1 AF mutations, S140G and V141M. KCNE1 residues starting at the extracellular end of the predicted KCNE1 helix (residues A44 through L51) were mutated because it was previously demonstrated that there is close proximity of this region of KCNE1 to KCNQ1 S1 (Figure 3-1A) (Chung et al., 2009). The specific mutations made on KCNE1 were initially designed to impact a putative KCNE1/KCNQ1 interface based on volume compensation. For the S140G mutation, there is a loss of volume when the residue is mutated from a serine to glycine, resulting in a volume loss of ~29.3 $Å^3$. In order to compensate

for this loss on KCNQ1 S1, one set of residues, starting from A44 - L51 in KCNE1, were mutated to have an added volume of ~29.3 $Å^{3.}$ For the V141M mutation, the same set of residues (A44 - L51) on KCNE1 were mutated to have a loss of volume of ~29.3 $Å^3$ to compensate for the V141M mutation.

We transiently co-expressed S140G KCNQ1 or V141M KCNQ1 with the appropriate volume compensated KCNE1 mutant in CHO cells and recorded currents by whole cell patch clamp. Recordings were done in a physiological K^+ solution. A series of depolarizing pulses were applied from -60 mV to +80 mV from a holding potential of -80 mV and repolarizing currents were measured at -40 mV. The pulse protocol was applied at 0.1Hz, and thus channels that open upon depolarization, but fail to close during the interpulse interval at the -80 mV holding potential generate time-independent currents that resemble "constituitively open channels". For channels that do close during the interval between test pulses, there is no open channel activity at the beginning of the test pulse. Normalized pedestal current (I_o/I defined in Methods) is used as a measure of restoration of KCNQ1/KCNE1 channel activity. For comparison, expression of WT KCNQ1/KCNE1channels yields I_o/I ratio of close to zero; expression of S140G/KCNE1 and V141M/KCNE1 channels yields I_o/I of 1.

L45F and Y46W KCNE1 Mutations Alter Deactivation in both KCNQ1 AF Mutations

KCNE1 residues, when co-expressed with KCNQ1 S140G, were screened for activity that reduced the accumulation of open channels during repetitive stimulation. Representative recordings are shown for S140G KCNQ1 co-expressed with KCNE1 residues: A44T and L45F (Figure 3-1B). The following KCNE1 mutations exhibited little open channel activity at the

beginning of the test pulse and were able to partially correct the markedly slow deactivation characteristic of the S140G mutation: L45F (0.24 ± 0.026 pA, *n*=15), Y46A (0.31 ± 0.014 pA, *n*=3) and Y46W (0.33 ± 0.029 pA, *n*=14). The functional impact of these and other mutations is summarized in a bar graph (Figure 3-1B).

When mutated KCNE1 subunits were co-expressed with KCNQ1 V141M, there was no change in channel function with any volume-compensated KCNE1 mutants (Data not shown). From the above results, we observed that KCNE1 mutations, L45F and Y46W, altered channel activity with the S140G mutation. Since S140G and V141M are adjacent residues, we tested whether L45F and Y46W would also have an effect on V141M. Representative recordings show that these two KCNE1 mutations also correct the slowed deactivation kinetics of the V141M mutation and the functional impact of these mutations is summarized in a bar graph (Figure 3-1C). Similar to the effects with the S140G mutation, these KCNE1 mutants co-expressed with V141M help restore channel activity towards a wild-type I_{Ks}-like phenotype.

These results suggest that a region on KCNE1, located on the amino terminus, is critical for altering channel function with the S140G and V141M mutations. To explore what aspect of function these KCNE1 mutations alter, we systematically compared co-expression of Y46W and L45F KCNE1 subunits with WT, S140G and V141M KCNQ1subunits. We compared the impact of these KCNE1 mutations on activation kinetics, absolute deactivation kinetics measured at -120 mV, and the fold difference in deactivation at -120 mV.

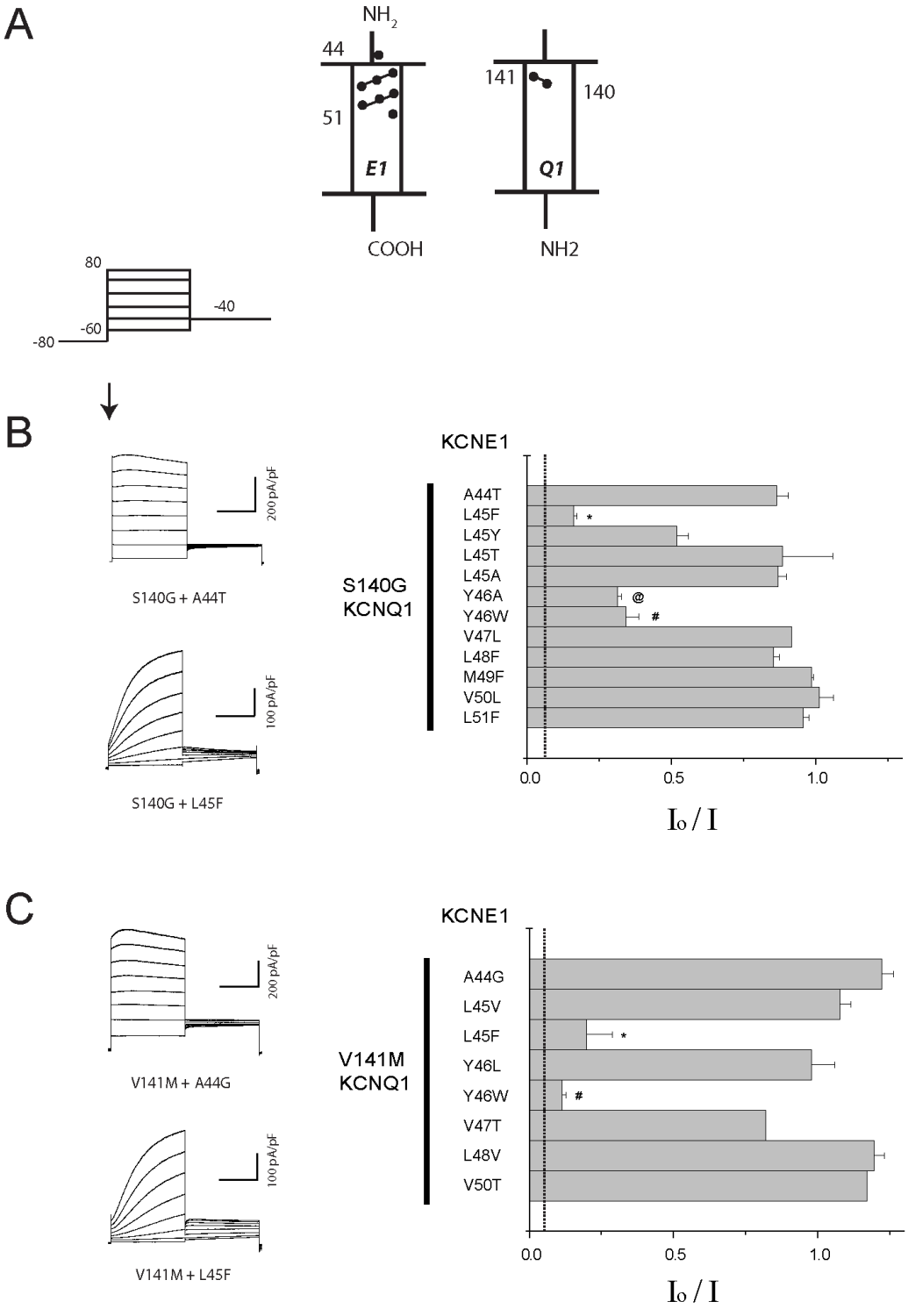

Figure 3-1. **Amino-terminal KCNE1 mutations preferentially impact deactivation: greater impact on V141M vs. S140G KCNQ1 subunits.** (A) Cartoon of KCNE1 and S1 KCNQ1,

with black dots indicating location of residues that were mutated and numbers represent amino acid position. The dashed line above KCNQ1 indicates continuation of the channel.
(B and C) Representative current traces are shown for the indicated S140G/KCNE1 pairs (B) and V141M/KCNE1 pairs (C). Recordings were done in 5 mM external K^+ solution. Holding potential = - 80 mV. Cells were depolarized from -60 mV to +80 mV in 20 mV increments for 2 s. Tail currents were measured at -40 mV for 2 s. The bar graph shows the normalized instantaneous current (I_o/I) measured at the beginning of the pulse at + 60 mV with each KCNQ1/KCNE1 pair. Twelve KCNE1 mutations were co-expressed with S140G. Eight KCNE1 mutations were co-expressed with V141M. The dashed line indicates the WT KCNQ1/KCNE1 condition. Data are shown as mean ± s.e.m. Symbols (*, @, #) indicate a significant difference ($p < 0.05$) using Student's t-test.

Characterization of KCNE1 Y46W co-expression with KCNQ1 Variants

Co-expression of Y46W with S140G or V141M exhibited little open channel activity at the beginning of each test pulse. To examine how Y46W is causing this effect in KCNQ1/KCNE1 channels, we compared the following parameters: voltage dependence of activation, kinetics of activation, and kinetics of deactivation upon co-expression with all KCNQ1 variants.

Co-expression of Y46W with all KCNQ1 variant channels resulted in slow activating, time-dependent currents for all assembled channels, however deactivation kinetics differed for these three subunit combinations (Figure 3-2A to 3-2C). There was a depolarizing shift in voltage dependence for KCNQ1/Y46W ($V_{1/2}$ = 91.5 ± 8.8 mV, n=5) compared to KCNQ1/KCNE1 ($V_{1/2}$ = 17.5 ± 2.6 mV, n=7) (Table 1). However, there is no significant difference in voltage dependence of activation for V141M/Y46W ($V_{1/2}$ = 20.8 ± 3.2 mV, n=3) and KCNQ1/KCNE1 ($p < 0.05$ for V141M/Y46W vs. KCNQ1/KCNE1). In contrast, for S140G/Y46W ($V_{1/2}$ = -25.3 ± 3.4 mV, n=5), there was a hyperpolarizing shift in voltage dependence that is significant from KCNQ1/KCNE1. Co-expression of Y46W with all KCNQ1 variants resulted

in similar kinetics of activation, while KCNQ1/KCNE1 Y46W resulted in a slightly faster time to half activation (KCNQ1/Y46W: 0.87 ± 0.29 s, *n*=6, S140G/Y46W: 1.09 ± 0.54 s, *n*=6, V141M/Y46W: 1.17 ± 0.31 s, *n*=8) (Figure 3-2D). Deactivating tail currents at -120 mV showed that the time course of deactivation for KCNQ1/ Y46W channels (τ_{deact} = 0.21 ± 0.05 s, *n*=5) is similar to KCNQ1/KCNE1 channels (τ_{deact} = 0.24 ± 0.004 s, *n*=9). In contrast, V141M/Y46W (τ_{deact} = 0.72 ± 0.04 s, n=9) and S140G/Y46W (τ_{deact} = 1.1 ± 0.13 s, n=6) channels both deactivate significantly slower than KCNQ1/KCNE1 channels.

There were differences in deactivation kinetics that are most dramatically seen in the comparison of the fold change in deactivation rate measured at a fixed voltage (-120 mV). Similar to the effect of WT KCNE1 expressed with KCNQ1, Y46W slows deactivation when co-expressed with each KCNQ1 variant. However, the impact on slowing deactivation from the Y46W mutant subunit is roughly 9-fold greater when co-expressed with V141M (8.94 ± 0.55, *n*=9) compared with either KCNQ1 (2.6 ± 0.62, *n*=6) or S140G (2.87 ± 0.28, *n*=6) (Figure 3-2E).

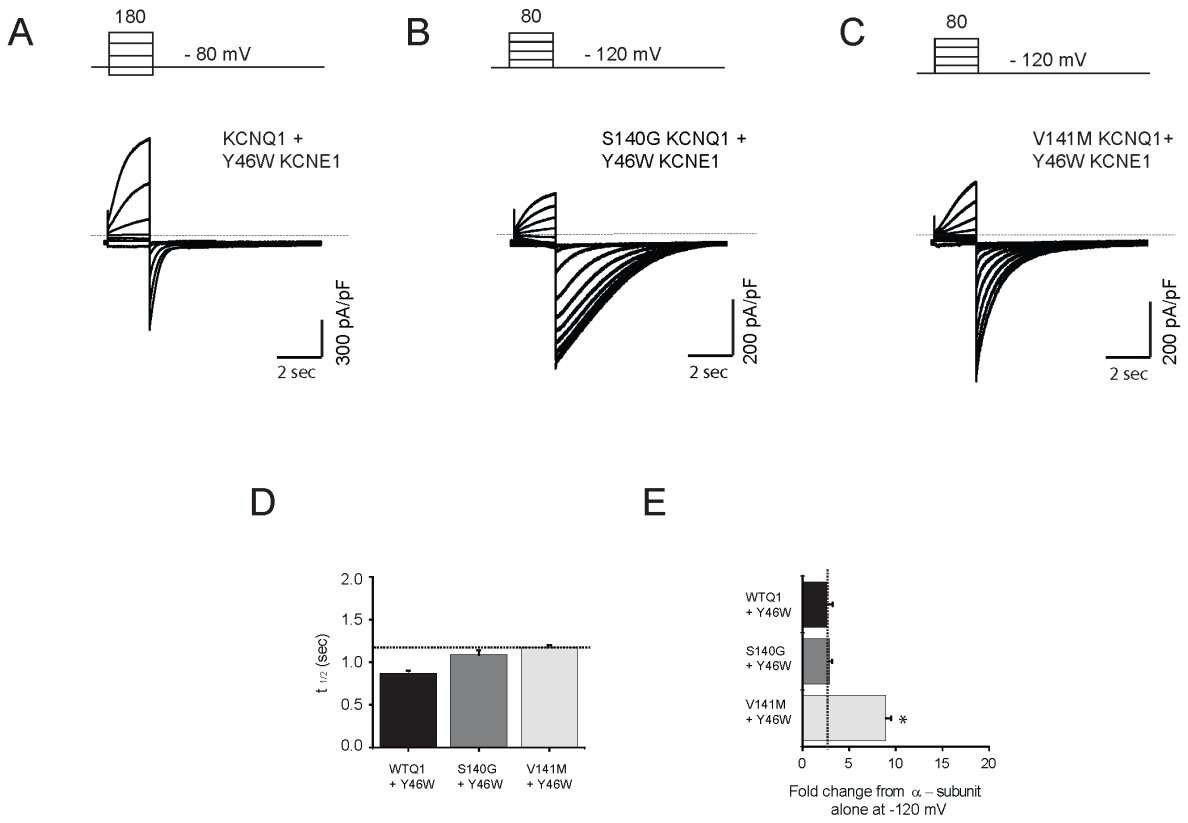

Figure 3-2. **Y46W co-expression has greater impact on deactivation kinetics for V141M vs. S140G KCNQ1 subunits.** (A to C) Representative current traces are shown for KCNQ1, S140G, and V141M, each co-expressed with Y46W. Recordings were done in 120 mM external K^+ solution. Stimulation protocols are shown above the trace. Activation $t_{1/2}$ (D) and fold change for τ_{deact} at -120 mV (E) was measured for KCNQ1, S140G, and V141M, each co-expressed with Y46W. The dashed line indicates WT KCNQ1/KCNE1. Data are shown as mean ± s.e.m. Asterisks indicate a significant difference ($p < 0.05$) using Student's t-test.

In the experiments investigating characteristics of Y46W co-expression, we co-expressed this residue with the WT KCNQ1 channel, which caused a large depolarizing shift (~70 mV) in voltage dependence of activation, compared to WT KCNQ1/KCNE1 channels. However, the time course of deactivation is roughly the same for WT KCNQ1/KCNE1 and WT KCNQ1/Y46W channels. Here, we first demonstrate a mutation that only affects activation

properties of the assembled channel, thus separating the mechanism of activation from deactivation. However, the story gets complicated when Y46W is co-expressed with either S140G or V141M channels. It seems that there are differential effects of the Y46W mutation with either mutation.

With S140G/Y46W channels, KCNE1 behaves like a less functional version of this subunit. We assume that the role of KCNE1, when co-expressed with KCNQ1 channels, is to slow deactivation and cause depolarizing shifts in voltage dependence. S140G/Y46W channels exhibit a depolarizing shift in voltage dependence, compared to S140G channels alone, but the shift is not as big as S140G/KCNE1 channels (Figure 3-3A). For deactivation, S140G/Y46W channels exhibit a slower time course of deactivation, but not nearly as slow as S140G/KCNE1 channels (Figure 3-3B).

For V141M/Y46W channels, again, we see separate of effects from activation versus deactivation. For activation, we observe a ~50 mV depolarizing shift in voltage dependence, compared to V141M channels alone (Figure 3-3C). This shift is similar to that of KCNQ1/KCNE1 channels, compared to KCNQ1 alone. This result demonstrates that Y46W co-expressed with V141M is behaving like KCNE1 with WT KCNQ1 channels. However, for deactivation, we again see a less functional version of KCNE1, where the time course of deactivation is slow for V141M/Y46W channels, but not nearly as slow as V141M/KCNE1 channels (Figure 3-3D).

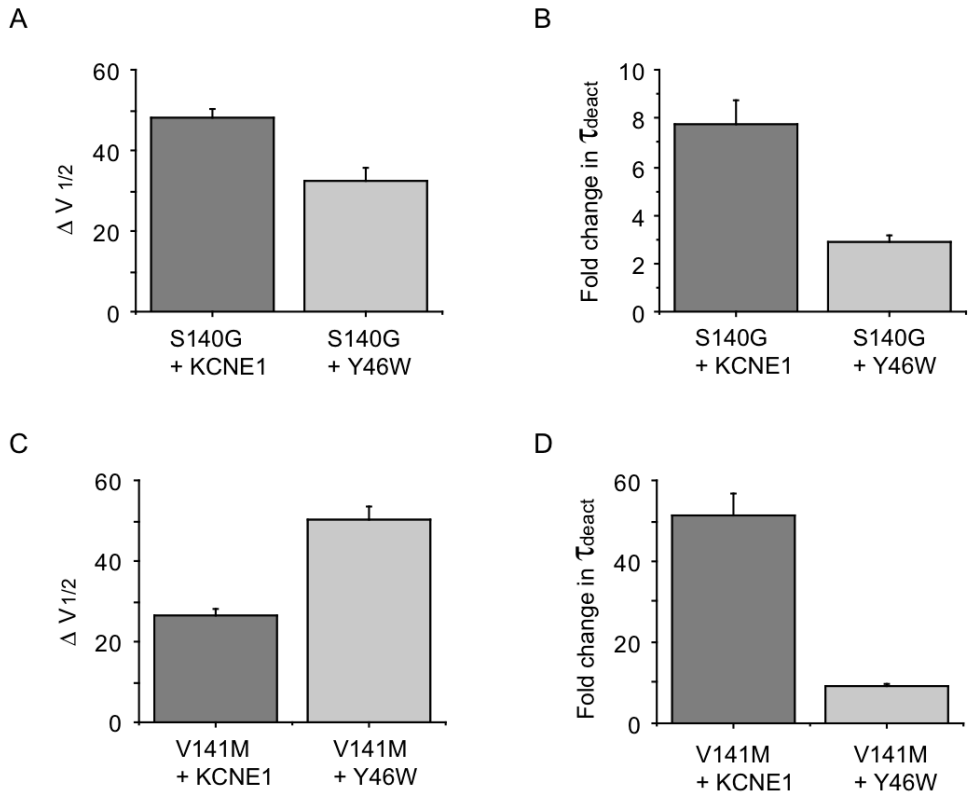

Figure 3-3. **The Y46W Mutation exhibit differential effects when co-expressed with S140G and V141M mutations.** $\Delta V_{1/2}$ (A) and fold change in deactivation tau (B) plotted for WT KCNE1 and Y46W co-expressed with S140G compared to S140G expressed alone. $\Delta V_{1/2}$ (A) and fold change in deactivation tau (B) plotted for WT KCNE1 and Y46W co-expressed with V141M compared to V141M expressed alone.

$V_{1/2}$ (mV)		KCNE1	L45F	Y46W
KCNQ1	-29.7 ± 2.1	17.5 ± 2.6	23.8 ± 3.1	91.5 ± 8.8
S140G	-57.5 ± 1.3	1.5 ± 2.7	-31.3 ± 6.8	-25.3 ± 3.4
V141M	-29.4 ± 0.9	2.4 ± 1.0	-18.3 ± 3.2	20.8 ± 3.2

τ_{deact} at -120 mV (ms)		KCNE1	L45F	Y46W
KCNQ1	89.4 ± 9.6	240.9 ± 4.2	238.7 ± 32.5	212.5 ± 50.8
S140G	672.7 ± 32.3	4093.3 ± 230.1	1271.2 ± 291.1	1916 ± 187.2
V141M	81.2 ± 14.6	6711.3 ± 637.9	1088.6 ± 131.4	716.1 ± 43.9

k		KCNE1	L45F	Y46W
KCNQ1	14.1 ± 1.6	15.9 ± 0.7	25.4 ± 0.6	29.1 ± 1.2
S140G	11.6 ± 1.4	20.6 ± 2.0	18.9 ± 0.8	27.6 ± 1.5
V141M	12.3 ± 1.7	16.6 ± 0.9	19.9 ± 0.9	28.8 ± 1.7

Table 1. **Voltage Dependence of Activation, Deactivation, and slope parameters for KCNQ1/KCNE1 subunit pairs used in study.**

Characterization of KCNE1 L45F co-expression with KCNQ1 Variants

KCNE1 L45F co-expression with KCNQ1 variants all exhibited slow activating, time dependent currents. However, for S140G/ L45F and V141M/ L45F channels, tail currents deactivated more slowly than KCNQ1/L45F (Figure 3-4A to 3-4C). L45F caused a minor depolarizing shift when co-expressed with KCNQ1 ($V_{1/2}$ = 23.8 ± 3.1 mV, *n*=4) compared to KCNQ1/KCNE1 ($V_{1/2}$ = 17.5 ± 2.6 mV, *n*=7), though not nearly as large as the Y46W mutation ($V_{1/2}$ = 91.5 ± 8.8 mV, *n*=5). L45F co-expression resulted in hyperpolarizing shifts for the S140G ($V_{1/2}$ = -31.3 ± 6.8 mV, *n*=4) and V141M mutations ($V_{1/2}$ = -18.3 ± 3.2 mV, *n*=5) compared to KCNQ1/KCNE1. Co-expression of L45F with all KCNQ1 variants resulted in kinetics of activation that are comparable to KCNQ1/KCNE1 channels (Figure 3-4D).

Deactivating tail currents were slower for S140G/L45F (τ_{deact} = 1.27 ± 0.29 s, *n*=4) and V141M/L45F channels (τ_{deact} = 1.09 ± 0.13 s, *n*=9), compared to KCNQ1/KCNE1 channels (τ_{deact} = 0.24 ± 0.004 s, *n*=9). The time course of deactivation for KCNQ1/L45F channels (τ_{deact} = 0.24 ± 0.03 s, *n*=6) was not significantly different from KCNQ1/ KCNE1. There is a differential response of V141M vs. S140G channels that is seen in the comparison of the L45F-induced fold change in channel deactivation kinetics. Here the impact of the KCNE1 subunit is roughly 14-fold greater when expressed with V141M (13.6 ± 1.64, *n*=9) compared with S140G (1.71 ± 0.36, *n*=4) or WT (2.91 ± 0.4, *n*=6) KCNQ1 subunits (Figure 3-4E). These results are similar to the Y46W mutation, where the impact of the KCNE1 subunit is much more substantial when co-expressed with the V141M mutation. All of the above functional results point to a much closer interdependence of channel function on assembly with KCNE1 for V141M vs. S140G KCNQ1 subunits.

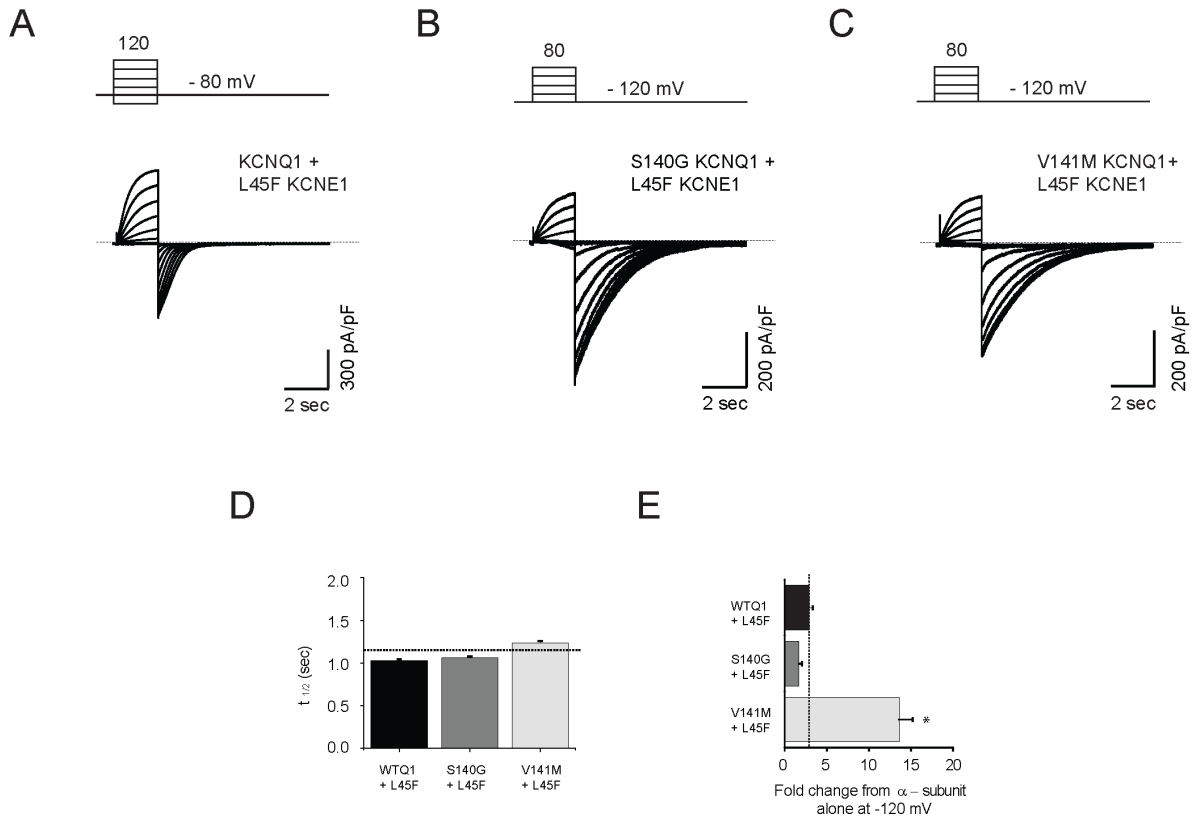

Figure 3-4. **L45F co-expression has greater impact on deactivation kinetics for V141M vs. S140G KCNQ1 subunits.** (A to C) Representative current traces are shown for KCNQ1, S140G, and V141M, each co-expressed with L45F. Recordings were done in 120 mM external K^+ solution. Stimulation protocols are shown above the trace. Activation $t_{1/2}$ (D) and fold change for τ_{deact} at -120 mV (E) was measured for KCNQ1, S140G, and V141M, each co-expressed with L45F. The dashed line indicates WT KCNQ1/KCNE1. Data are shown as mean ± s.e.m. Asterisks indicate a significant difference ($p < 0.05$) using Student's t-test.

The L45F mutation, when co-expressed with KCNQ1, results in channels with similar voltage dependence and deactivation time course to KCNQ1/KCNE1 channels. Already, the L45F and Y46W mutations do not behave the same when co-expressed with the WT KCNQ1 channel. However, what is interesting is that both mutations co-expresssed with the AF mutants produce channels resembling I_{Ks} channels.

When L45F is co-expressed with either S140G or V141M, we see channels that are roughly the same in voltage dependence and deactivation time course (Figure 3-5). In both S140G/L45F and V141M/L45F channels, the L45F mutant behaves like a less functional version of KCNE1. For voltage dependence of activation, the L45F mutation causes a depolarizing shift in voltage dependence for S140G and V141M channels, but nearly as much as WT KCNE1 with S140G or V141M. Similarly, for time course of deactivation at -120 mV, the L45F mutation slows deactivation with both S140G and V141M channels, but not nearly as slow as the WT KCNE1 subunit.

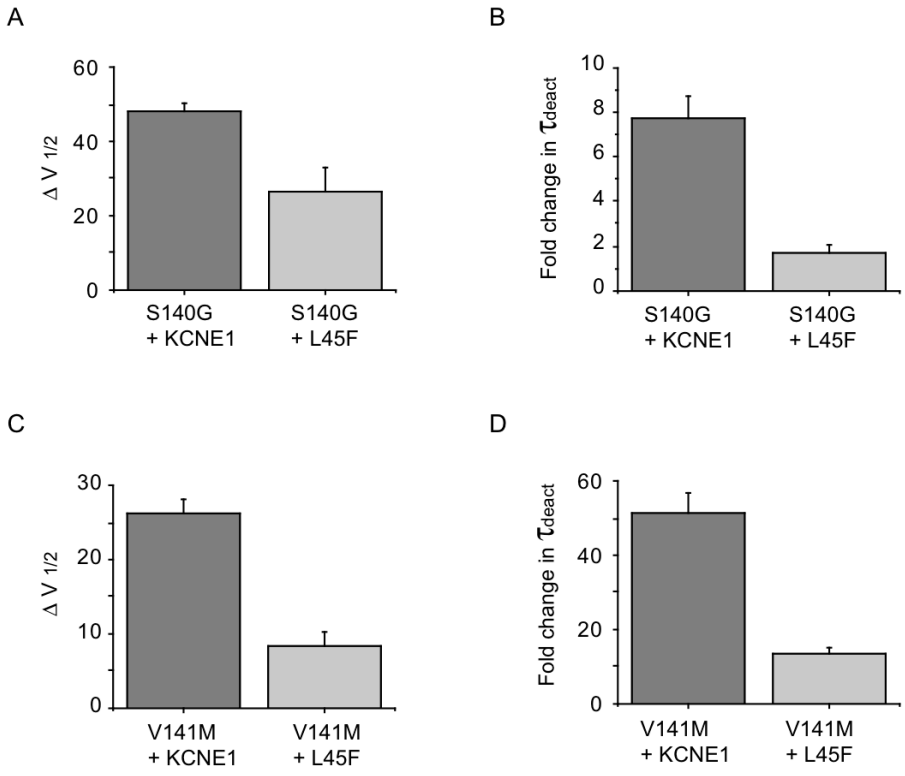

Figure 3-5. **The L45F Mutation exhibit similar changes in channel function when co-expressed with S140G and V141M mutations.** $\Delta V_{1/2}$ (A) and fold change in deactivation tau (B) plotted for WT KCNE1 and L45F co-expressed with S140G compared to S140G expressed

alone. $\Delta V_{1/2}$ (A) and fold change in deactivation tau (B) plotted for WT KCNE1 and L45F co-expressed with V141M compared to V141M expressed alone.

Function of KCNE1 Mutations with WT KCNQ1

The functional characteristics of the single KCNE1 mutants were tested with WT KCNQ1. Substitutions of amino acids in residues A44T – L51F in KCNE1 co-expressed with KCNQ1 exhibited subtle changes in activation and deactivation kinetics, but all resembled currents similar to I_{Ks} (Figure 3-6).

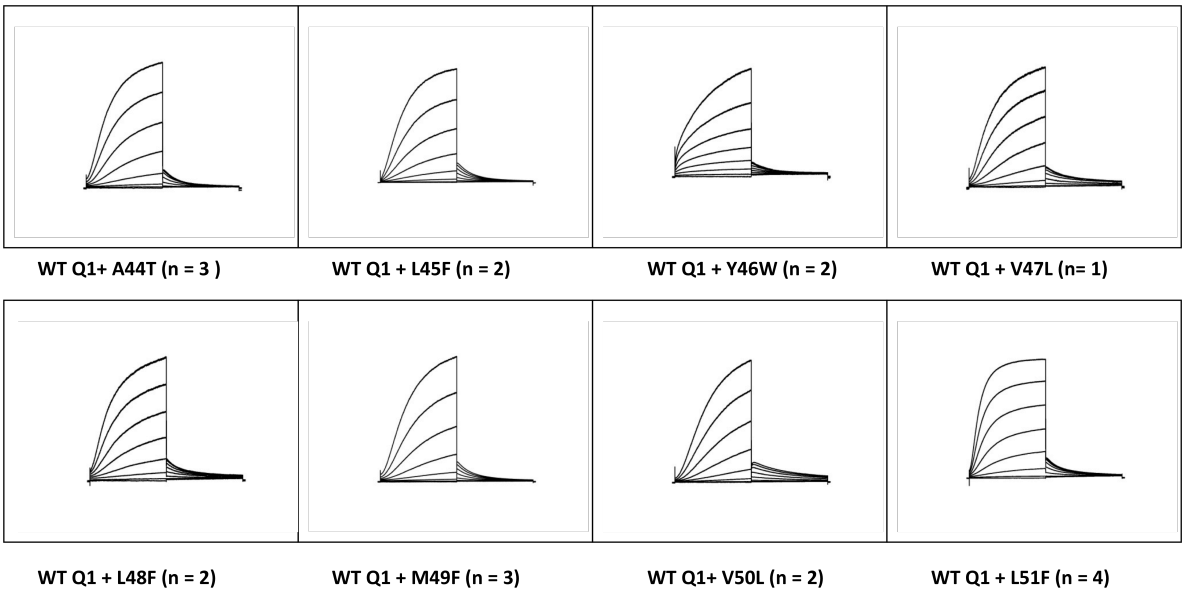

Figure 3-6. **Amino-terminal KCNE1 mutations co-expressed with WT KCNQ1.** Families of current traces shown for KCNQ1 co-expressed with KCNE1 residues: A44T, L45F, Y46W, V47L, L48F, M49F, V50L, and L51F. Currents in response to 2 s pulses from -60 mV to +80 mV in 20 mV increments from -80 mV holding potential.

Effect of Different Size Amino acids at positions L45 and Y46

From the initial experiments done in Figure 3-1, it was clear that our origninal volume hypothesis to compensate for volume change in the V141M mutations was unsuccessful, so we wanted to investigate the effect of different sized amino acids as a factor in compensating function of the channel. We tested the effects of substituting various sized amino acids at positions L45 and Y46 to see whether these two KCNE1 residues caused changes in function due to the amino acid or due to its position on the KCNE1 helix relative to the mutations in the S1 segment of KCNQ1. Prevously, we had substituted phenylalanine at position L45, which when co-expressed with S140G or V141M, restored I_{Ks}-like channel activity. Here we substituted the leucine at position 45 with alanine, threonine, and tyrosine (Figure 3-7A). Alanine was chosen because it was a reduction in volume. Threonine was chosen because it incurs a similar volume change as the phenylalanine, but without the aromatic ring. Tyrosine was chosen because it has an aromatic ring like the phenylalanine, but also incurs a larger volume change. Here, we find that the substitution of smaller and larger amino acids at positon L45 on KCNE1 did not compensate the effects of the S140G mutation. Additionally, we see that substitution of a threonine at L45 did not alter S140G channel function. To summarize, the L45F mutation is specific and unique in its ability to compensate for both the S140G and V141M mutations.

For residue Y46, we substituted the tyrosine with alanine to investigate a reduction in size at this position (Figure 3-7B). We find that Y46A resembles the effects of Y46W, when each are co-expressed with the S140G mutation. These results indicate that the specific amino acid, tryptophan, substituted at Y46 is not unique in compensating the AF KCNQ1 mutants, because substituting an alanine at Y46 produces the same functional results. However, these data suggest that the specific position of Y46 in KCNE1 is significant in affecting S140G channel function.

A) L45 Mutations

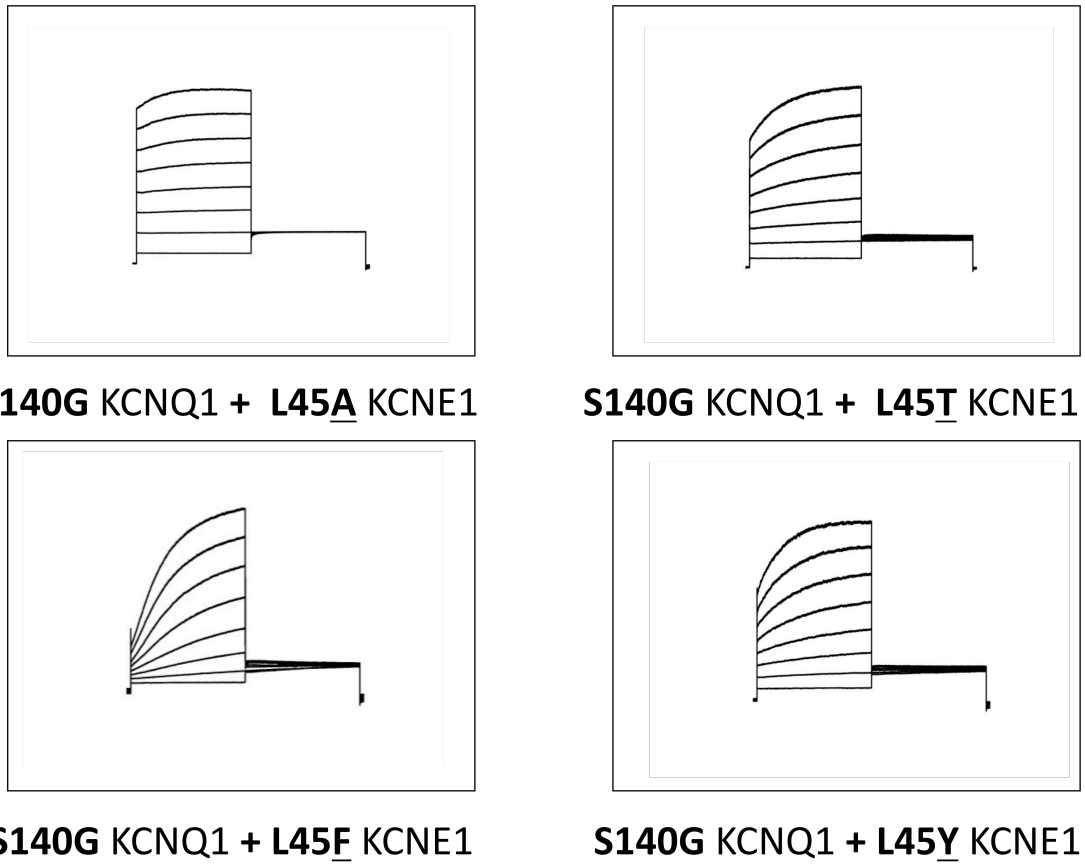

B) **Y46 Mutations**

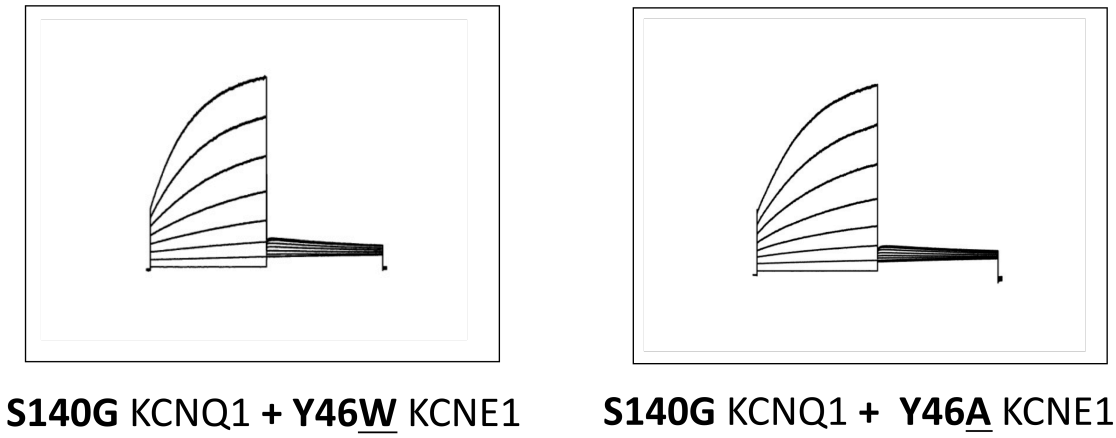

Figure 3-7. **Effects of different sized amino acids at positions L45 and Y46 on KCNE1.** Families of current traces recorded for S140G co-expressed with KCNE1 mutations made on

L45: Alanine, Threonine, Phenylalanine, Tyrosine (A) and made on Y46: Tryptophan, Alanine (B). Cells were depolarized from -60 mV to +80 mV in 20 mV increments for 2 s. Tail currents were measured at -40 mV for 2 s.

Discussion

Until recently, the amino-terminus of KCNE1 has not been studied in detail in terms of modulation of KCNQ1 channels. It was thought that this region was not necessary for control of channel gating (Takumi et al., 1991; Romey et al., 1997). The Kass lab group and others first show evidence that this region is involved in interactions with the S1 domain and the pore region of KCNQ1, shown through crosslinking studies (Xu et al., 2008; Chung et al., 2009). Here, we demonstrate for the first time that the amino-terminus of KCNE1 is likely an important region for control of deactivation kinetics and may play a role in modulation of the KCNQ1 channel.

We scanned the KCNE1 amino-terminus for mutations that could restore channel function when co-expressed with the KCNQ1 AF mutants, S140G and V141M. We looked for mutations that fixed the slow deactivation effect of the mutations, thus resulting in channels that would exhibit less pedestal current during repetitive pulses. Two mutations, L45F and Y46W, when co-expressed with either S140G or V141M, both helped to fix the slow deactivation defect and produced channels that resembled WT I_{Ks} channels. Upon further analysis, we find that the Y46W mutation, when co-expressed with WT KCNQ1 separates the effects of activation from deactivation in the channel.

Altogether, these results point out several findings: (1) the Y46W mutation in KCNE1 separates the effects of activation from deactivation and (2) L45F is a unique mutation able to alter S140G and V141M channel function, (3) Y46 is in a specific location able to alter S140G and V141M channel function, and (4) the L45F and Y46W mutations behave like a less

functional KCNE1 subunit. These results highlight this region of KCNE1 as an important region of modulatory control of the KCNQ1 channel.

Previously, in Chapter II, we demonstrated that the V141M mutation relies on KCNE1 co-expression for the channel to exhibit slow deactivation kinetics and additionally, there is a structural proximity of KCNE1 to this residue. Based on these results, it is understandable that mutations made at the upper TM region of KCNE1, L45F and Y46W, would have large effects on channel function. In this case, these two KCNE1 mutants are located in the same upper TM region where there is structural proximity and functionally, they fix the slow deactivation defect when co-expressed with the V141M mutation, by allowing channels to be closed during the interpulse interval (11 s) at a relatively physiological holding potential (-80 mV), thus producing channels that resemble I_{Ks}.

Co-expression of the L45F and Y46W mutations with the S140G mutation could be rescuing the channels via a different route, which can also be applied to the V141M mutation. In a previous study, it was demonstrated that certain salt bridge interactions were involved in the mechanism of slowing of the S140G and V141M mutations (Restier et al 2008). It is possible that the L45F and Y46W mutations could be affecting the stability of the salt bridges formed between S2 and S4. For the L45F mutation specficially, this leucine residue is mutated to a larger phenylalanine residue, which may alter the packing of the KCNQ1 channel complex. This residue is also oriented towards the S1 domain, so it could be directly pushing on the S1 domain, which could alter the salt bridge interactions that seem to stabilize the open states of the S140G or V141M mutations (Smith et al., 2007). For the Y46W mutation, the tyrosine residue is also mutated to a larger residue, tryptophan, and is facing the other direction, away from the S1 domain and is oriented towards S6, based on the current KCNQ1 structural model. It is possible

that the Y46W mutation could be interacting the pore domain in the upper TM region and affecting channel gating via a different route. This hypothesis is supported by evidence indicating proximity of the S6 domain and KCNE1 in the extracellular regions flanking the TM region (Chung et al. 2009).

CHAPTER IV

Functional Studies of the KCNQ1 S140T Mutation

Background and Significance

Ion channels must maintain a specific intra-membrane structure, with specific interactions between its individual transmembrane segments. Mutation of residues, which are involved in these specific interactions, are expected to disrupt the structure and thus the function of the protein. In Chapter II, two mutations in the KCNQ1 channel (S140G and V141M) were investigated and shown to specifically disrupt channel deactivation kinetics. In Chapter III, scanning mutagenesis of amino-terminal KCNE1 residues were characterized for mutations that would restore channel function in the S140G and V141M mutations. We find that several KCNE1 mutations fit this role, L45F and Y46W. However, one question that remains is why are those specific mutations, S140G and V141M, able to disrupt channel deactivation so dramatically? One group substituted various amino acids at positions 140 and 141 to see what were the effects of other mutations, but they concluded that only the S140G and V141M mutations caused the most dramatic changes in channel deactivation (Restier et al., 2008). Here, we characterize the functional effects of one mutation in KCNQ1, S140T, which causes a significant change in channel function. In contrast to the S140G mutation, the functional effects include a large depolarizing shift in voltage dependence of activation, and very rapid deactivation kinetics.

Residue S140 was mutated to a polar residue, Threonine, and the biophysical changes in channel function were characterized in a mammalian expression system. The S140T channels

expressed well in CHO cells in contrast to a previous report of this mutation, S140T, which was reported to cause a complete loss of KCNQ1 function. However, those experiments were conducted in *Xenopus* oocytes, in which depolarizations to voltages greater than +60 mV could not be performed due to possible activation of endogenous K^+ currents (Restier et al., 2008). Threonine was chosen as the amino acid for substitution at position 140 based on the volume change it would incur: the S140T mutation would have an added volume of 27 $Å^3$, in contrast to the loss of 29 $Å^3$ with the S140G mutation.

Results

Functional Characterization of S140T in the absence of KCNE1

The functional effects of the S140T mutation were characterized in cells expressing only KCNQ1 channels (Figure 4-1B). The following experiments were carried out in external solutions containing physiological K^+ concentration (5 mM). These experiments were also done in elevated K^+ solution (120 mM) to better evaluate the tail currents, but the data produced the same results as those shown here. Channels assembled with the S140T mutation resemble WT channels (Figure 4-1A and 4-1B). S140T channels ($V_{1/2}$ = -24.08 ± 0.9 mV, *n*=4) and WT KCNQ1 channels ($V_{1/2}$ = -26. 27 ± 1.8 mV, *n*=6) exhibited similar activation $V_{1/2}$'s, in contrast to that of S140G channels with ($V_{1/2}$ = - 57.5 ± 1.3 mV, *n*= 5) (Figure 4-1D). Deactivation kinetics were significantly different for S140T channels (τ_{deact} = 0.21 ± 0.018 s, *n*=6) compared with both WT KCNQ1 (τ_{deact} = 0.081 ± 0.014 s, *n*=6) and S140G channels (τ_{deact} = 0.67 ± 0.11 s, *n*=6) (Figure 4-1E).

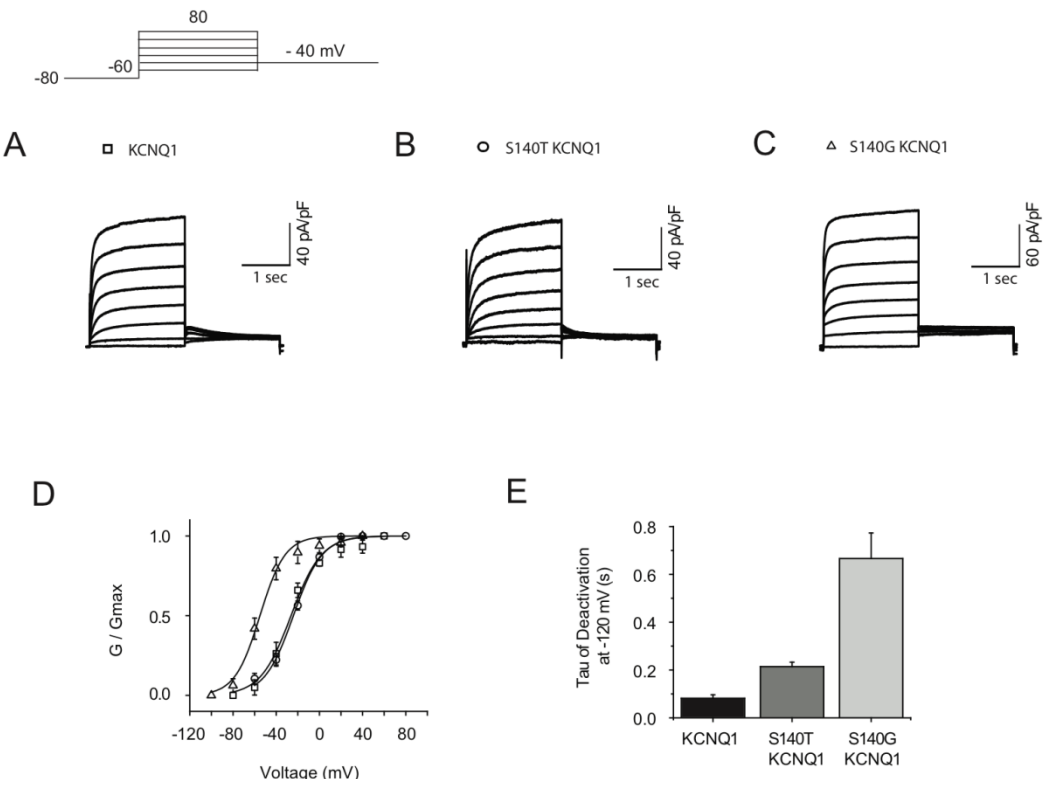

Figure 4-1. **S140T, in contrast to S140G, resembles homomeric WT KCNQ1 channels.** Representative families of currents traces in cells expressing WT KCNQ1 (A), S140T (B), and S140G (C) in the absence of KCNE1. Currents in response to 2 s pulses from -60 mV to +80 mV in 20 mV increments from a -80 mV holding potential. (D) Normalized isochronal (2 s) activation curves for KCNQ1 (squares), S140T (circles), and S140G (triangles). (E) Deactivation time constant (tau) obtained at -120 mV from single exponential fits to tail currents following conditioning pulses (+20 mV, 2 sec). Data are shown as mean ± s.e.m.

Functional Characterization of S140T in the presence of KCNE1

The impact of KCNE1 co-expression on channel properties was investigated with KCNQ1 carrying the S140T mutation. A pulse protocol consisting of a series of 2 s isochronal activating pulses (-60 mV to + 80 mV) was applied as we measured the impact of KCNE1 co-expression on activation gating. Representative current traces for S140T KCNQ1, assembled with KCNE1, reveal channels that do not exhibit much activation using the voltage protocol shown above trace, in contrast with WT I_{Ks} channels (Figure 4-2A and 4-2B). Because of this,

we applied a different protocol, consisting of 2 s activating pulses starting from +20 mV to +160 mV, applied at the same rate as the original protocol. We observed more channel opening in S140T/KCNE1 channels using this depolarized voltage range (Figure 4-2C).

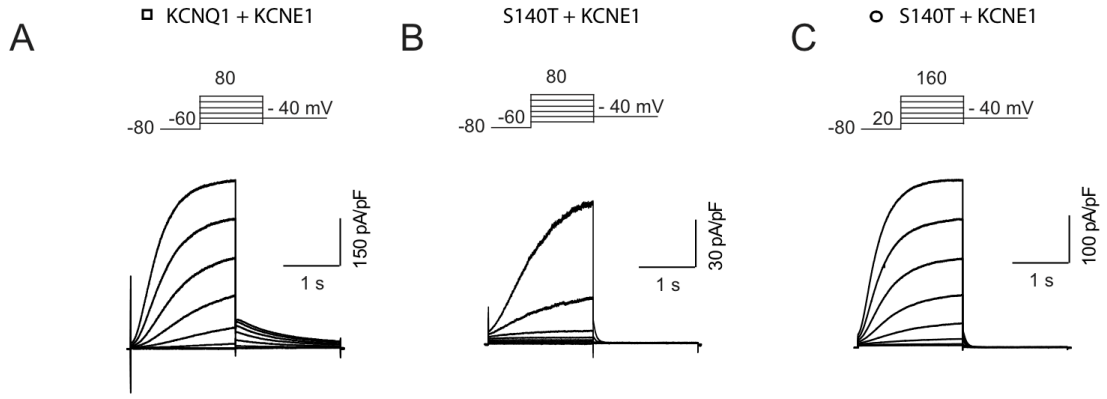

Figure 4-2. **S140T exhibits depolarizing shift in voltage dependence and fast deactivation kinetics.** Representative families of currents traces in cells expressing WT KCNQ1/KCNE1 (A) and S140T/KCNE1 (B and C) using stimulation protocol shown above traces.

The voltages for half maximal (isochronal) activation for channels consisting of KCNE1 co-expressed with three KCNQ1 variants were measured to compare voltage dependence of activation gating. S140T/KCNE1 channels ($V_{1/2}$ = 112 ± 1.86 mV, *n*=5) exhibited a significant depolarizing shift in voltage dependence from WT KCNQ1/KCNE1 channels ($V_{1/2}$ = 17.5 ± 2.6 mV, *n*=6) in contrast to S140G/KCNE1 ($V_{1/2}$ = 1.5 ± 2.7 mV, *n*=4) channels, which exhibited a hyperpolarizing shift from WT KCNQ1/KCNE1 channels (Figure 4-3A). Next, I_{Ks} activation kinetics were compared by measuring the time ($t_{1/2}$) at which I_{Ks} current is half maximally activated at the voltage closest to the $V_{1/2}$ for each subunit combination. Activation kinetics for the S140T/KCNE1 channel ($t_{1/2}$ = 0.6 ± 0.06 s, *n*=4) are two-fold faster than WT

KCNQ1/KCNE1 channels ($t_{1/2}$ = 1.1 ± 0.031 s, n=4), and nearly three-fold faster than S140G/KCNE1 channels ($t_{1/2}$ = 1.5 ± 0.035 s, n=4) (Figure 4-3B).

Deactivation kinetics of the S140T mutant channels with KCNE1 were subsequently investigated. To compare deactivation for the different KCNQ1/KCNE1 pairs, the deactivation time constants (tau) were measured from tail currents at -120 mV in response to a 2 s depolarizing pulse. The deactivation tau for S140T / KCNE1 (τ_{deact} = 0.045 ± 0.006 s, n=4) is significantly faster than both KCNQ1 / KCNE1 channels (τ_{deact}= 0.24 ± 0.004 s, n=5) and S140G (τ_{deact}= 4.09 ± 0.2 s, n=6) (Figure 4-3C).

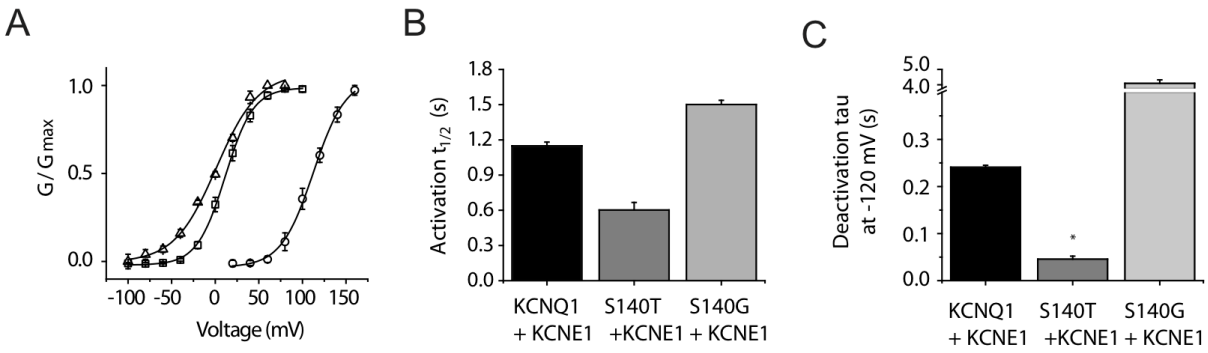

Figure 4-3. **S140T and S140G channels exhibit contrasting biophysical effects in the presence of KCNE1.** (A) Normalized isochronal (2 s) activation curves for KCNQ1 (squares), S140T (circles), and S140G (triangles) in the presence of KCNE1. Activation $t_{1/2}$ (B) and deactivation time constant (tau) (C) obtained at -120 mV from single exponential fits to tail currents following conditioning pulses (+20 mV, 2 sec). Data are shown as mean ± s.e.m. * (p <0.05)

Influence of KCNE1

Expression of the S140T mutation in KCNQ1 subunits alone exhibited properties similar to WT KCNQ1 channels. However, upon KCNE1 co-expression, S140T channels exhibited a

large shift in voltage dependence and a speeding of deactivation, so we wanted to compare the impact of KCNE1 co-expression in all KCNQ1 variants. To evaluate the effect of KCNE1 on the channel's voltage dependence, we measured the $\Delta V_{1/2}$ by subtracting the $V_{1/2}$ from KCNQ1 subunits alone from the $V_{1/2}$ of KCNQ1 subunits in the presence of KCNE1 (Figure 4-4A). The co-expression of KCNE1 with S140T channels exhibited a 137 ± 0.62 mV (n=5) depolarizing shift in voltage dependence, while KCNE1 co-expression with WT KCNQ1 or S140G channels exhibit similar shifts of 45 ± 0.6 mV (n=6) and 48 ± 2.2 mV (n=6), respectively. Next, to evaluate the effect of KCNE1 on channel deactivation, we examined the fold change in deactivation time constants of the KCNQ1 mutations in the absence and presence of KCNE1. The fold change is the ratio of deactivation tau from the KCNQ1 / KCNE1 channels: deactivation tau from the KCNQ1 subunit alone. S140T/KCNE1 channels exhibited less than 0.5 fold difference in channel deactivation, in contrast to S140G/KCNE1 channels, which exhibited a 8-fold difference (Figure 4-4B).

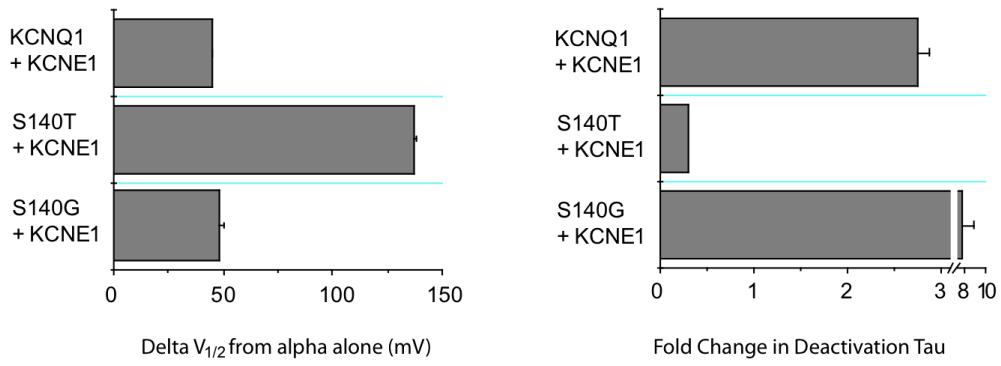

Figure 4-4. **The impact of KCNE1 exhibits opposing effects when co-expressed with S140T vs. S140G.** $\Delta V_{1/2}$ (A) and fold change in deactivation time constant (tau) (B) analyzed for KCNQ1, S140T, and S140G to demonstrate the influence of KCNE1 on voltage dependence of activation and deactivation kinetics. Data are shown as mean ± s.e.m.

Amino-Terminal KCNE1 Mutations

As had been previously described in Chapter III, the amino terminus of KCNE1 was screened for residues that might counter the functional consequences of the S140T mutation. KCNE1 residues starting at the extracellular end of the predicted KCNE1 helix (residues A44 through L51) were mutated to amino acids that would incur a loss of volume of 27 $Å^3$ at that residue.

KCNE1 mutations, when co-expressed with S140T KCNQ1, were tested for activity that restored channel activity similar to WT IKs channels. Representative recordings are shown for S140T KCNQ1 co-expressed with KCNE1 residues: A44G, L45V, Y46L, V47T, L48V, M49V, and L51V (Figure 4-5).

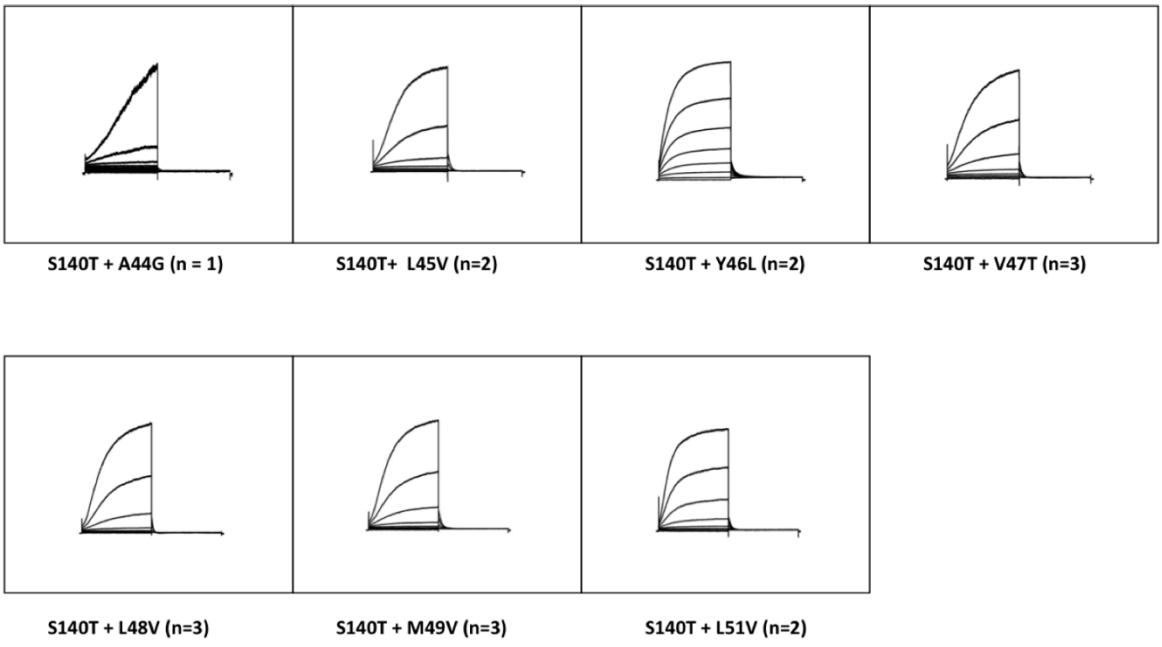

Figure 4-5. **Amino-terminal KCNE1 mutations co-expressed with S140T mutation.** Families of current traces shown for S140T KCNQ1 co-expressed with KCNE1 residues: A44G, L45V, Y46L, V47T, L48V, M49V, and L51V. Currents in response to 2 s pulses from -60 mV to +80 mV in 20 mV increments from -80 mV holding potential.

Among the KCNE1 mutants tested, the Y46L KCNE1 mutation exhibited more open channel activity at the beginning of the test pulse. The functional impact of these mutations on voltage dependence of activation is summarized in a graph (Figure 4-6A). S140T/Y46L channels ($V_{1/2}$ = 19.8 ± 1.7 mV, *n*=4) exhibited a hyperpolarizing shift in voltage dependence from S140T/KCNE1 channels ($V_{1/2}$ = 114 ± 3.7 mV, *n*=6), bringing the $V_{1/2}$ closer to that of WT KCNQ1/KCNE1 channels ($V_{1/2}$ = 17.5 ± 2.6 mV, *n*=6). Other KCNE1 mutations expressed with S140T exhibited a range of voltage dependences of activation, indicating biophysical changes from those mutations.

Deactivation kinetics of the KCNE1 mutations co-expressed with S140T were analyzed next. The tau of deactivation was measured from repolarizing currents at – 40 mV in response to 2 s depolarizing pulses at +60 mV and the results are summarized in a bar graph (Figure 4-6B). Co-expression of WT and mutant KCNE1 subunits with S140T speeds deactivation dramatically compared with WT I_{Ks} channels. However, Y46L co-expression with S140T exhibited a slower deactivation tau (τ_{deact} = 0.13 ± 0.005 s, *n*=6) compared to the rest of the mutations (τ_{deact} < 0.1 s).

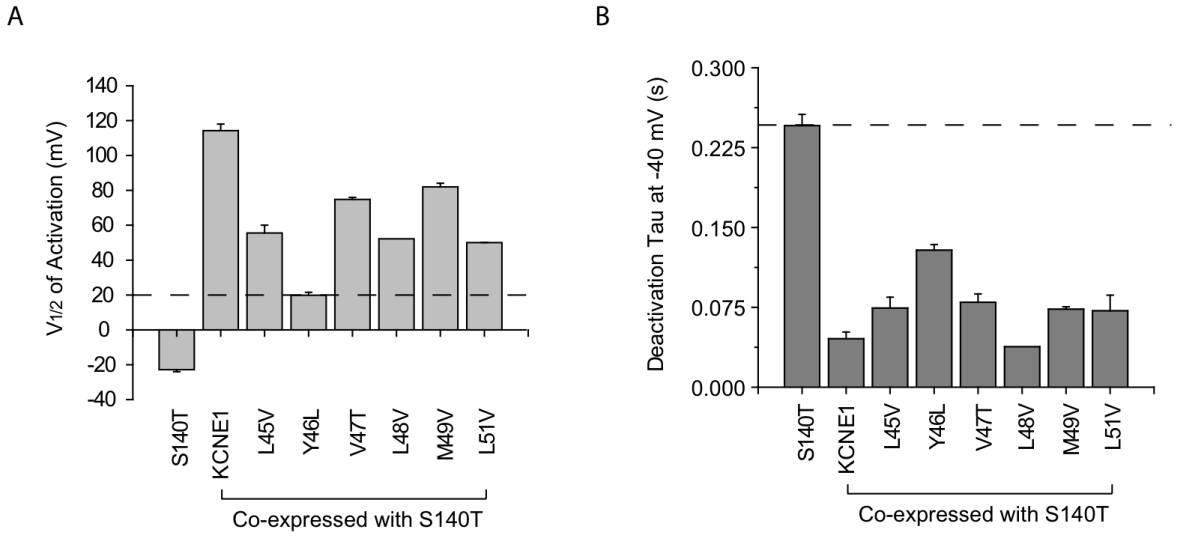

Figure 4-6. **Y46L KCNE1 mutation co-expressed with S140T produce channels that resemble WT KCNQ1/KCNE1 channels.** $V_{1/2}$ of activation (A) and deactivation time constant (tau) measured at -40 mV (B) for KCNE1 mutations co-expressed with S140T mutation. Dashed line indicates WT KCNQ1/KCNE1 channels.

Function of Single KCNE1 Mutations with WT KCNQ1

The functional characteristics of the single KCNE1 mutants were tested with WT KCNQ1 (Figure 4-7A). Substitutions of amino acids in residues A44 – L51 in KCNE1 co-expressed with KCNQ1 exhibited various shifts in voltage dependence of activation (Figure 4-7B). These mutations caused various effects on channel gating, but this data did not contribute much to determine the mechanism of the S140T mutation on channel function.

A

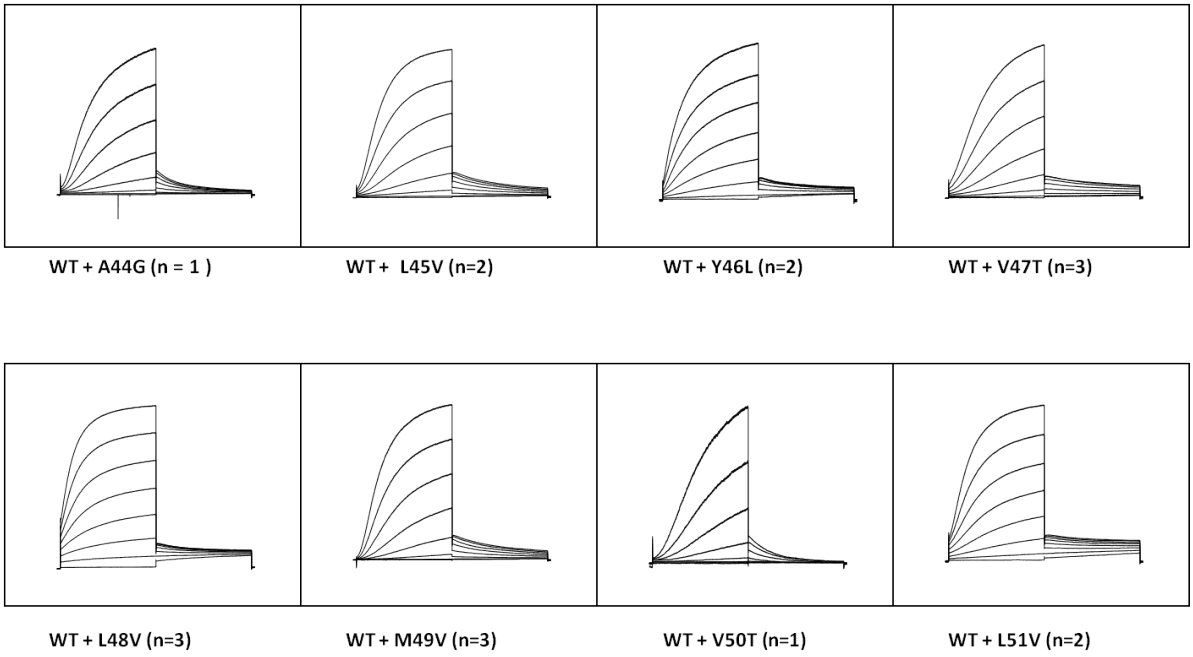

B

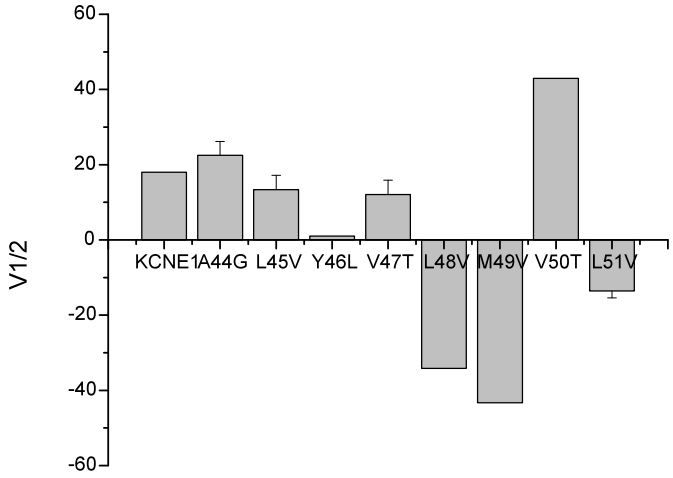

Figure 4-7. **Function of single KCNE1 mutations co-expressed with WT KCNQ1 channels.** Representative families of current traces (A) and $V_{1/2}$ of activation (B) summarized for KCNE1 mutations co-expressed with WT KCNQ1.

Discussion

Here, we find distinct effects of two mutations engineered at the same residue S140. A glycine at position 140 causes a hyperpolarizing shift in voltage dependence of activation gating and markedly slow deactivation kinetics. In contrast, a threonine at position 140 causes the opposite effects, a depolarizing shift in voltage dependence and a speeding of deactivation kinetics. Originally, we had set out to investigate whether the partial dependence on KCNE1 of the S140G mutation and its effects on KCNQ1 homomeric channel function is due to the specific glycine mutation at this position. We find that the S140G mutation is distinct from the S140T mutation in that S140G alters homomeric KCNQ1 channel function, while S140T does not. S140T expressed in KCNQ1 channels resembles WT KCNQ1 channel behavior, both in voltage dependence of activation and deactivation kinetics.

In Chapter II, we had demonstrated a unique dependence on KCNE1 for two different mutations, S140G and V141M, which we correlated with the orientation of the two residues relative to KCNE1. V141M is positioned next to KCNE1, while S140G is positioned away from KCNE1. However, here we demonstrate that a mutation at S140T is dependent on KCNE1 for its dramatic biophysical changes on channel function. In the presence of KCNE1, we see a large depolarizing shift of about ~90 mV in voltage dependence and a five-fold speeding of deactivation, compared to WT IKs channels. Due to the contrasting dependencies on KCNE1 for two mutations made at the same residue, we cannot explain the mechanism of these mutations in terms of orientation relative to the KCNE1 subunit.

However, KCNE1 mutations made at residue Y46, when co-expressed with S140G or S140T, dramatically alter channel behavior and these assembled channels resemble WT I_{Ks} channels. It is hard to say exactly how the mutations in each subunit are interacting to make the

channel more wild-type like, but we know that there is some type of interaction between S140 on KCNQ1 and Y46 on KCNE1, which may not be a direct physical interaction, but an allosteric interaction that has a big effect on altering channel behavior, perhaps by destabilizing salt bridge interactions. Another hypothesis for why the Y46 residue is a particular hotspot for altering channel function is based on predictions from the current KCNQ1 structural model. Using this model, the Y46 residue on KCNE1 is predicted to be oriented away from the S1 domain where S140 is located and is instead oriented towards the S6 domain. These predictions suggest that mutations made on the Y46 residue could somehow be interacting with the channel pore and affect channel gating via this route.

To summarize, the S140G mutation is a unique mutation that is interacting with a region of the channel that controls KCNQ1 channel function, and is not completely dependent on KCNE1 for these changes. S140T is a mutation that dramatically alters channel function, but these changes are dependent on the presence of KCNE1. The behavior of both mutations can be changed with co-expression of a mutant at Y46 on KCNE1, in which the assembled channels resemble WT I_{Ks} channels. Altogether, residue S140 is sensitive to mutation and must be located in or near an area of the channel complex important for control of the channel's function.

CHAPTER V

Significance of KCNE1 Location and Assembly in the I_{Ks} Channel Complex

Background and Significance

Currently, there is no evidence for coordinated transcription of KCNQ1 and KCNE1 genes. However, there have been studies investigating the transcriptional control for the KCNQ1 or KCNE1 genes, individually. In a study by Mustapha et al 2007, this group characterized the promoter for the cardiac KCNE1 gene. They demonstrate that there are specific regions in the KCNE1 promoter, which are important for transcriptional and tissue specific control. Additionally, differences in the core promoter sequences for KCNE1 for different species may account for the species variation in KCNE1 expression, such as in mouse there is low I_{Ks} density vs. in human, where there is much higher I_{Ks} density. In another study characterizing the transcriptional control of both hERG and KCNQ1 genes, it was concluded that both promoters of these potassium channel genes were GC-rich, contained multiple Sp1 (stimulating protein) binding sites and lacked consensus TATA boxes (Luo et al. 2008). These three elements of the promoter for two potassium channel genes were also found to be present in the KCNE1 promoter (Mustapha et al. 2007). Although it has not been investigated, it is possible that there is coordinated transcriptional control of the KCNQ1 and KCNE1 genes due to the similarity in promoter elements for both genes.

Following the transcription of both KCNQ1 and KCNE1 genes, how exactly do these proteins coassmeble to form I_{Ks} channels? A recent study demonstrated that co-expression with KCNQ1 subunits promotes KCNE1 trafficking to the cell surface (Chandrasekhar et al. 2006).

They also show that KCNQ1 coassembles with KCNE1 early in the secretory pathway and that KCNE1 subunits alone do not get fully glycosylated unless they are assembled with KCNQ1. After co-assembly of KCNQ1 and KCNE1 subunits, how is the stoichiometry determined for these channels?

The co-assembly of a KCNQ1 tetrameric channel with two KCNE1 subunits is sufficient for modulation of channel function (Chen et al., 2003a; Morin and Kobertz, 2008), although the possibility of multiple stoichiometries was not ruled out in these studies (Wang et al., 1998). A recent study reported that the stoichiometry of the KCNQ1 and KCNE1 complex is variable, ranging from 4:1 to 4:4, in which up to 4 KCNE1 subunits can associate with the KCNQ1 tetramer (Nakajo et al., 2010). Currently, there is no evidence of stoichiometry regulation for KCNQ1/KCNE1 subunits given that the stoichiometry can vary, indicating that all stoichiometries are possible. In the heart, it is possible that stoichiometry is controlled by the relative amount of KCNE1 expressed in a specific chamber (Soma et al. 2010). In the studies by both the Kass and Isacoff groups, they also find that channels formed by tandem KCNQ1/KCNE1 constructs could be further modulated by co-expression of additional KCNE1 protein. For the 2:1 fusion protein, two KCNQ1s linked to one KCNE1, they observe currents similar to I_{Ks} that could be modulated with additional KCNE1 protein, altering activation kinetics. However, the fusion protein with one KCNQ1 and one KCNE1 could not be further modulated, indicating that 4 is the maximal number of KCNE1 subunits that can associate with the KCNQ1 tetramer. Now that the stoichiometry of KCNQ1/KCNE1 subunits in the channel complex is determined to be variable, the importance of how and where KCNE1 assembles is the next step in fully understanding how this subunit modulates the KCNQ1 channel.

Results

Part I – Significance of Location of KCNE1 in Channel Complex

Recent studies demonstrate variable stoichiometry in the channel complex (Nakajo et al., 2010), indicating that there will not only be KCNQ1/KCNE1 channels with a 4:4 stoichiometry expressed at the cell membrane, but that there could be channels 4:1, 4:2, and 4:3 stoichiometry, in which for these channels, not every KCNQ1 subunit will be associated with a KCNE1 subunit. We set out to investigate the importance of KCNE1 assembly next to a specific KCNQ1 subunit, using the V141M and S140G mutations. In Chapter II, we learn that the V141M mutation, but not S140G, is dependent on the presence of KCNE1, functionally and structurally, for the mutation-induced effects on channel function. In the absence of KCNE1, we observed that KCNQ1 channels encoded with V141M exhibit WT KCNQ1 channel behavior. First, we functionally characterize channels with a 4:4 and 4:2 stoichiometries encoded with the S140G and V141M mutations. With the 4:2 channel constructs, we engineer the S140G or V141M mutations into the proximal (close to KCNE1) or distal (far from KCNE1) KCNQ1 subunits and measure the effects on channel properties (Figure 5-1). We find that channels with a 4:2 stoichiometry exhibit less of the mutation-induced slowing of deactivation kinetics on channel function, compared with channels with a 4:4 stoichiometry. Additionally, channels with 4:2 stoichiometry, in which KCNE1 is assembled next to the mutated KCNQ1 subunit, exhibit slower deactivation kinetics, compared to constructs where KCNE1 is not assembled next to the mutated KCNQ1 subunit.

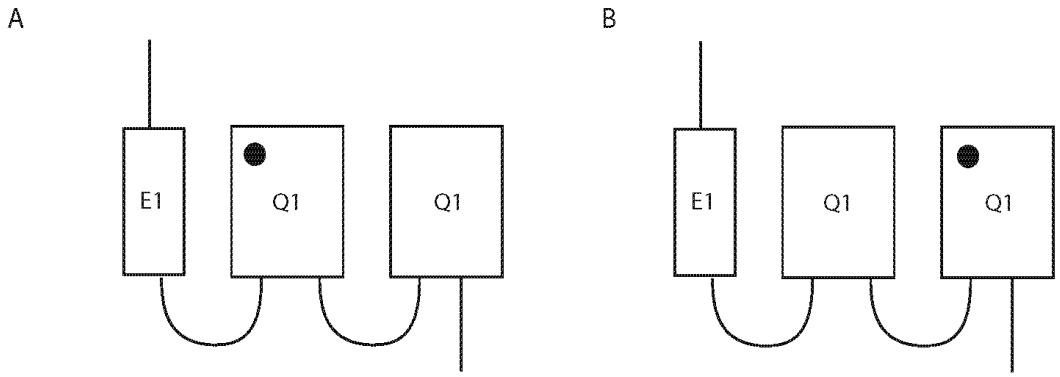

Figure 5-1. **Schematic of EQQ Tandem Constructs.** (A) EQQ with mutation (black circle) in proximal KCNQ1 subunit, closest to KCNE1 (B) EQQ with mutation in distal KCNQ1 subunit, furthest from KCNE1

Functional Studies

EQ S140G and EQ V141M (4:4 stoichiometry)

We measured the effect of the S140G and V141M mutations in a fusion construct, where one KCNQ1 is linked to one KCNE1, thus fixing a 4:4 stoichiometry in channel complexes. A series of 2 s isochronal activating pulses was applied from -60 mV to + 80 mV to measure the effect of theses mutations on channel gating. Current traces shown for both S140G and V141M EQ channels display an accumulation of open channels resulting from channels that did not have time to close in between depolarizing pulses due to mutation-altered slowing of deactivation kinetics (Figure 5-2A and 5-2B). For channels containing the V141M mutation, current traces indicated a time-dependent decay after depolarization, which is typical for these channels expressed in CHO cells. It is possible that after applying a depolarizing pulse, all channels are open due to the large pedestal current that is seen on current traces. Then, during the depolarization, a large amount of potassium has exited the cell due to the open channels, causing an increase in the extracellular potassium concentration. So the decay in current could reflect

the fact that intra/extracellular potassium concentrations have changed and perhaps the driving force for potassium efflux is not as big as it was during the initial depolarization.

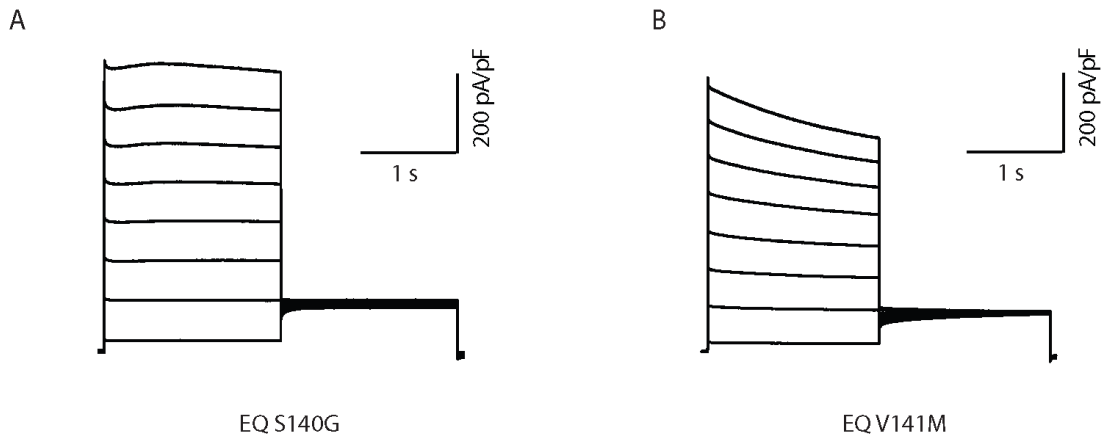

Figure 5-2. **S140G and V141M Channels in Fixed 4:4 Stoichiometry display constituitive currents.** Representative families of currents traces in cells expressing S140G (A) and V141M (B) in EQ fusion constructs. Currents in response to 2 s pulses from -60 mV to +80 mV in 20 mV increments from -80 mV holding potential.

EQQ S140G Proximal vs. EQQ S140G Distal

The impact of the S140G mutation, engineered into the proximal (EQQ Q1 S140G) or distal (EQQ Q2 S140G) KCNQ1 subunit in tandem constructs, on channel properties was investigated next. A pulse protocol consisting of a series of 2 s isochronal activating pulses (-60 mV to + 80 mV) was applied as we measured the effect of the S140G mutation on different KCNQ1 subunits on channel gating. Representative current traces shown for EQQ Q1 S140G constructs reveal channels that exhibit slow deactivation kinetics and some pedestal current compared with WT I_{Ks} channels, whereas current traces shown for EQQ Q2 S140G channels exhibit faster deactivation kinetics than EQQ Q1 S140G channels (Figure 5-3A and 5-3B). The

voltage at which half the channels are activated was measured from tail current amplitudes and EQQ Q1 S140G ($V_{1/2}$ = -2.3 ± 3.39 mV) and Q2 S140G ($V_{1/2}$ = -5.4 ± 1.99 mV) channels both exhibit a slight hyperpolarizing shift in voltage dependence of activation from WT I_{Ks} channels ($V_{1/2}$ = 33.6 ± 2.4 mV) (Figure 5-3C). Further examination of deactivation kinetics indicates that the $t_{1/2}$ of deactivation measured at -120 mV for EQQ Q2 S140G channels ($t_{1/2}$ = 0.309 s) is not significantly different from WT I_{Ks} channels ($t_{1/2}$ = 0.159 s), but for EQQ Q1 S140G channels deactivation is much slower than EQQ Q2 S140G channels ($t_{1/2}$ = 1.306 s) (Figure 5-4A and 5-4B).

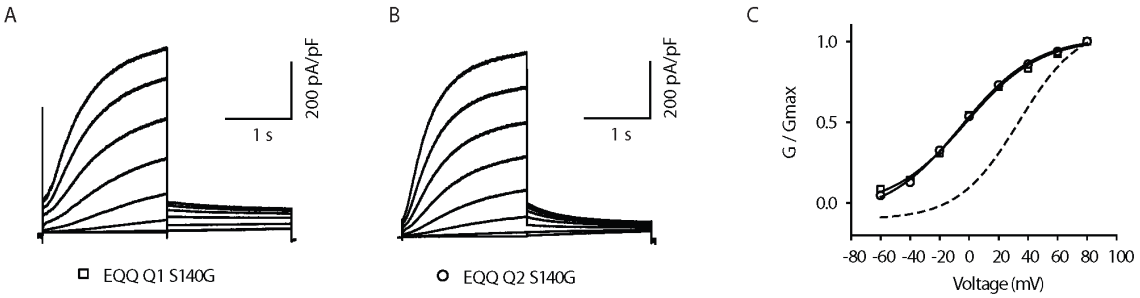

Figure 5-3. **Proximal and Distal S140G Channels in Fixed 4:2 Stoichiometry display similar shifts in voltage dependence.** Representative families of currents traces in cells expressing Q1 S140G (A) Q2 S140G (B) in EQQ fusion constructs. Currents in response to 2 s pulses from -60 mV to +80 mV in 20 mV increments from a -80 mV holding potential. (C) Normalized isochronal (2 s) activation curves for Q1 S140G (squares) and Q2 S140G (circles) and WT KCNQ1/KCNE1 (dashed line).

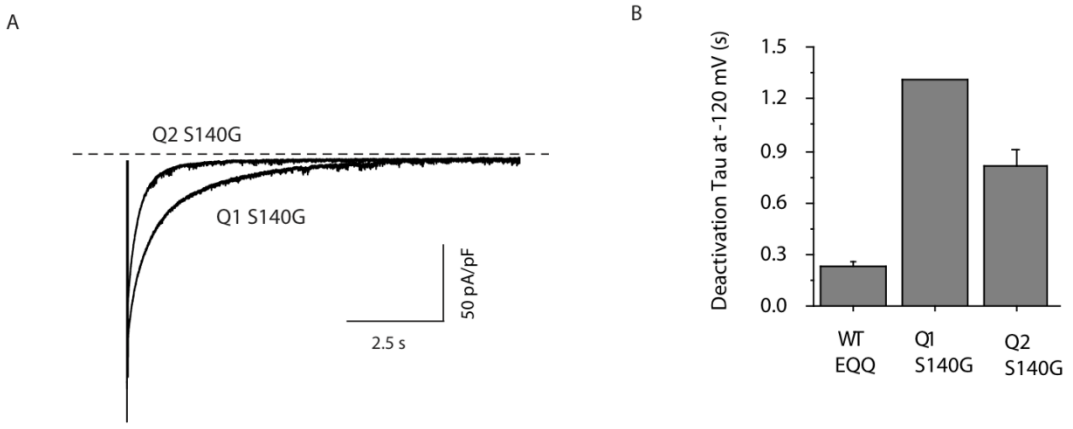

Figure 5-4. **S140G Channels in Fixed 4:2 Stoichiometry display slower deactivation kinetics in proximal vs. distal KCNQ1 subunit.** (A) Representative tail current traces in cells expressing Q1 S140G (A) Q2 S140G (B) in EQQ fusion constructs. (B) Deactivation $t_{1/2}$ obtained at -120 mV from single exponential fits to tail currents following conditioning pulses (+20 mV, 2 sec).

EQQ V141M Proximal vs. EQQ V141M Distal

We next investigated the impact of the V141M mutation, engineered into the proximal (EQQ Q1 V141M) or distal (EQQ Q2 V141M) KCNQ1 subunits of tandem constructs. The same pulse protocol consisting of a series of 2 s isochronal activating pulses (-60 mV to + 80 mV) was applied as we measured the effect of different locations of the V141M mutation with respect to the KCNE1 subunit. Current traces shown for EQQ Q1 V141M constructs reveal channels that exhibit slow deactivation kinetics and pedestal current similar to what was seen for EQQ Q1 S140G channels. Current traces shown for EQQ Q2 V141M channels exhibit faster deactivation kinetics than EQQ Q1 V141M channels (Figure 5-5A and 5-5B). The $V_{1/2}$ of activation gating was measured, showing that channels with the V141M mutations assembled next to KCNE1 exhibit a hyperpolarizing shift in voltage dependence. Channels with the V141M mutation ($V_{1/2}$ = 9.91 ± 0.91 mV, n=3) in the distal subunit exhibit similar voltage

dependence as WT I_{Ks} channels ($V_{1/2}$ = 13.04 ± 0.75 mV, n=7), while channels with V141M in the proximal KCNQ1 subunit exhibit a hyperpolarizing shift in voltage dependence ($V_{1/2}$ = -10.93 ± 1.28 mV, n=3) (Figure 5-5C). Further examination of deactivation kinetics indicates that the tau of deactivation measured at -120 mV for EQQ Q2 V141M channels (τ_{deact} = 0.32 ± 0.071 s, n=6) is slower than WT I_{Ks} channels (τ_{deact} = 0.24 ± 0.004 s, n=7) but is not as slow as that for EQQ Q1 V141M channels (τ_{deact} = 0.59 ± 0.05 s, n=7) (Figure 5-6).

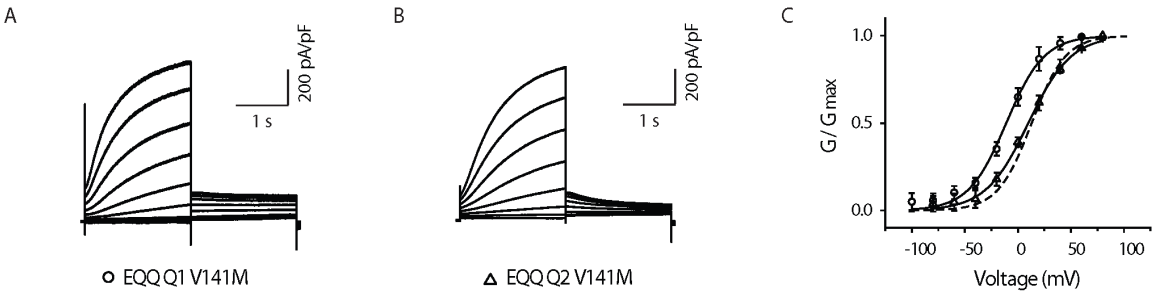

Figure 5-5. **Proximal V141M Channels in Fixed 4:2 Stoichiometry exhibit hyperpolarizing shift in voltage dependence vs. distal V141M Channels.** Representative families of currents traces in cells expressing Q1 V141M (A) Q2 V141M (B) in EQQ fusion constructs. Currents in response to 2 s pulses from -60 mV to +80 mV in 20 mV increments from a -80 mV holding potential. (C) Normalized isochronal (2 s) activation curves for Q1 V141M (circles) and Q2 V141M (triangles) and WT KCNQ1/KCNE1 (dashed line).

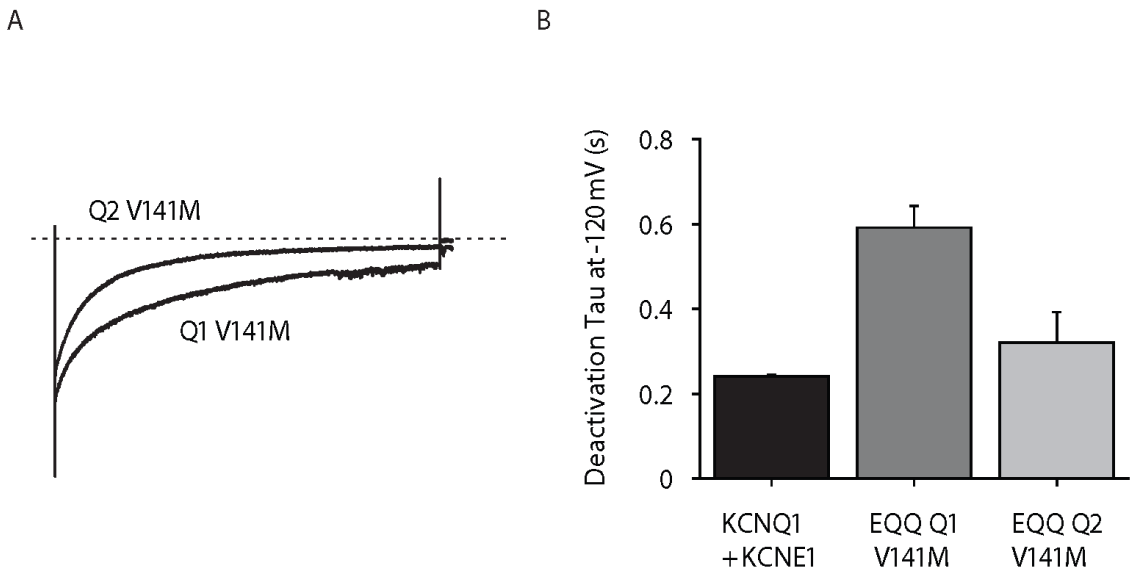

Figure 5-6. **V141M Channels in Fixed 4:2 Stoichiometry display slower deactivation kinetics in proximal vs. distal KCNQ1 subunit.** (A) Representative tail current traces in cells expressing Q1 V141M (A) Q2 V141M (B) in EQQ fusion constructs. (B) Deactivation time constant (tau) obtained at -120 mV from single exponential fits to tail currents following conditioning pulses (+20 mV, 2 sec). Data expressed as mean ± s.e.m.

Titrating additional KCNE1 Subunits

To investigate whether the fusion protein EQQ Q2 V141M could be modulated by additional KCNE1, we co-expressed KCNE1 with this fusion protein and characterized channel activity. As had been previously demonstrated by two separate groups, co-expression of fusion constructs can be further modulated by KCNE1 (Wang and Kass 1998, Nakajo and Isacoff 2010). Co-expression with additional KCNE1 slows EQQ Q2 V141M channel activation and deactivation kinetics of the EQQ Q2 V141M channels, compared to channels without additional KCNE1 (Figure 5-7A and 5-7B). In order to quantify these differences, we measured the voltage dependence of activation. Channels with the EQQ Q2 V141M mutation co-expressed with additional KCNE1 ($V_{1/2}$ = 3.32 ± 4.49 mV, n=4) exhibit a hyperpolarizing shift in voltage dependence, in contrast to WT EQQ channels with additional KCNE1 ($V_{1/2}$ = 43.6 ± 1.47 mV,

n=5), which exhibit a depolarizing shift (Figure 5-7C). WT EQQ ($V_{1/2}$ = 27.5 ± 4.56 mV, n=7) and EQQ Q2 V141M ($V_{1/2}$ = 22.7 ± 2.77 mV, n=7) channels exhibited similar voltage dependences on activation gating.

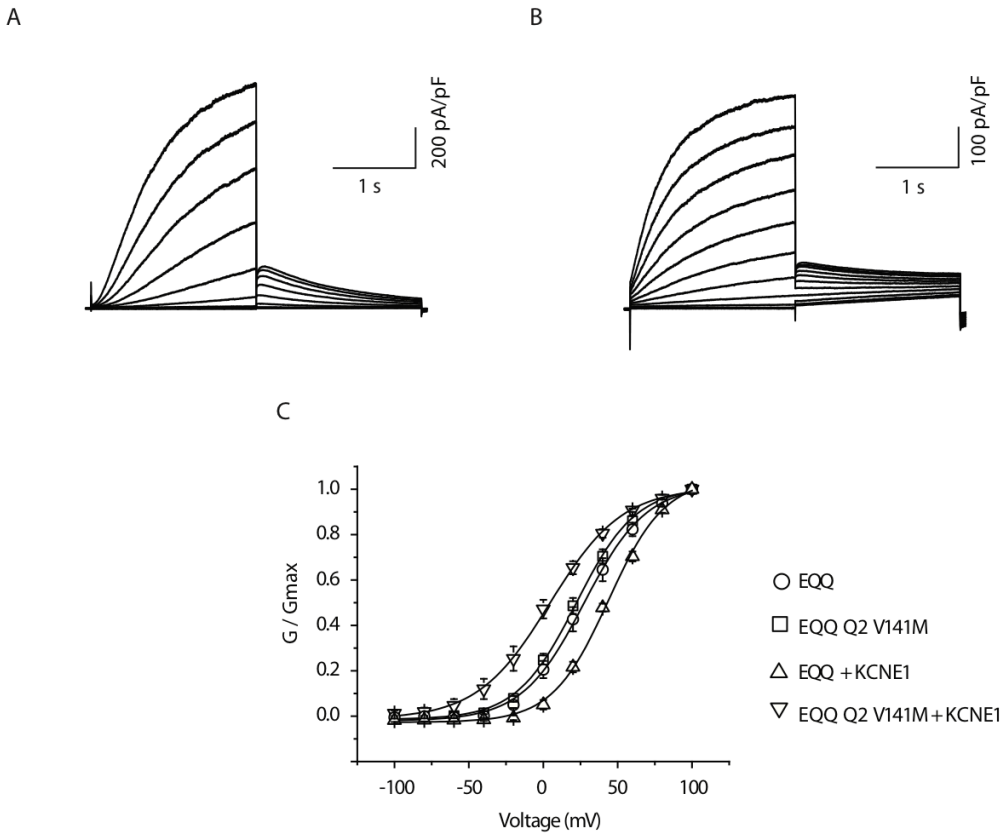

Figure 5-7. **Additional KCNE1 Subunits can further modulate V141M Channels in Fixed 4:2 Stoichiometry by slowing activation kinetics.** (A) Representative families of current traces in cells expressing EQQ Q2 V141M, without additional KCNE1 (A) and with additional KCNE1 subunits (B). (C) Normalized isochronal (2 s) activation curves for EQQ (circles), EQQ + KCNE1 (triangles), EQQ Q2 V141M (squares) and EQQ Q2 V141M + KCNE1 (inverted triangles). Data expressed as mean ± s.e.m.

To compare the effect of KCNE1 co-expression on deactivation kinetics, the deactivation time constant (tau) was measured from tail currents at -120 mV in response to a 2 s depolarizing pulse

to + 60 mV. Addition of KCNE1 to EQQ Q2 V141M channels exhibited much slower deactivation compared to cells without additional KCNE1 (Figure 5-8A). The deactivation time constant for EQQ Q2 V141M channels with additional KCNE1 (τ_{deact} = 0.664 ± 0.067 s, n=6) reveal a significantly slower time course for deactivation compared to channels without additional KCNE1 (τ_{deact} = 0.277 ± 0.017 s, n=7) and WT EQQ channels (τ_{deact} = 0.235 ± 0.024 s, n=5) and WT EQQ with additional KCNE1 (τ_{deact} = 0.329 ± 0.011 s, n=5) (Figure 5-8B).

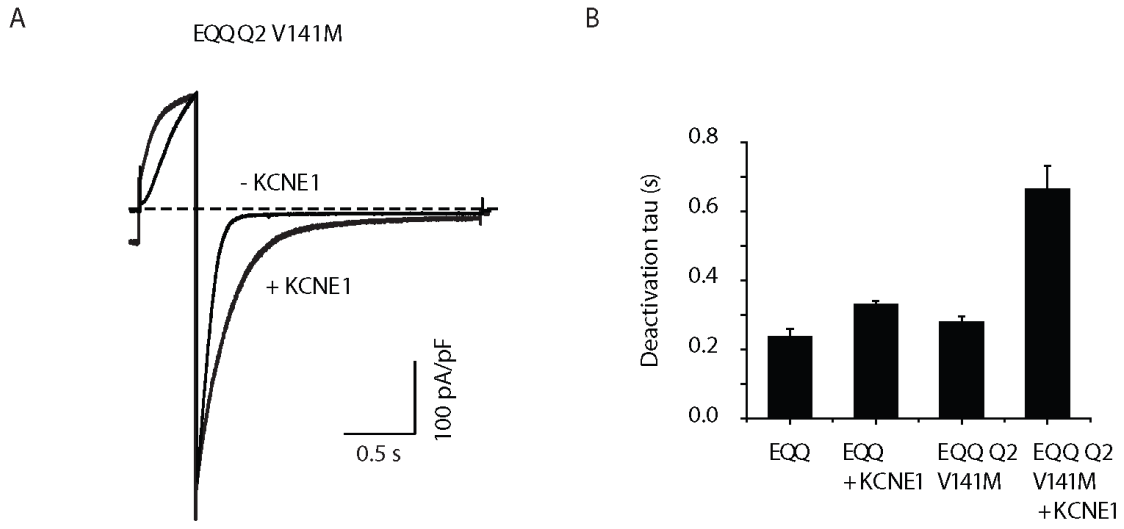

Figure 5-8. **Distal V141M Channels in Fixed 4:2 Stoichiometry are further modulated with additional KCNE1 subunits.** (A) Representative tail current traces in cells expressing EQQ Q2 V141M fusion constructs without additional KCNE1 and with additional KCNE1 (A). (B) Deactivation time constant (tau) obtained at -120 mV from single exponential fits to tail currents following conditioning pulses (+20 mV, 2 sec). Data expressed as mean ± s.e.m.

Part II –Assembly of KCNE1 in Channel Complex

Crosslinking Studies

The I_{Ks} channel is composed of a tetramer of pore-forming alpha subunits, KCNQ1, and accessory beta subunits, KCNE1. The location of KCNE1 has been positioned between the S1

and S6 domains of different alpha subunits (Xu et al., 2008; Chung et al., 2009). However, this positioning of KCNE1 is based on co-expression of individual alpha and beta subunits so it is not confirmed how the hetero-tetrameric channel assembles. In order to verify that KCNE1 assembles between the S1 segment from one KCNQ1 subunit and the S6 segment of an opposing KCNQ1 subunit, we monitor crosslinking between substituted cysteines engineered into the following tandem constructs: EQ (one KCNE1 tethered to one KCNQ1), and EQQ (one KCNE1 tethered to two KCNQ1s) to mimic the possibilities of a 4:4 and 4:2 stoichiometries. If the KCNQ1/KCNE1 channel assembles how we believe it does, then we would expect the same crosslinks to form in these tandem constructs. Additionally, we engineered an HRV-3C protease cleavage site between the C-terminus of KCNE1 and the N-terminus of the proximal KCNQ1. By monitoring the fully assembled KCNQ1/KCNE1 channel complex before and after cleavage, we will be able to identify how the channel assembles by monitoring a shift in molecular weights on the western blot.

In these constructs, we use specific cysteine substitutions shown to have the strongest crosslinks (~80%), based on previous work from our group. To demonstrate crosslinking between KCNE1 to S1 in the proximal KCNQ1 subunit, cysteines were substituted for the following residues, K41 in KCNE1 and I145 in KCNQ1 and this will be referred to as the S1 crosslink from now on. To demonstrate crosslinking between KCNE1 to S6 in the distal KCNQ1 subunit, cysteines were substituted for the following residues, L42 in KCNE1 and V324 in KCNQ1, which will be referred to as the S6 crosslink from here on.

EQ Crosslinking

We first set out to demonstrate that KCNE1 is positioned between the S1 and S6 domains of two different KCNQ1 subunits using constructs which have a forced 4:4 stoichiometry. Using EQ tandem constructs, with one KCNE1 tethered to one KCNQ1, we tested crosslinking for constructs $E_{K41C}Q_{I145C}$ to observe a crosslink between the S1 domain and KCNE1 and $E_{L42C}Q_{V324C}$ to observe a crosslink between the S6 domain and KCNE1. In these constructs, a HRV3C-cleavage site was engineered between the C-terminus of KCNE1 and N-terminus of KCNQ1 in order to fix the stoichiometry of channels first and then monitor crosslinking. Here, we observe the expected molecular weight band for the S1 crosslink at ~90 kD (E1: 20 kD + Q1: 70 kD) (Figure 5-9, *top panel*). However, for the S6 crosslink, we observe a high molecular weight band ~ 300 kD, which we suspect is an aggregate band consisting of a tetramer or more of KCNQ1/KCNE1 subunits. Upon addition of the HRV-3C protease, we cleave the EQ construct into individual subunits, KCNE1 and KCNQ1 to monitor the crosslinks that were formed. Here, we observe DTT-sensitive crosslinking with both the S1 and S6 crosslink constructs (Figure 5-9, *bottom panel*). The results for the S1 and S6 crosslinks confirm the findings from Chung et al 2009. However, the result that was hard to interpret was the S6 crosslink before HRV-3C cleavage. We believe that this channel may be in a conformation in which it is aggregated at the top of the gel and cannot be separated out, so it is possible that the EQ constructs are tangled up in a knot. Upon HRV-3C cleavage though, these subunits are separated and a crosslink can be monitored between the S6 domain and KCNE1, so the aggregate must be due to the linkage between E1 and Q1.

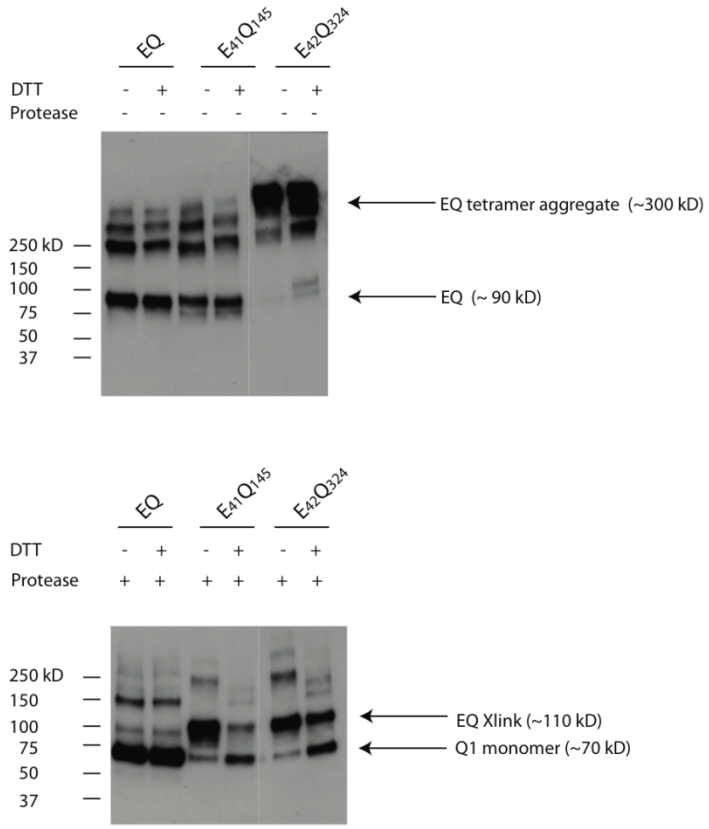

Figure 5-9. **EQ Crosslinking demonstrates crosslinking of KCNE1 between S1 and S6 KCNQ1 subunits.** Western blot of tandem constructs: $E_{K41C}Q_{I145C}$ to observe the crosslink between S1 and KCNE1 and $E_{L42C}Q_{V324C}$ to observe the crosslink between S6 and KCNE1 without (top panel) and with (bottom panel) HRV-3C protease treatment.

EQQ Crosslinking

Next, we set out to investigate crosslinking using EQQ tandem constructs, fixing the KCNQ1/KCNE1 channel in a 4:2 stoichiometry. The extents of KCNE1 to S1 and KCNE1 to S6 crosslinking will be determined by the density of the EQQ band at ~160 kD divided by the sum of densities of the bands at 70 kD (KCNQ1 monomer) and 280 kD (KCNQ1 tetramer). There

are two possible conclusions that we can draw from these experiments. The first possibility is that the tandem EQQ constructs are assembling in an anti-parallel manner to form a heterotetramer, as E-Q-Q. We will observe crosslinking between KCNE1 and S1 of the proximal KCNQ1 subunit and between KCNE1 and S6 of the distal subunit (Figure 5-10A). These results will support the idea that S1 on the proximal KCNQ1 and S6 on the distal KCNQ1 are not cross-linking to the same KCNE1 subunit. The second possibility is that the tandem EQQ construct is assembling in a different manner to form a heterotetramer, as Q-E-Q. In this case, we will observe a variety of crosslinks between KCNE1 and S1 of the proximal or distal KCNQ1 subunits and between KCNE1 and S6 of the proximal or distal subunits. These results will tell us that the heteromeric channel does not assemble in the way we think it is.

(A)

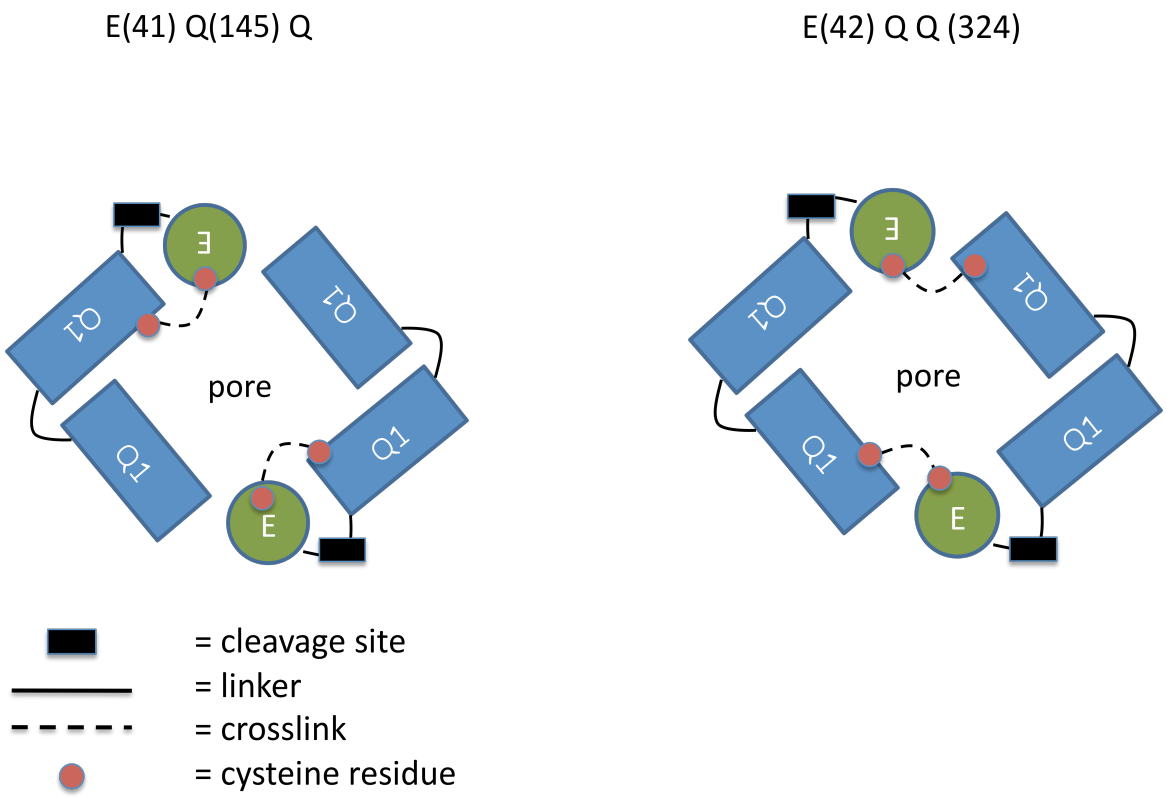

Figure 5-10. **Schematic Illustration of two possible outcomes for EQQ Tandem Crosslinking.** (A) Cartoon of expected crosslinking for $E_{K41C}Q_{I145C}Q$ and $E_{L42C}QQ_{V324C}$

As expected, we observe a molecular weight band at 160 kD, corresponding to the EQQ band for $E_{K41C}Q_{I145C}Q$ (Figure 5-11, *top panel*). For our two negative controls, $E_{K41C}QQ_{I145C}$ and $E_{L42C}Q_{V324C}Q$, we observed high molecular weight bands, which we suspect are aggregates of the channel. These two constructs are negative controls because if we expect the S1 crosslink to form between the cysteines in KCNE1 and the proximal KCNQ1 subunit, we would expect KCNE1 to not form crosslinks with the cysteine in the distal KCNQ1 subunit. Similarly, if we expect the S6 crosslink to form between KCNE1 and the distal KCNQ1 subunit, we would not observe crosslinking in the proximal KCNQ1 subunit.

Upon treatment with the HRV-3C protease, we observe the expected DTT-sensitive crosslink band for the $E_{K41C}Q_{I145C}Q$ (Figure 5-11, *bottom panel*). However, we also observe DTT-sensitive crosslink bands for the two negative control constructs, which is unexpected. These results suggest two ideas, one is that the channel is not assembling the way we think it is and the second is that there are unexpected crosslinks occurring.

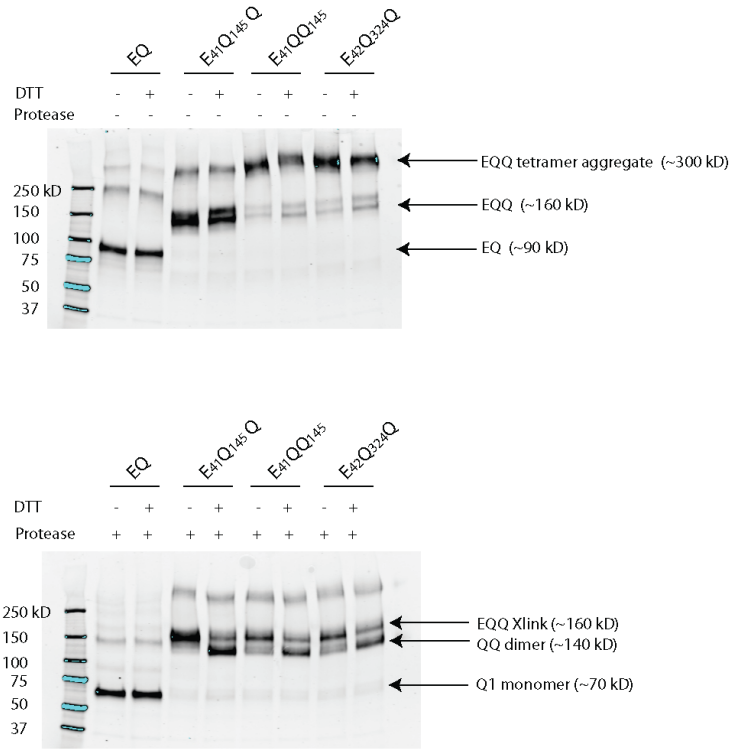

Figure 5-11. **EQQ Crosslinking demonstrates crosslinking of KCNE1 and S1 KCNQ1 subunit.** Western blot of tandem construct, $E_{K41C}Q_{I145C}Q$, to observe the crosslink between S1 and KCNE1 without (top panel) and with (bottom panel) HRV-3C protease treatement. $E_{K41C}QQ_{I145C}$ and $E_{L42C}Q_{V324C}Q$ are used for negative controls.

Discussion

In the current study, we studied the significance of KCNE1 assembly in the I_{Ks} channel complex. We find that assembly of KCNE1 next to a specific KCNQ1 subunit can determine the

severity of two AF KCNQ1 mutations, S140G and V141M. We functionally characterized the effect of having a mutation in a channel with 4:4 stoichiometry, where there are KCNE1 subunits assembled next to all KCNQ1 subunits and channels with 4:2 stoichiometry, in which KCNE1 is not assembled next to every KCNQ1 subunit. We observed that channels with 4:2 stoichiometry exhibit less severe effects of the mutation, compared to channels with 4:4 stoichiometry. This result demonstrates that having less than 4 KCNE1 subunits produces a channel with a less severe phenotype when KCNQ1 contains either AF mutation. Next, in channels with 4:2 stoichiometry, we functionally characterized two constructs, one to investigate the effect of having KCNE1 assembled next to the mutated KCNQ1 subunit and one where KCNE1 is not assembled next to the mutated KCNQ1. Channels where KCNE1 is assembled next to the mutated KCNQ1 subunit exhibit more severe effects of the mutation-induced slowing of deactivation kinetics, compared with channels where KCNE1 is not assembled next to the mutated KCNQ1. Due to the variable stoichiometry of KCNQ1/KCNE1 channels, we next investigated whether we could change the stoichiometry of the 4:2 channels to 4:4 channels by co-expressing additional KCNE1 subunits. We find that these 4:2 channels can be modulated with the addition of extra KCNE1 subunits, supporting the finding that the stoichiometry can be variable, ranging from 4:1 and up to 4:4 KCNQ1 to KCNE1 subunits.

CHAPTER VI

CONCLUSION

In the current thesis study, we investigated the nature of KCNQ1 / KCNE1 interactions in the I_{Ks} channel complex and their roles in altering the channel's biophysical properties. Chapter II examined two AF-associated KCNQ1 mutations and the complete dependence on the KCNE1 subunit for the mutation-induced slowing of deactivation kinetics for the V141M mutation, but not for S140G. In this section, biochemical evidence reveals a KCNQ1/KCNE1 interaction that is likely important in the mutation-altered channel properties for V141M, highlighting the amino-terminal end of KCNE1 and the proximal end of the S1 segment in KCNQ1 as important regions for control of channel deactivation. In Chapter III, we screened the amino-terminal region of KCNE1 and found two mutations that restored the slowed deactivation defect in the AF channels back towards a WT I_{Ks} channel. Chapter IV focused on the characterization of a mutation, S140T, in the proximal end of S1 KCNQ1, which had considerable effects on speeding channel deactivation. Chapter V focuses on the significance of the location and assembly of KCNE1 within the I_{Ks} channel complex. The results from these investigations emphasize the importance of the presence, proximity, orientation, location, and assembly of KCNE1 within the channel complex, which will guide us in eventually determining the mechanism of KCNE1 modulation of the KCNQ1 channel.

In Chapter II, we learn that the AF-associated mutations, S140G and V141M, depend differently on the presence of KCNE1 in order to exhibit slow deactivation kinetics. There are two possible mechanisms in which slowing of channel deactivation kinetics can occur, which include slowing by affecting the channel gate or slowing by affecting voltage sensor movement.

The V141M mutation relies entirely on KCNE1 to see a defect in channel deactivation and without this accessory subunit; the channel looks like a wild-type channel. In this case, KCNE1 could be interacting with the channel gate in order to slow channel closing which is supported by evidence demonstrating proximity between KCNE1 and the S6 domain of KCNQ1 (Chung et al. 2009). However, the S140G mutation slows channel closing in the absence of KCNE1, so it does not depend entirely on this subunit for changes in channel properties and must rely on a different mechanism of slowing deactivation kinetics. In this case, the S140G mutation could be affecting voltage sensor movement based on the predictions from the KCNQ1 structural model showing that the S140 residue is oriented towards the S4 domain.

These are only two examples of AF mutations that previously were both shown to depend entirely on KCNE1, but now display differential dependence on this subunit. There are other gain of function mutations, Q147R, S209P, R231C, I274V, A300T, and V307L, that are reported to rely on the presence of KCNE1 in order to see the mutation-induced effects on channel function, but perhaps more in depth analysis is needed to fully determine whether these mutation-altered channels depend on this accessory subunit (Bartos et al. 2009; Bianchi et al., 2000; Bellocq et al., 2004; Lundby et al., 2007; Rhodes et al., 2008; Das et al., 2009).

Subunit Orientation of KCNQ1 and KCNE1

Based on our functional experiments in Chapter II, the results of biochemical crosslinking results reveal a specific orientation of the S1 KCNQ1 domain, where residue V141 is in closest proximity to residue A44 on the KCNE1 subunit (Figure 2-17).

Amino-Terminus of KCNE1

Previously, the N-terminus of KCNE1 has been recognized as a region not necessary for modulatory control of KCNQ1 channels (Takumi et al., 1988; Tapper and George, 2000; Melman et al., 2004; Lvov et al., 2010). However, the Kass lab group highlighted the extracellular N-terminal region of KCNE1 in a crosslinking study, where the discovery of close KCNQ1/KCNE1 interactions led to the placement of KCNE1 within the I_{Ks} channel complex (Chung et al., 2009). In the current investigation, we emphasize the amino-terminus of KCNE1 as a region important for control of channel deactivation kinetics.

In Chapter III, two mutations in the amino terminal region of KCNE1, L45F and Y46W, were found to improve the slow deactivation defect characteristic of the AF mutants. Functional characterization of the KCNE1 mutants co-expressed with the AF mutants was done to determine how deactivation kinetics was being affected. The effects of the two mutations, L45F and Y46W, when co-expressed with the AF mutants, produce channels that resemble WT I I_{Ks} channels. However, upon further analysis of channel properties, these two KCNE1 mutations behave differently, when co-expressed with the WT KCNQ1 channel. The differential effects of the L45F and Y46W mutations is likely due to their orientation on the KCNE1 helix, where L45F is oriented towards the S1 helix, but Y46W is not. We conclude that KCNE1 mutations, L45F and Y46W, are helping to speed the deactivation process, but the mechanism of this effect is undetermined. Thus far, we have highlighted four residues in KCNE1, E43, A44, L45, and Y46, in which each have either a structural and/or functional role in altering KCNQ1 channel properties.

Chapter IV focuses on the significance of position S140 in the S1 helix of KCNQ1. Substitution of a glycine at S140 produced channels that exhibited extremely slow deactivation kinetics, however substitution of a threonine at S140 produced channels that speed deactivation

kinetics greatly. Here, we demonstrate that the proximal end of the S1 helix is sensitive to mutations that greatly alter deactivation kinetics of the channel.

In order to further test the upper TM region of KCNQ1 and KCNE1 as an area of important control of deactivation kinetics, mutations can be engineered into the KCNE1 subunit to see whether deactivation kinetics can be specifically controlled. For example, from our experiments in the current investigation, we know the KCNE1 residues A44, L45, and Y46 are hotspots in altering channel deactivation properties. For future experiments, these three residues could be mutated to all possible amino acids to see if hydrophobicity or polarity of residue may play a role in affecting the ability of the mutated KCNE1 to alter KCNQ1 channel gating properties.

Having established the importance of proximity of KCNE1 to the S1 segment of KCNQ1, we investigated this property in populations of channels where there are multiple stoichiometries of KCNQ1: KCNE1 subunits in Chapter V. We explored the functional consequences of the S140G and V141M mutations in channels with a fixed 4:2 stoichiometry, compared to channels with a 4:4 stoichiometry. In channels with a 4:2 stoichiometry, we find that channels where KCNE1 is in proximity to the mutation exhibit more mutation-induced changes compared to channels where KCNE1 is not assembled next to the mutation. Thus, when KCNQ1 and KCNE1 subunits assemble into channels in the endoplasmic reticulum, the location of KCNE1 assembly within the KCNQ1 channel complex is important for the resultant channel that traffics to the surface, especially if it is a mutation that is dependent on KCNE1 for altering channel properties. In the case of S140G, if KCNE1 does not assemble next to this mutation, the resultant channel will still have a defect in deactivation. In contrast, for the V141M mutation, if KCNE1 does not assemble next to this mutation, the channel will behave like a WT I_{Ks} channel.

In this section, we attempt to confirm the assembly of the I_{Ks} channel, using tandem constructs in a 4:4 or 4:2 fixed KCNQ1: KCNE1 subunit ratios. We wanted to demonstrate crosslinking of KCNE1 between the S1 and S6 domains of KCNQ1, as had been shown previously (Chung et al 2009). Using the EQ constructs, to fix channels in a 4:4 stoichiometry, we were able to clearly demonstrate crosslinking between KCNE1 and the S1 helix. Similarly, with the EQQ constructs, to fix channels in a 4:2 stoichiometry, we observe crosslinking between KCNE1 and S1 KCNQ1. However, for crosslinking with the S6 domain of KCNQ1, the results were inconclusive.

In order to assemble a more complete story for the tandem constructs in Chapter V, other control experiments and constructs must be functionally characterized. It would be interesting to engineer either the S140G or V141M mutations into both KCNQ1 subunits in the EQQ construct to see how channel gating is affected and subsequently co-expressing additional KCNE1 subunits to see if stoichiometry can be maximized. We would compare these experiments to the individual co-expression of KCNQ1 containing either AF mutation and KCNE1. Another experiment would be to see how channels containing either the S140G or V141M mutation in both subunits of a QQ dimer construct might behave and comparing these results to our functional results testing the mutation in a single KCNQ1 subunit.

Taken together, the work in this thesis reveals the distinct dependence of KCNE1 for the mutation-altered deactivation kinetics of the S140G and V141M mutations. Not only is the presence of KCNE1 within the channel complex important, but also the proximity of this accessory subunit to the S1 segment of KCNQ1. The thesis also establishes a role for the N-terminus of KCNE1 in modulation of KCNQ1 channels, specifically in control of deactivation kinetics. The modulation of KCNE1 is not only provided by the transmembrane domain and the

C-terminus, but also by the association of the N-terminus. Furthermore, the significance of location and assembly of KCNE1 within the channel complex is essential in understanding the variable effects that can result from channels with multiple stoichiometries of KCNQ1: KCNE1 subunits.

REFERENCES

Abbott, G.W., F. Sesti, I. Splawski, M.E. Buck, M.H. Lehmann, K.W. Timothy, M.T. Keating, and S.A. Goldstein. 1999. MiRP1 forms IKr potassium channels with HERG and is associated with cardiac arrhythmia. *Cell*. 97:175-187.

Abitbol, I., A. Peretz, C. Lerche, A.E. Busch, and B. Attali. 1999. Stilbenes and fenamates rescue the loss of I(KS) channel function induced by an LQT5 mutation and other IsK mutants. 18:4137-4148.

Aggeli, A., M.L. Bannister, M. Bell, N. Boden, J.B. Findlay, M. Hunter, P.F. Knowles, and J.C. Yang. 1998. Conformation and ion-channeling activity of a 27-residue peptide modeled on the single-transmembrane segment of the IsK (minK) protein. *Biochemistry*. 37:8121-8131.

Ahern, C.A., and R. Horn. 2004. Specificity of charge-carrying residues in the voltage sensor of potassium channels. *J Gen Physiol*. 123:205-216.

Akabas, M.H., D.A. Stauffer, M. Xu, and A. Karlin. 1992. Acetylcholine receptor channel structure probed in cysteine- substitution mutants. 258:307-310.

Angelo, K., T. Jespersen, M. Grunnet, M.S. Nielsen, D.A. Klaerke, and S.P. Olesen. 2002. KCNE5 induces time- and voltage-dependent modulation of the KCNQ1 current. *Biophysical journal*. 83:1997-2006.

Barhanin, J., F. Lesage, E. Guillemare, M. Fink, M. Lazdunski, and G. Romey. 1996. K(V)LQT1 and lsK (minK) proteins associate to form the I(Ks) cardiac potassium current. *Nature*. 384:78-80.

Bartos, D.C., S. Duchatelet, D.E. Burgess, D. Klug, I. Denjoy, R. Peat, J.M. Lupoglazoff, V. Fressart, M. Berthet, M.J. Ackerman, C.T. January, P. Guicheney, and B.P. Delisle. 2009. R231C mutation in KCNQ1 causes long QT syndrome type 1 and familial atrial fibrillation. *Heart Rhythm*. 8:48-55.

Bell, D.C., H. Yao, R.C. Saenger, J.H. Riley, and S.A. Siegelbaum. 2004. Changes in local S4 environment provide a voltage-sensing mechanism for mammalian hyperpolarization-activated HCN channels. *J Gen Physiol*. 123:5-19.

Bellocq, C., A.C. van Ginneken, C.R. Bezzina, M. Alders, D. Escande, M.M. Mannens, I. Baro, and A.A. Wilde. 2004. Mutation in the KCNQ1 gene leading to the short QT-interval syndrome. *Circulation*. 109:2394-2397.

Ben-Efraim, I., Y. Shai, and B. Attali. 1996. Cytoplasmic and extracellular IsK peptides activate endogenous K+ and Cl- channels in Xenopus oocytes. Evidence for regulatory function. *J Biol Chem*. 271:8768-8771.

Bendahhou, S., C. Marionneau, K. Haurogne, M.M. Larroque, R. Derand, V. Szuts, D. Escande, S. Demolombe, and J. Barhanin. 2005. In vitro molecular interactions and distribution of KCNE family with KCNQ1 in the human heart. *Cardiovasc Res*. 67:529-538.

Bezanilla, F. 2005. The voltage-sensor structure in a voltage-gated channel. *Trends Biochem Sci*.

Bianchi, L., S.G. Priori, C. Napolitano, K.A. Surewicz, A.T. Dennis, M. Memmi, P.J. Schwartz, and A.M. Brown. 2000. Mechanisms of I(Ks) suppression in LQT1 mutants. *Am J Physiol Heart Circ Physiol*. 279:H3003-3011.

Blumenthal, E.M., and L.K. Kaczmarek. 1994. The minK potassium channel exists in functional and nonfunctional forms when expressed in the plasma membrane of Xenopus oocytes. *Journal of Neuroscience*. 14:3097-3105.

Chandrasekhar, K.D., T. Bas, and W.R. Kobertz. 2006. KCNE1 subunits require co-assembly with K+ channels for efficient trafficking and cell surface expression. *J Biol Chem*.

Chen, H., and S.A. Goldstein. 2007. Serial perturbation of MinK in IKs implies an alpha-helical transmembrane span traversing the channel corpus. *Biophysical journal*. 93:2332-2340.

Chen, H., L.A. Kim, S. Rajan, S. Xu, and S.A. Goldstein. 2003a. Charybdotoxin binding in the I(Ks) pore demonstrates two MinK subunits in each channel complex. *Neuron*. 40:15-23.

Chen, H., F. Sesti, and S.A. Goldstein. 2003b. Pore- and state-dependent cadmium block of I(Ks) channels formed with MinK-55C and wild-type KCNQ1 subunits. *Biophysical journal*. 84:3679-3689.

Chen, J., R. Zheng, Y.F. Melman, and T.V. McDonald. 2009. Functional interactions between KCNE1 C-terminus and the KCNQ1 channel. *PLoS One*. 4:e5143.

Chen, Y.H., S.J. Xu, S. Bendahhou, X.L. Wang, Y. Wang, W.Y. Xu, H.W. Jin, H. Sun, X.Y. Su, Q.N. Zhuang, Y.Q. Yang, Y.B. Li, Y. Liu, H.J. Xu, X.F. Li, N. Ma, C.P. Mou, Z. Chen, J. Barhanin, and W. Huang. 2003c. KCNQ1 gain-of-function mutation in familial atrial fibrillation. *Science*. 299:251-254.

Chung, D.Y., P.J. Chan, J.R. Bankston, L. Yang, G. Liu, S.O. Marx, A. Karlin, and R.S. Kass. 2009. Location of KCNE1 relative to KCNQ1 in the I(KS) potassium channel by disulfide cross-linking of substituted cysteines. *Proc Natl Acad Sci U S A*. 106:743-748.

Curran, M., D. Atkinson, K Timothy, G.M. Vincent, A.J. Moss, M. Leppert, M. Keating. 1993. Locus Heterogeneity of autosomal dominant long QT syndrome. *J Clin Invest*. 92: 799-803.

Das, S., S. Makino, Y.F. Melman, M.A. Shea, S.B. Goyal, A. Rosenzweig, C.A. Macrae, and P.T. Ellinor. 2009. Mutation in the S3 segment of KCNQ1 results in familial lone atrial fibrillation. *Heart Rhythm*. 6:1146-1153.

Dedek, K., and S. Waldegger. 2001. Colocalization of KCNQ1/KCNE channel subunits in the mouse gastrointestinal tract. *Pflugers Arch*. 442:896-902.

Doyle, D.A., J. Morais Cabral, R.A. Pfuetzner, A. Kuo, J.M. Gulbis, S.L. Cohen, B.T. Chait, and R. MacKinnon. 1998. The structure of the potassium channel: molecular basis of K+ conduction and selectivity. *Science*. 280:69-77.

Drici, M.D., I. Arrighi, C. Chouabe, J.R. Mann, M. Lazdunski, G. Romey, and J. Barhanin. 1998. Involvement of IsK-associated K+ channel in heart rate control of repolarization in a murine engineered model of Jervell and Lange- Nielsen syndrome. *Circulation Research*. 83:95-102.

Durell, S.R., I.H. Shrivastava, and H.R. Guy. 2004. Models of the structure and voltage-gating mechanism of the shaker K+ channel. *Biophysical journal*. 87:2116-2130.

Folander, K., J.S. Smith, J. Antanavage, C. Bennett, R.B. Stein, and R. Swanson. 1990. Cloning and expression of the delayed-rectifier IsK channel from neonatal rat heart and diethylstilbestrol-primed rat uterus. *Proceedings of the National Academy of Sciences of the United States of America*. 87:2975-2979.

Gage, S.D., and W.R. Kobertz. 2004. KCNE3 truncation mutants reveal a bipartite modulation of KCNQ1 K+ channels. *J Gen Physiol*. 124:759-771.

Goldstein, S.A., and C. Miller. 1993. Mechanism of charybdotoxin block of a voltage-gated K+ channel. *Biophysical journal*. 65:1613-1619.

Goldstein, S.A.N., and C. Miller. 1991. Site-specific mutations in a minimal voltage-dependent K+ channel alter ion selectivity and open-channel block. *Neuron*. 7:403-408.

Grunnet, M., T. Jespersen, H.B. Rasmussen, T. Ljungstrom, N.K. Jorgensen, S.P. Olesen, and D.A. Klaerke. 2002. KCNE4 is an inhibitory subunit to the KCNQ1 channel. *The Journal of physiology*. 542:119-130.

Haitin, Y., I. Yisharel, E. Malka, L. Shamgar, H. Schottelndreier, A. Peretz, Y. Paas, and B. Attali. 2008. S1 constrains S4 in the voltage sensor domain of Kv7.1 K+ channels. *PLoS ONE*. 3:e1935.

Heitzmann, D., V. Koren, M. Wagner, C. Sterner, M. Reichold, I. Tegtmeier, T. Volk, and R. Warth. 2007. KCNE beta subunits determine pH sensitivity of KCNQ1 potassium channels. *Cell Physiol Biochem*. 19:21-32.

Hong, K., D.R. Piper, A. Diaz-Valdecantos, J. Brugada, A. Oliva, E. Burashnikov, J. Santos-de-Soto, J. Grueso-Montero, E. Diaz-Enfante, P. Brugada, F. Sachse, M.C. Sanguinetti, and R. Brugada. 2005. De novo KCNQ1 mutation responsible for atrial fibrillation and short QT syndrome in utero. *Cardiovasc Res*. 68:433-440.

Howard, R.J., K.A. Clark, J.M. Holton, and D.L. Minor, Jr. 2007. Structural insight into KCNQ (Kv7) channel assembly and channelopathy. *Neuron*. 53:663-675.

Hwang, C., A.J. Sinskey, and H.F. Lodish. 1992. Oxidized redox state of glutathione in the endoplasmic reticulum. *Science*. 257:1496-1502.

Jan, L.Y., and Y.N. Jan. 1997. Voltage-gated and inwardly rectifying potassium channels. *The Journal of physiology*. 505 (Pt 2):267-282.

Jiang, Y., A. Lee, J. Chen, V. Ruta, M. Cadene, B.T. Chait, and R. MacKinnon. 2003a. X-ray structure of a voltage-dependent K+ channel. *Nature*. 423:33-41.

Jiang, Y., V. Ruta, J. Chen, A. Lee, and R. MacKinnon. 2003b. The principle of gating charge movement in a voltage-dependent K+ channel. *Nature*. 423:42-48.

Kang, C., C. Tian, F.D. Sonnichsen, J.A. Smith, J. Meiler, A.L. George, Jr., C.G. Vanoye, H.J. Kim, and C.R. Sanders. 2008. Structure of KCNE1 and implications for how it modulates the KCNQ1 potassium channel. *Biochemistry*. 47:7999-8006.

Kurokawa, J., J.R. Bankston, A. Kaihara, L. Chen, T. Furukawa, and R.S. Kass. 2009. KCNE variants reveal a critical role of the beta subunit carboxyl terminus in PKA-dependent regulation of the IKs potassium channel. *Channels (Austin)*. 3:16-24.

Kurokawa, J., L. Chen, and R.S. Kass. 2003. Requirement of subunit expression for cAMP-mediated regulation of a heart potassium channel. *Proc Natl Acad Sci U S A*. 100:2122-2127.

Kurokawa, J., H.K. Motoike, and R.S. Kass. 2001. TEA(+)-sensitive KCNQ1 constructs reveal pore-independent access to KCNE1 in assembled I(Ks) channels. *J Gen Physiol*. 117:43-52.

Kurz, L.L., R.D. Zuhlke, H.J. Zhang, and R.H. Joho. 1995. Side-chain accessibilities in the pore of a K+ channel probed by sulfhydryl-specific reagents after cysteine-scanning mutagenesis. *Biophysical journal*. 68:900-905.

Larsson, H.P., O.S. Baker, D.S. Dhillon, and E.Y. Isacoff. 1996. Transmembrane movement of the shaker K+ channel S4. *Neuron*. 16:387-397.

Lee, M.P., J.D. Ravenel, R.J. Hu, L.R. Lustig, G. Tomaselli, R.D. Berger, S.A. Brandenburg, T.J. Litzi, T.E. Bunton, C. Limb, H. Francis, M. Gorelikow, H. Gu, K. Washington, P. Argani,

J.R. Goldenring, R.J. Coffey, and A.P. Feinberg. 2000. Targeted disruption of the kvlqt1 gene causes deafness and gastric hyperplasia in mice. 106:1447-1455.

Lee, S.Y., A. Banerjee, and R. MacKinnon. 2009. Two separate interfaces between the voltage sensor and pore are required for the function of voltage-dependent K(+) channels. *PLoS Biol*. 7:e47.

Lesage, F., B. Attali, J. Lakey, E. Honore, G. Romey, E. Faurobert, M. Lazdunski, and J. Barhanin. 1993. Are Xenopus oocytes unique in displaying functional IsK channel heterologous expression? *Receptors Channels*. 1:143-152.

Liu, G., S.I. Zakharov, L. Yang, S.X. Deng, D.W. Landry, A. Karlin, and S.O. Marx. 2008a. Position and Role of the BK Channel {alpha} Subunit S0 Helix Inferred from Disulfide Crosslinking. *J Gen Physiol*. 131:537-548.

Liu, G., S.I. Zakharov, L. Yang, R.S. Wu, S.X. Deng, D.W. Landry, A. Karlin, and S.O. Marx. 2008b. Locations of the beta1 transmembrane helices in the BK potassium channel. *Proc Natl Acad Sci U S A*. 105:10727-10732.

Long, S.B., E.B. Campbell, and R. Mackinnon. 2005a. Crystal structure of a mammalian voltage-dependent Shaker family K+ channel. *Science*. 309:897-903.

Long, S.B., E.B. Campbell, and R. Mackinnon. 2005b. Voltage sensor of Kv1.2: structural basis of electromechanical coupling. *Science*. 309:903-908.

Long, S.B., X. Tao, E.B. Campbell, and R. MacKinnon. 2007. Atomic structure of a voltage-dependent K+ channel in a lipid membrane-like environment. *Nature*. 450:376-382.

Lundby, A., L.S. Ravn, J.H. Svendsen, S.P. Olesen, and N. Schmitt. 2007. KCNQ1 mutation Q147R is associated with atrial fibrillation and prolonged QT interval. *Heart Rhythm*. 4:1532-1541.

Luo, X., J. Xiao, H. Lin, Y. Lu, B. Yang, and Z. Wang. 2008. Genomic structure, transcriptional control, and tissue distribution of HERG1 and KCNQ1 genes. *Am J Physiol Heart Circ Physiol.* 294:1371-80.

Lvov, A., S.D. Gage, V.M. Berrios, and W.R. Kobertz. 2010. Identification of a protein-protein interaction between KCNE1 and the activation gate machinery of KCNQ1. *J Gen Physiol*. 135:607-618.

MacKinnon, R. 1991. Determination of the subunit stoichiometry of a voltage-activated potassium channel. *Nature*. 350:232-235.

MacKinnon, R. 1995. Pore loops: an emerging theme in ion channel structure. [Review]. *Neuron*. 14:889-892.

MacKinnon, R., and C. Miller. 1988. Mechanism of charybdotoxin block of the high-conductance, Ca2+- activated K+ channel. *Journal of General Physiology*. 91:335-349.

MacKinnon, R., and G. Yellen. 1990. Mutations affecting TEA blockade and ion permeation in voltage- activated K+ channels. 250:276-279.

Marx, S.O., J. Kurokawa, S. Reiken, H. Motoike, J. D'Armiento, A.R. Marks, and R.S. Kass. 2002. Requirement of a macromolecular signaling complex for beta adrenergic receptor modulation of the KCNQ1-KCNE1 potassium channel. *Science*. 295:496-499.

Melman, Y.F., A. Domenech, S. de la Luna, and T.V. McDonald. 2001. Structural determinants of KvLQT1 control by the KCNE family of proteins. *J Biol Chem*. 276:6439-6444.

Melman, Y.F., A. Krumerman, and T.V. McDonald. 2002. A single transmembrane site in the KCNE-encoded proteins controls the specificity of KvLQT1 channel gating. *J Biol Chem*. 277:25187-25194.

Melman, Y.F., S.Y. Um, A. Krumerman, A. Kagan, and T.V. McDonald. 2004. KCNE1 binds to the KCNQ1 pore to regulate potassium channel activity. *Neuron*. 42:927-937.

Miller, C., E. Moczydlowski, R. Latorre, and M. Phillips. 1985. Charybdotoxin, a protein inhibitor of single Ca2+-activated K+ channels from mammalian skeletal muscle. *Nature*. 313:316-318.

Morin, T.J., and W.R. Kobertz. 2007. A derivatized scorpion toxin reveals the functional output of heteromeric KCNQ1-KCNE K+ channel complexes. *ACS Chem Biol*. 2:469-473.

Morin, T.J., and W.R. Kobertz. 2008. Counting membrane-embedded KCNE beta-subunits in functioning K+ channel complexes. *Proc Natl Acad Sci U S A*. 105:1478-1482.

Murai, T., A. Kazikuza, T. Takumi, H. Ohkubo, and S. Nakanishi. 1989. Molecular cloning and sequence analysis of human genomic DNA encoding a novel membrane protein which exhibits a slowly activating potassium channel activity. *Biochemical and biophysical research communications*. 161:176-181.

Mustapha, Z., L. Pang, and S. Nattel. 2007. Characterization of the cardiac KCNE1 gene promoter. *Cardiovasc Res*. 73:82-91.

Nakajo, K., and Y. Kubo. 2007. KCNE1 and KCNE3 stabilize and/or slow voltage sensing S4 segment of KCNQ1 channel. *J Gen Physiol*. 130:269-281.

Nakajo, K., M.H. Ulbrich, Y. Kubo, and E.Y. Isacoff. 2010. Stoichiometry of the KCNQ1 - KCNE1 ion channel complex. *Proc Natl Acad Sci U S A*. 107:18862-18867.

Nattel, S. 2002. New ideas about atrial fibrillation 50 years on. *Nature*. 415:219-226.

Neyroud, N., F. Tesson, I. Denjoy, M. Leibovici, C. Donger, J. Barhanin, S. Faure, F. Gary, P. Coumel, C. Petit, K. Schwartz, and P. Guicheney. 1997. A novel mutation in the potassium channel gene KVLQT1 causes the Jervell and Lange-Nielsen cardioauditory syndrome. 15:186-189.

Noble, D., and R.W. Tsien. 1969. Outward membrane currents activated in the plateau range of potentials in cardiac Purkinje fibres. *Journal of Physiology*. 200:205-231.

Osteen, J.D., C. Gonzalez, K.J. Sampson, V. Iyer, S. Rebolledo, H.P. Larsson, and R.S. Kass. 2010. KCNE1 alters the voltage sensor movements necessary to open the KCNQ1 channel gate. *Proc Natl Acad Sci U S A*.

Panaghie, G., and G.W. Abbott. 2007. The Role of S4 Charges in Voltage-dependent and Voltage-independent KCNQ1 Potassium Channel Complexes. *J Gen Physiol*.

Panaghie, G., K.K. Tai, and G.W. Abbott. 2006. Interaction of KCNE subunits with the KCNQ1 K+ channel pore. *The Journal of physiology*. 570:455-467.

Papazian, D.M. 1999. Potassium channels: some assembly required. *Neuron*. 23:7-10.

Papazian, D.M., X.M. Shao, S.A. Seoh, A.F. Mock, Y. Huang, and D.H. Wainstock. 1995. Electrostatic interactions of S4 voltage sensor in Shaker K+ channel. *Neuron*. 14:1293-1301.

Pascual, J.M., C.C. Shieh, G.E. Kirsch, and A.M. Brown. 1995. Multiple residues specify external tetraethylammonium blockade in voltage-gated potassium channels. 69:428-434.

Peretz, A., H. Schottelndreier, L.B. Aharon-Shamgar, and B. Attali. 2002. Modulation of homomeric and heteromeric KCNQ1 channels by external acidification. *The Journal of physiology*. 545:751-766.

Piccini, M., F. Vitelli, M. Seri, L.J. Galietta, O. Moran, A. Bulfone, S. Banfi, B. Pober, and A. Renieri. 1999. KCNE1-like gene is deleted in AMME contiguous gene syndrome: identification and characterization of the human and mouse homologs. 60:251-257.

Pusch, M., R. Magrassi, B. Wollnik, and F. Conti. 1998. Activation and inactivation of homomeric KvLQT1 potassium channels. 75:785-792.

Restier, L., L. Cheng, and M.C. Sanguinetti. 2008. Mechanisms by which atrial fibrillation-associated mutations in the S1 domain of KCNQ1 slow deactivation of IKs channels. *The Journal of physiology*. 586:4179-4191.

Rhodes, T.E., R.L. Abraham, R.C. Welch, C.G. Vanoye, L. Crotti, M. Arnestad, R. Insolia, M. Pedrazzini, C. Ferrandi, A. Vege, T. Rognum, D.M. Roden, P.J. Schwartz, and A.L. George, Jr. 2008. Cardiac potassium channel dysfunction in sudden infant death syndrome. *J Mol Cell Cardiol*. 44:571-581.

Rocheleau, J.M., S.D. Gage, and W.R. Kobertz. 2006. Secondary structure of a KCNE cytoplasmic domain. *J Gen Physiol*. 128:721-729.

Rocheleau, J.M., and W.R. Kobertz. 2008. KCNE peptides differently affect voltage sensor equilibrium and equilibration rates in KCNQ1 K+ channels. *J Gen Physiol*. 131:59-68.

Roepke, T.K., K. Purtell, E.C. King, K.M. La Perle, D.J. Lerner, and G.W. Abbott. 2010. Targeted deletion of Kcne2 causes gastritis cystica profunda and gastric neoplasia. *PLoS One*.

Romey, G., B. Attali, C. Chouabe, I. Abitbol, E. Guillemare, J. Barhanin, and M. Lazdunski. 1997. Molecular mechanism and functional significance of the MinK control of the KvLQT1 channel activity. *J Biol Chem*. 272:16713-16716.

Sanguinetti, M.C., M.E. Curran, A. Zou, J. Shen, P.S. Spector, D.L. Atkinson, and M.T. Keating. 1996. Coassembly of K(V)LQT1 and minK (IsK) proteins to form cardiac I(Ks) potassium channel. *Nature*. 384:80-83.

Sanguinetti, M.C., and N.K. Jurkiewicz. 1990. Two components of cardiac delayed rectifier K+ current. Differential sensitivity to block by class III antiarrhythmic agents. *Journal of General Physiology*. 96:195-215.

Schroeder, B.C., S. Waldegger, S. Fehr, M. Bleich, R. Warth, R. Greger, and T.J. Jentsch. 2000. A constitutively open potassium channel formed by KCNQ1 and KCNE3. *Nature*. 403:196-199.

Schulze-Bahr, E., W. Haverkamp, H. Wedekind, C. Rubie, M. Hordt, M. Borggrefe, G. Assmann, G. Breithardt, and H. Funke. 1997. Autosomal recessive long-QT syndrome (Jervell Lange-Nielsen syndrome) is genetically heterogeneous. 100:573-576.

Seebohm, G., N. Strutz-Seebohm, R. Birkin, G. Dell, C. Bucci, M.R. Spinosa, R. Baltaev, A.F. Mack, G. Korniychuk, A. Choudhury, D. Marks, R.E. Pagano, B. Attali, A. Pfeufer, R.S. Kass, M.C. Sanguinetti, J.M. Tavare, and F. Lang. 2007. Regulation of endocytic recycling of KCNQ1/KCNE1 potassium channels. *Circ Res*. 100:686-692.

Sesti, F., K.K. Tai, and S.A. Goldstein. 2000. MinK endows the I(Ks) potassium channel pore with sensitivity to internal tetraethylammonium. *Biophysical journal*. 79:1369-1378.

Shamgar, L., Y. Haitin, I. Yisharel, E. Malka, H. Schottelndreier, A. Peretz, Y. Paas, and B. Attali. 2008. KCNE1 constrains the voltage sensor of Kv7.1 K+ channels. *PLoS ONE*. 3:e1943. doi:10.1371/journal.pone.0001943.

Smith, J.A., C.G. Vanoye, A.L. George, Jr., J. Meiler, and C.R. Sanders. 2007. Structural models for the KCNQ1 voltage-gated potassium channel. *Biochemistry*. 46:14141-14152.

Soma, K., K. Nagaoka, M. Kuwahara, H. Tsubone, and K. Ito. 2010. Abundant expression of KCNE1 in the left ventricle of the miniature pig. *Heart Vessels*. 26:353-356.

Tai, K.K., and S.A. Goldstein. 1998. The conduction pore of a cardiac potassium channel. *Nature*. 391:605-608.

Takumi, T., K. Moriyoshi, I. Aramori, T. Ishii, S. Oiki, Y. Okada, OhkuboH., and S. Nakanishi. 1991. Alteration of channel activities and gating by mutations of slow ISK potassium channel. *J Biol Chem*. 266:22192-22198.

Takumi, T., H. Ohkubo, and S. Nakanishi. 1988. Cloning of a membrane protein that induces a slow voltage-gated potassium current. *Science J1 - sci*. 242:1042-1045.

Tamargo, J., R. Caballero, R. Gomez, C. Valenzuela, and E. Delpon. 2004. Pharmacology of cardiac potassium channels. *Cardiovasc Res*. 62:9-33.

Tapper, A.R., and A.L. George, Jr. 2000. MinK subdomains that mediate modulation of and association with KvLQT1. 116:379-390.

Tapper, A.R., and A.L. George, Jr. 2001. Location and orientation of minK within the I(Ks) potassium channel complex. *J Biol Chem*. 276:38249-38254.

Tian, C., C.G. Vanoye, C. Kang, R.C. Welch, H.J. Kim, A.L. George, Jr., and C.R. Sanders. 2007a. Preparation, functional characterization, and NMR studies of human KCNE1, a voltage-gated potassium channel accessory subunit associated with deafness and long QT syndrome. *Biochemistry*. 46:11459-11472.

Tian, X.L., Y. Cheng, T. Zhang, M.L. Liao, S.L. Yong, and Q.K. Wang. 2007b. Optical mapping of ventricular arrhythmias in LQTS mice with SCN5A mutation N1325S. *Biochemical and biophysical research communications*. 352:879-883.

Tinel, N., S. Diochot, M. Borsotto, M. Lazdunski, and J. Barhanin. 2000. KCNE2 confers background current characteristics to the cardiac KCNQ1 potassium channel. 19:6326-6330.

Tiwari-Woodruff, S.K., M.A. Lin, C.T. Schulteis, and D.M. Papazian. 2000. Voltage-dependent structural interactions in the Shaker K(+) channel. *J Gen Physiol*. 115:123-138.

Tristani-Firouzi, M., and M.C. Sanguinetti. 1998. Voltage-dependent inactivation of the human K+ channel KvLQT1 is eliminated by association with minimal K+ channel (minK) subunits. *The Journal of physiology*. 510 (Pt 1):37-45.

Tyson, J., L. Tranebjaerg, S. Bellman, C. Wren, J.F. Taylor, J. Bathen, B. Aslaksen, S.J. Sorland, O. Lund, S. Malcolm, M. Pembrey, S. Bhattacharya, and M. Bitner-Glindzicz. 1997. IsK and KvLQT1: mutation in either of the two subunits of the slow component of the

delayed rectifier potassium channel can cause Jervell and Lange-Nielsen syndrome. 6:2179-2185.

Tzounopoulos, T., H.R. Guy, S. Durell, J.P. Adelman, and J. Maylie. 1995. min K channels form by assembly of at least 14 subunits. *Proc Natl Acad Sci U S A*. 92:9593-9597.

Van Horn, W.D., C.G. Vanoye, and C.R. Sanders. 2011. Working model for the structural basis for KCNE1 modulation of the KCNQ1 potassium channel. *Curr Opin Struct Biol*. 21:283-291.

Vemana, S., S. Pandey, and H.P. Larsson. 2004. S4 movement in a mammalian HCN channel. *J Gen Physiol*. 123:21-32.

Wang, K.W., and S.A. Goldstein. 1995. Subunit composition of minK potassium channels. *Neuron*. 14:1303-1309.

Wang, Q., J. Shen, I. Splawski, D. Atkinson, Z. Li, J.L. Robinson, A.J. Moss, J.A. Towbin, M.T. Keating. 1995. SCN5A mutations associated with an inherited cardiac arrhythmia, long QT syndrome. *Cell*. 80: 805-11.

Wang, K.W., K.K. Tai, and S.A. Goldstein. 1996a. MinK residues line a potassium channel pore. *Neuron*. 16:571-577.

Wang, Q., M.E. Curran, I. Splawski, T.C. Burn, J.M. Millholland, T.J. VanRaay, J. Shen, K.W. Timothy, G.M. Vincent, T. de Jager, P.J. Schwartz, J.A. Toubin, A.J. Moss, D.L. Atkinson, G.M. Landes, T.D. Connors, and M.T. Keating. 1996b. Positional cloning of a novel potassium channel gene: KVLQT1 mutations cause cardiac arrhythmias. *Nat Genet*. 12:17-23.

Wang, W., J. Xia, and R.S. Kass. 1998. MinK-KvLQT1 fusion proteins, evidence for multiple stoichiometries of the assembled IsK channel. *J Biol Chem*. 273:34069-34074.

Wiener, R., Y. Haitin, L. Shamgar, M.C. Fernandez-Alonso, A. Martos, O. Chomsky-Hecht, G. Rivas, B. Attali, and J.A. Hirsch. 2008. The KCNQ1 (Kv7.1) COOH terminus, a multitiered scaffold for subunit assembly and protein interaction. *J Biol Chem*. 283:5815-5830.

Woycechowsky, K.J., and R.T. Raines. 2000. Native disulfide bond formation in proteins. *Curr Opin Chem Biol*. 4:533-539.

Xu, X., M. Jiang, K.L. Hsu, M. Zhang, and G.N. Tseng. 2008. KCNQ1 and KCNE1 in the IKs channel complex make state-dependent contacts in their extracellular domains. *J Gen Physiol*. 131:589-603.

Xu, X., V.A. Kanda, E. Choi, G. Panaghie, T.K. Roepke, S.A. Gaeta, D.J. Christini, D.J. Lerner, and G.W. Abbott. 2009. MinK-dependent internalization of the IKs potassium channel.

Cardiovasc Res. 82:430-438. Yang, N., A.L. George, Jr., and R. Horn. 1997a. Probing the outer vestibule of a sodium channel voltage sensor. *Biophysical journal*. 73:2260-2268.

Yang, W.P., P.C. Levesque, W.A. Little, M.L. Conder, F.Y. Shalaby, and M.A. Blanar. 1997b. KvLQT1, a voltage-gated potassium channel responsible for human cardiac arrhythmias. *Proc.Natl.Acad.Sci.U.S.A.* 94:4017-4021.

Yarov-Yarovoy, V., D. Baker, and W.A. Catterall. 2006. Voltage sensor conformations in the open and closed states in ROSETTA structural models of K(+) channels. *Proc Natl Acad Sci U S A*. 103:7292-7297.

Yellen, G., M.E. Jurman, T. Abramson, and R. MacKinnon. 1991. Mutations affecting internal TEA blockade identify the probable pore- forming region of a K+ channel. 251:939-942.

Zheng, R., K. Thompson, E. Obeng-Gyimah, D. Alessi, J. Chen, H. Cheng, and T.V. McDonald. 2010. Analysis of the interactions between the C-terminal cytoplasmic domains of KCNQ1 and KCNE1 channel subunits. *Biochem J*. 428:75-84.